U.PORTO

MASTER IN MARINE SCIENCES – MARINE RESOURCES
MARINE BIOLOGY AND ECOLOGY

The effect of rising ocean temperatures on the behaviour and thermoregulation of large endothermic fish.

Maria Eduarda Costa Vieira

M

2024

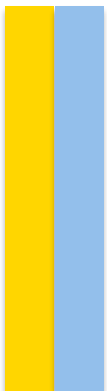

MARIA EDUARDA COSTA VIEIRA

THE EFFECT OF RISING OCEAN TEMPERATURES ON THE BEHAVIOUR AND THERMOREGULATION OF LARGE ENDOTHERMIC FISH.

Dissertação de Candidatura ao grau de Mestre em Ciências do Mar – Recursos Marinhos ao Instituto de Ciências Biomédicas de Abel Salazar da Universidade do Porto.

Orientador – Dr. Nuno Miguel Cabral Queiroz
Categoria – Investigador Principal
Afiliação – CIBIO/InBIO, Centro de Investigação em Biodiversidade e Recursos Genéticos, Universidade do Porto

Co-orientador – Não aplicável.
Categoria – Não aplicável.
Afiliação – Não aplicável.

Declaração de Honra

Declaro que a presente dissertação é de minha autoria e não foi utilizada previamente noutro curso ou unidade curricular, desta ou de outra instituição. As referências a outros autores (afirmações, ideias, pensamentos) respeitam escrupulosamente as regras da atribuição, e encontram-se devidamente indicadas no texto e nas referências bibliográficas, de acordo com as normas de referenciação. Tenho consciência de que a prática de plágio e autoplágio constitui um ilícito académico.

30 de setembro de 2024

A estudante,

Maria Eduarda Costa Vieira

Resumo

Este estudo investiga o comportamento, movimentos e termorregulação de atuns da espécie *Thunnus obesus*, uma espécie classificada como vulnerável pela IUCN. Com as alterações climáticas a impulsionarem o aumento das temperaturas do oceano, a expansão das zonas de oxigénio mínimo (OMZs) e a alteração dos habitats, compreender como essas mudanças afetam grandes predadores endotérmicos é crucial para a gestão e conservação dos ecossistemas marinhos. Os objetivos do estudo focaram-se na validação e aplicação de um modelo de balanço térmico para determinar se surgem problemas de termorregulação ou mudanças no comportamento devido a gradientes ambientais. Três indivíduos foram inicialmente utilizados para capturar a dinâmica da temperatura interna e ambiental, e a equação final foi posteriormente aplicada a seis indivíduos adicionais. Os resultados mostraram que, embora os modelos capturassem eficazmente as tendências gerais de temperatura, houve enviesamentos, particularmente durante períodos de rápidas flutuações de temperatura. O estudo também analisou os padrões de distribuição espacial, observando diferenças significativas entre os atuns que permaneceram em latitudes mais altas (região das Ilhas Canárias e Açores) e os que migraram para sul (em torno de Cabo Verde), com tendências de aquecimento mais acentuadas nas regiões do norte. As variações sazonais indicaram o outono como um período de transição no comportamento, enquanto a ausência de dados no verão e na primavera pode ter ocultado informações importantes. Os resultados também demonstram que o atum patudo exibe resiliência a condições de baixo oxigénio e temperaturas frias devido a adaptações fisiológicas, mas pode enfrentar riscos crescentes. A expansão das OMZs, combinada com o aumento da temperatura da água e uma acentuação nos efeitos da termoclina, pode provocar alterações no comportamento dos indivíduos e causar agregações em certas profundidades, levando a uma maior vulnerabilidade às pressões da pesca comercial. Isto afirma a necessidade urgente de medidas de conservação mais direcionadas, incluindo práticas de gestão das pescas. Ao fornecer informações sobre as interações entre atuns, mudanças climáticas e pescas, este estudo contribui para a previsão dos impactos futuros do aquecimento dos oceanos e destaca a necessidade de estratégias mais sustentáveis para proteger esses animais e manter o equilíbrio ecológico.

Palavras-chave: Atum patudo, *Thunnus obesus*, Alterações climáticas, Padrões de movimento, Pescas.

Abstract

This study investigates the behaviour, movements, and thermoregulation of bigeye tuna (*Thunnus obesus*), a species listed as vulnerable by the IUCN. With climate change driving rising ocean temperatures, expanding oxygen minimum zones (OMZs), and altering habitats, understanding how these changes affect large endothermic fish is crucial for marine ecosystem management and conservation. The research focuses on fitting, validating, and applying a heat budget model to assess if thermoregulation challenges or changes in behaviour happen due to environmental gradients. Three individuals were initially used to record internal and ambient temperature dynamics, and the final model was then applied to six additional individuals. Results showed that while the models effectively captured general temperature trends, there were biases, particularly during periods of rapid temperature fluctuations. Spatial distribution patterns were also analysed, noting significant differences between tuna that remained in higher latitudes (Canary Islands and Azores region) and those migrating southward (around Cabo Verde), with warming trends more pronounced in the northern regions. Seasonal variations indicated autumn as a transitional period, while gaps in summer and spring data could have masked import information. The findings demonstrate that bigeye tuna exhibit resilience to low-oxygen and cold conditions due to physiological adaptations but face growing risks from climate-induced stressors. OMZ expansion, combined with increasing water temperatures and a sharper thermocline, may cause shifts in the behaviour and cause aggregations at certain depths, leading to greater vulnerability to commercial fishing pressures. This underscores the urgent need for more specific conservation measures, including fisheries management practices. By providing insights into the interactions between tuna, climate change, and fisheries, this study contributes to predicting the future impacts of ocean warming and highlights the need for sustainable strategies to protect these marine predators and maintain ecological balance.

Keywords: Bigeye tuna, *Thunnus obesus*, Climate change, Movement patterns, Fisheries.

List of contents

List of tables

List of figures

List of abbreviations

ETA	Eastern Tropical Atlantic
GPS	Global Positioning System
ID	Individual Identification
DO	Dissolved Oxygen
IUCN	International Union for the Conservation of Nature
OMZ	Oxygen Minimum Zone
NOAA	National Oceanic and Atmospheric Administration
WMO	World Meteorological Organization
ICCAT	International Commission for the Conservation of Atlantic Tunas
DO	Dissolved Oxygen
SST	Sea Surface Temperature
FL	Fork Length
BW	Body Weight
RMSE	Root Mean Squared Error
MAE	Mean Absolute Error
i.e.	That is
et al.	And others
e.g.	For example
m	Meters

1. Introduction

1.1. Bio-logging as a scientific tool and how to study marine species

Understanding the behaviour of marine free-living animals is challenging, as they spend most of their time underwater and travel great distances, making direct observation difficult (Wilmers et al., 2015; Heylen & Nachtsheim, 2018). This also complicates efforts to study their habitat use, both horizontally and vertically. However, with the development of transmitters and advances in technology, scientists can now monitor marine species using electronic devices attached to them (e.g., Sato et al., 2004; Okuyama et al., 2012; Watanabe & Takahashi, 2013). These devices collect high-resolution data on their movements, biology, and interactions with the environment, providing crucial insights into habitat preferences, distribution patterns, and spatial dynamics (Sims et al., 2008). Due to these advantages, bio-logging has become a widely adopted and valuable tool across fields such as environmental science, ecology, oceanography, and zoology (Hussey et al., 2015).

The high diversity of marine animals has led to a variety of sensors and tagging methods. Traditional capture-tag-recapture techniques have been used for centuries to track both marine and freshwater fish (Kohler & Turner, 2001). This method involves tagging fish, releasing them back into their habitats, and recapturing them later to have access to the data. Moreover, this conventional method needs a high amount of time for data accumulation and it is entirely dependent on the successful recapture of the fish (Chung, Lee & Lee, 2021). Over the years, alternative methods have emerged. Acoustic tagging, which began in the 1980s, introduced long-term track of fish movements, with tagged individuals transmitting signals whenever they pass near a receiver (Hussey et al., 2015). By the 1990s, advancements in data logger technology made them small enough to reduce interference with fish movement, although low tag recovery rates remained a challenge (Klimley et al., 1988). A significant leap came with the advent of satellite tracking systems, particularly the Argos system, launched in 1978, which revolutionized ecological research. Archival tags capable of transmitting data via satellite, such as pop-off satellite archival transmitters (PSATs), greatly reduced the need for fish recapture (Metcalfe & Arnold, 1997). These devices detach from fish at a set time, float to the surface, and send their data to satellites (Block et al., 1998). Today, the data collected ranges from low-resolution geolocation based on light levels to precise GPS coordinates, and even highly detailed daily movement tracks and environmental variables recording (Wilson et al., 2015), further

enhancing the understanding of fish behaviour and migration. While bio-logging provides invaluable insights, it comes with limitations, including high costs, limited battery life, data storage capacity, signal loss in complex environments, and gaps in movement data (Wilson & McMahon, 2006; Hussey et al., 2015). In order to overcome these barriers, newer tagging technologies are appearing. An example of this is the method of incorporating tri-axial accelerometers that have been developed, enabling more accurate movement tracking (Shepard et al., 2008). Despite these challenges, bio-logging continues to be a crucial tool for studying the often-inaccessible marine environment (Cooke et al., 2004), linking behaviour to environment, driving advancements in fisheries management, species conservation, and research on future environmental changes such as increased ocean temperatures (Greene et al., 2009).

1.2. Climate change and rising ocean temperatures

Global climate change, primarily driven by the rising of anthropogenic greenhouse gas emissions, has led to significant alterations in the Earth's climate system (Parmesan, 2006). Ranked as one of the greatest threats to terrestrial biodiversity and being the cause of shifts in species distributions, less is known about marine impacts (Thomas et al., 2004; Burrows et al., 2011), even with the oceans absorbing a significant amount of this heat generated (> 93%) and also approximately 26% of CO_2 emissions from 2011 to 2020 (Cheng et al., 2019; Johnson & Lyman, 2020; Gruber et al., 2021). In the last years, the warming of ocean waters is leading to multifaceted changes, affecting physical, chemical, and biological processes, and disrupting its natural balance (Nagelkerken & Connell, 2015). As oceans cover 71% of Earth's surface (NOAA), they are crucial not only for supporting global economies but also for sustaining an enormous range of biodiversity, from microscopic plankton to large marine mammals (FAO, 2018). Given these and others fundamental roles, there is an urgent need to understand and address these changes.

When discussing climate change, the rising temperatures of oceans and sea surfaces are often one of the first consequences considered. The Intergovernmental Panel on Climate Change (IPCC) reports that over the last two centuries, global ocean surface temperatures have increased by approximately 0.76°C, with projections indicating sharp increases in the coming decades. This trend has accelerated notably in recent years, as confirmed by the National Oceanic and Atmospheric Administration (NOAA). 2023 stands out as the warmest year on record, with global land and ocean temperatures reaching unprecedented levels and record-high SSTs observed (NOAA's 2023 Annual Climate Report). According to the

World Meteorological Organization (WMO), the global mean surface temperature through October 2023 was about 1.40°C higher than the pre-industrial average (1850–1900), surpassing previous records set in 2016 and 2020, and according to Hazen et al. (2012), climate change scenarios have predicted an average SST rise of 1-6ºC by 2100. These changes not only disrupt marine ecosystems, but also contribute to the intensification of extreme and adverse events. Warmer ocean waters can lead to frequent marine heatwaves, defined as periods when temperatures are warmer than normal for at least five consecutive days (Holbrook et al., 2020). Additionally, warmer waters increase stratification of the water column, creating a barrier to mixing (Li et al., 2020). This stratification reduces oxygen solubility in surface waters, limits ventilation of deeper waters, and slows the rate of oxygen resupply from the atmosphere (Breitburg et al., 2019).

Over the last five decades, ocean oxygen loss has been estimated at 2%, with a continuous decline observed (Breitburg et al., 2019). In shallow coastal waters, increased eutrophication is recognized as the primary cause of declining levels of dissolved oxygen (DO) and the formation of hypoxic and even anoxic zones (Kessouri et al., 2021). However, in the open ocean, the mechanism is more complex, largely due to climate change, as noted earlier (Gruber et al., 2021). DO concentrations at depth are known to decrease due to microbial respiration of particulate organic matter that sinks from more productive surface waters into the intermediate layers (Breitburg et al., 2018). In areas with upwellings, a mix of stratification, restricted DO ventilation, elevated primary production, and microbial respiration contributes to this substantial decline, also leading to the formation of oxygen minimum zones (OMZs) (Diaz & Rosenberg, 2008; Chan et al., 2008). OMZs are globally distributed, covering approximately 8% of the oceanic area (see Figure 1, a), and are characterized by extremely low oxygen concentrations (Paulmier & Ruiz-Pino, 2009; Wright, Konwar & Hallam, 2012; Gilly et al., 2013). In these regions, dissolved oxygen declines with depth, reaching minimal levels before increasing again, forming a hypoxic zone typically found between 200 and 800 meters (OMZ core; see Figure 1, b) (Stramma et al., 2008; Gilly et al., 2013). The eastern tropical Atlantic (ETA) OMZ, located along the west coast of Africa and around Cabo Verde, is of particular interest due to its significant expansion in recent years compared to other OMZs (Stramma et al., 2008). Though not the largest one, it continues to expand, with hypoxic waters spreading into regions above its core (Karstensen et al., 2015). The same study also reported critically low DO concentrations below 0.05 ml O_2 l^{-1} in this area, leading to the formation of called "dead zones".

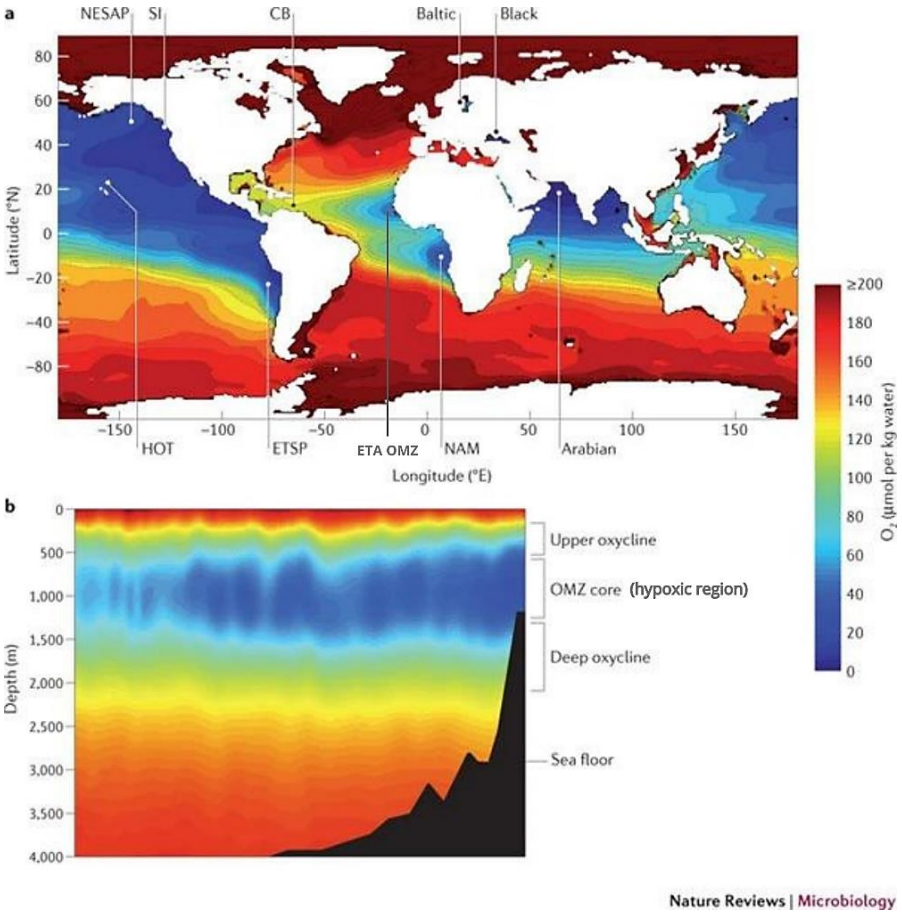

Figure 1. (a) Oxygen concentrations across different ocean regions - Hawaii Ocean Time-series (HOT), the northeast subarctic Pacific (NESAP), Saanich Inlet (SI), the eastern tropical South Pacific (ETSP), the Cariaco Basin (CB), the eastern tropical Atlantic (ETA) OMZ, Namibian upwelling (NAM), and the Baltic, Black and Arabian seas. (b) A cross-section of the northeast subarctic Pacific OMZ that shows O_2 levels from surface waters to the sea floor, with the upper oxycline marking the transition to the OMZ core, known as hypoxic zone, and the deep oxycline indicating the shift from the OMZ to abyssal waters. Adapted from Wright, Konwar & Hallam (2012).

Still less is known about the combination of all these mentioned factors and its impacts in various species, however, temperature is considered the most important environmental variable influencing horizontal and vertical distributions, abundance and movement patterns of marine animals (Hubbs, 1948; McCormick & Molony, 1995; Herbing, 2002; Takahashi et al., 2012).

1.3. Vertical movements and thermoregulation

Vertical movements in water species refer to their up-and-down movement through different ocean layers, typically in response to environmental conditions such as light, temperature, and food availability. One common type of vertical movement is the diel vertical migration, where species ascend to surface waters at night to feed and descend to deeper waters during the day to avoid predators (Brierley, 2014).

Vertical movements in marine species are not limited to daily migrations; they are also influenced by seasonal variations and environmental factors like the thermocline. Thermocline is a transitional layer where temperature rapidly decreases with depth, separating the warmer surface waters from the cooler deep waters (Kitagawa et al., 2007; Nordstrom et al., 2013). Above this, the epipelagic zone interacts with wind and waves, mixing the water and distributing heat (Mellor & Durbin, 1975; Aspillaga et al., 2017). The thermocline plays a critical role in diving behaviour, acting as a barrier that traps prey, making it a key zone for predator-prey interactions (Sogard & Olla, 1993). For example, some species dive deeper during the day to escape warmer surface waters or to forage for prey found below the thermocline (Potier et al., 2014). The depth and strength of the thermocline also vary seasonally, annually, and regionally (Welander, 1971). Vertical movements are crucial for maintaining energy balance and regulating body temperature as individuals experience a wide range of environmental variables throughout the water column, particularly as ocean conditions shift due to climate change (Seibel, 2011; Keeling et al., 2010). The homeostasis mechanism is vital for living beings, also known as thermoregulation, and consists of a set of systems and adaptations responsible for regulating the body temperature. Its main objective is to maintain the balance between the heat generated by the organism and the heat exchanged with - lost to or acquired from - the environment in which it is inserted (Kurz, 2008; Cutler & Haesemeyer, 2024).

Endothermy is an adaptation that allows animals to generate and regulate body heat through metabolic processes, enabling them to maintain body temperatures above the environment temperatures. This trait has independently evolved multiple times among vertebrates and is most observed in mammals and birds, which are capable of sustaining stable internal temperatures regardless of external conditions (Clarke & Pörtner, 2010; Grady et al., 2014; Legendre & Davesne, 2020). In contrast, ectothermic animals, such as reptiles, rely on external heat sources to regulate their body temperature, resulting in fluctuating internal temperatures that mirror their surroundings (Huey & Kingsolver, 2019).

In most fish, body temperature depends on the surrounding water, as metabolic heat is quickly lost through the body surface or gills, making them predominantly ectothermic (Stevenson, 1985). However, regional endothermy has independently evolved in certain fish lineages, such as some sharks (e.g., white and mako sharks), tuna, and billfishes. This adaptation allows them to generate metabolic heat and maintain their core body regions (i.e., red muscle) and other areas (i.e., viscera, eyes, brain) warmer than the ambient temperature (Wegner et al., 2015). Stevens et al. (2011) described how this is made by their lateral blood circulation, with red muscle situated near the vertebral column and distributed

along the body. They also noted modifications in the vascular supply to and from the red muscle, eyes, brain, and viscera that form counter-current heat exchangers. As venous blood passes through the tissues, it absorbs the metabolic heat produced by those tissues and carries it to the gills. Due to the large surface area of the gills for gas exchange and the high heat capacity of the water flowing over them, the blood temperature equilibrates with the ambient water. Consequently, all metabolic heat is lost to the water, and the arterial blood delivering oxygen to the tissues matches the temperature of the water, promoting thermal equilibrium. The flow rate through the vessels and the contact surface area between them also influence the efficiency of this exchange.

Regional endothermy enabled these animals to maintain higher activity levels, offering significant advantages such as elevated cruising speeds, improved brain and eye function, and greater metabolic efficiency. This adaptation also allowed them to explore a wider range of environments, including colder waters (Farrell, 2002; Wegner et al., 2015). These combined factors highlight the metabolic differences between endotherms and ectotherms, influencing their trophic roles and competitive interactions. For instance, heat conservation by the red muscle and vascular heat exchangers enables tunas to sustain elevated and stable muscle temperatures, both at high latitudes and when swimming beneath the thermocline (Carey, Kanwisher & Stevens, 1984; Marcinek et al., 2001). Although faster cruising speeds lead to increased exploration and higher prey encounter rates (with annual migration ranges 2-3 times greater than those of ectothermic fishes), they also come with a high energetic cost.

Oxygen (O_2) consumption is another important part of thermoregulation, as the gas is consumed during cellular respiration. The faster an organism consumes oxygen, the higher its metabolic rate is, and more heat it generates (Dickson & Graham, 2004). The variations in oxygen and temperature caused by the climate change affect blood-oxygen binding capacity, and consequently, the tolerance of individuals to hypoxia (Deutsch et al., 2015). Besides that, higher temperatures result in higher energetic expenditures and faster rates of important physiological processes. Tunas, with high oxygen requirements, are likely to be one of the most affected animals by changes in the distribution of low DO, temperature increases and stratification in the oceans (Malte et al., 2007; Gilly et al., 2013). Consequently, bigeye tuna is an appropriate species to test for the effect of low DO, as they have relatively high metabolic rates among fish with consequently high O_2 demands and are therefore likely to be more sensitive to it and to the rising ocean water temperatures (Bernal et al., 2017).

1.4. Bigeye tuna

Bigeye tuna (*Thunnus obesus*) is a highly migratory species found in tropical and temperate marine waters worldwide (Erdaide et al., 2016). Known for its large eyes, metallic blue upper body, and silvery white underbelly (see Figure 2), the bigeye tuna, as a top predator, feed opportunistically on cephalopods, crustaceans, and teleosts, which form the primary components of its diet (Olson et al., 2016; da Silva et al., 2019). Analyses of its diet also provide valuable insights into the marine ecosystems and food webs of its habitats (Polovina et al., 2009). The species' large eyes and well-developed visual centres suggest that vision plays a vital role in its feeding and other behavioural patterns (Kawamura et al., 1981). Its vertical distribution ranges from the surface to depths exceeding 1000 m, influenced by factors such as diel vertical migration, seasonal changes, and water temperature (Matsumoto, Kitagawa & Kimura, 2013; Lam, Galuardi & Lutcavage, 2014).

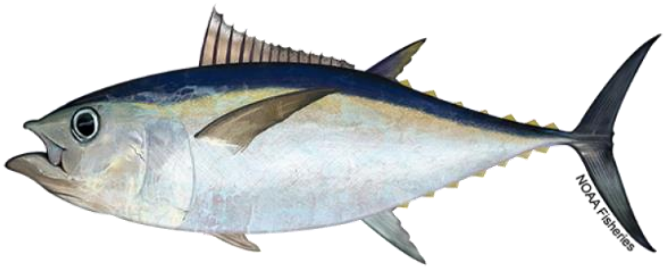

Figure 2. Illustration of Bigeye tuna. Credits: NOAA.

Economically, bigeye tuna is highly valued, particularly in sashimi markets due to its taste and nutritional benefits (Wang & Xie, 2019). The global demand for tuna, driven by markets for canned tuna and sushi, has led to intense exploitation. Tropical tuna species account for 95% of the 5.1 million tonnes of tuna caught globally in 2018 (FAO, 2018; ISSF, 2020). This level of exploitation highlights the need for careful management, especially as bigeye tuna is classified as vulnerable on the IUCN Red List.

Sustainable management initiatives, led by organizations like the International Commission for the Conservation of Atlantic Tunas (ICCAT), work to regulate catch limits and promote responsible fishing practices (Galland et al., 2018). As a member of the Scombridae family, the bigeye tuna is not only vital to marine ecosystems but also serves as a key food and economic source for coastal communities worldwide (Arrizabalaga et al., 2015; FAO, 2016).

However, global marine ecosystems and fisheries are nearing collapse due to decades of overfishing (Pauly et al., 1998; Sethi, Branch & Watson, 2010; McCauley et al., 2015). Changes in the behaviour and habitat utilization of bigeye tuna affect their susceptibility to capture, making it essential to understand their responses to environmental changes for improved stock assessments (Brill et al., 2005; Maunder et al., 2006). Studying temperature fluctuations and tuna's adaptations to these changes is crucial, as it provides a window into future scenarios and the long-term impacts of climate change on this species (Ekau et al., 2010; Hussey et al., 2015).

2. General objectives

This study investigates behaviour and thermal biology of nine individuals of the bigeye tuna species listed by the IUCN as vulnerable with a decreasing population trend, highlighting the need for new information on their movements, behaviour and thermoregulation in relation to environmental gradients (e.g., rising ocean temperatures, thermocline, hypoxia zones) to support marine ecosystem management and conservation. Thus, in this context, the objectives were:

1. Fit a temperature model using internal and ambient temperature data from three tracked tuna;

2. Validate and apply the model to six additional individuals.

By achieving these objectives, the study aims to answer two main questions:

- Do bigeye tuna exhibit altered behaviour in response to sharp changes or increasing ocean temperatures?

- Can these environmental changes lead to thermoregulation challenges?

The goals align with the UN Global Goals for Sustainable Development - Goal 13 (Climate Action) and Goal 14 (Life Below Water). Goal 13 aims to improve resilience and adaptive capacity in response to climate-related threats, while Goal 14 focuses on conserving and sustainably using the oceans, seas, and marine resources, including managing fishing practices.

This research will explore how temperature affects behaviour and distribution, contributing to predictions of how future warming scenarios may impact this and other endothermic species. The main hypothesis is that climate change-induced high temperatures can interfere with the thermoregulation of large endothermic fish, shifting their habitat use and making them more vulnerable to commercial fishing.

3. Materials and Methods

3.1. Tagging

A total of nine archival tags from Wildlife Computers (Redmond, WA, USA) were deployed on bigeye tuna individuals. The tagging was conducted at different locations and across different years, with all procedures approved by institutional ethical review committees and performed by trained personnel. After tagging, the fish were released within a few minutes, showing no apparent adverse effects.

In September 2005, the first tags were deployed aboard the M/P El Grande Primero, a 26-meter vessel with a gross registered tonnage of 124 tons. The fishing method involved the use of live bait, and catches were made near floating objects known as Fish Aggregation Devices (FADs), which attract tuna and other species, facilitating their capture (Ariz et al., 1999). The fishing occurred northeast of the Canary Islands, between latitudes 29º11'N – 29º26'N and longitudes 12º21'W – 12º24'W. Three archival tags, model Mk9 (Figure 3), were implanted in the peritoneal cavity of the tuna. These tags have two temperature sensors - one in the tag body to measure internal temperature and another on the stalk to measure ambient temperature. Once the fish were brought on deck, they were swiftly measured, and the tags were inserted through a small incision approximately 2 cm long, which was then sutured (Figures 4 and 5). The entire procedure took between 1.44 and 3.50 minutes per fish.

To enhance the chances of locating tagged individuals for data recovery, a conventional ICCAT (spaghetti-type) red tag was also attached. The Mk9 tags require retrieval to access the collected data, making them suitable for animals that can be recaptured. Details on the tag identification numbers (ID) and additional information on the tagging and recapture dates are provided in Table 1. Each tag recorded daily data on depth (pressure), ambient temperature, internal temperature, and light level. Using specialized software provided by the tags' manufacturer (WC-GPE, global position estimator program suite), the position (latitude and longitude) of the tagged fish was estimated based on light level curves. Longitude estimates were based on the local time of midnight or midday, estimated through the daily maximal rate of change in light intensity, and latitude was determined via day-length estimates (Wilson, 1992). Data were recorded every sixteen seconds, generating substantial volumes of information from specimens that remained at liberty for extended

periods, potentially up to a year. Although the tags could be set to record data at longer intervals, the shorter sixteen-second interval was chosen due to concerns regarding the likelihood of long-term tag recovery.

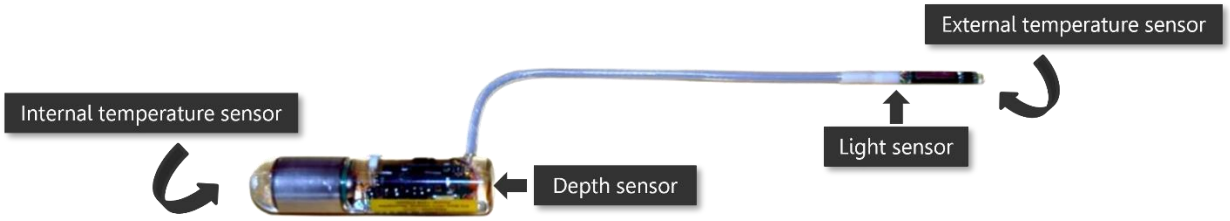

Figure 3. Photograph of Wildlife Computers' MK9 archival tag model pointing for the location of depth, light, internal and external temperature sensors.

Figure 4. After making a small incision and attaching the tag, the wound was stitched up. Photo by Francisco Abascal.

Figure 5. Tag implanted in the peritoneal cavity on a recaptured individual. Photo by Francisco Abascal.

The subsequent tagging operations were conducted in the Azores, specifically along the south shore of São Miguel Island, between 2019 and 2022. Six individuals were caught and tagged aboard a private boat using the live bait fishing method. Once hooked, they were brought close to the boat and carefully lifted onboard. On deck (Figure 6), the fish were measured and tagged with MiniPAT pop-up satellite archival tags (Figure 7). This tagging process (Figure 8) was executed as quickly and carefully as possible to ensure the fish's survival. Details on the tag identification numbers (ID) and additional information on the tagging and pop-up dates are provided in Table 2. The MiniPAT tags are archival devices equipped with Argos transmitters and corrodible attachment links designed to tether the tags to the animal. The corrodible burn pin releases the tag from the tether on a pre-programmed date or when the tag detects that it is no longer attached to the fish. Data on depth, ambient temperature, and light levels were collected and summarized for transmission via Argos, which began once the tag was released and floating on the ocean surface (Whitney et al., 2018).

Figure 6. Bigeye tuna positioned on boat deck, on a tagging cradle with a hose providing seawater. Photo by Miguel Furtado.

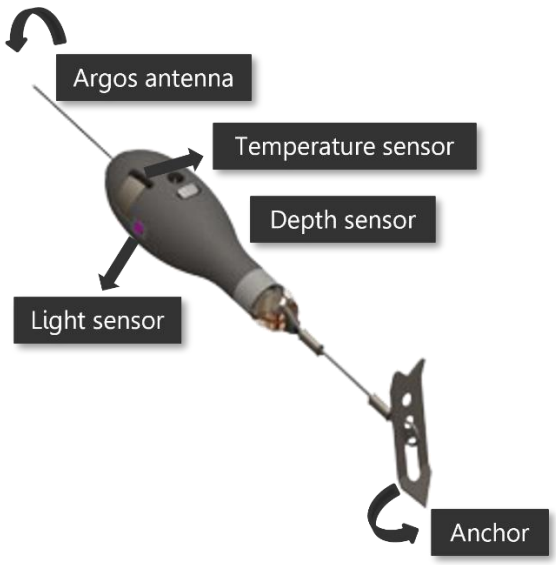

Figure 7. Photograph of a Wildlife Computers' MiniPAT pop-up satellite archival tag rigged with a stainless-steel tether, an Argos antenna and a Titanium anchor, pointing also for the location of depth, light and external temperature sensors. Image adapted from Wildlife Computers.

Figure 8. Tagging process. Photo by Miguel Furtado.

In this study, the fork length (FL) was used as a measure method as it provides the most reproducible and reliable results compared to other length measurements such as standard length or total length. The FL measurement utilizes a consistent anatomical landmark, the fork of the tail, which minimizes measurement variability and error. This standardization is crucial in tagging and fisheries research, ensuring consistency and accuracy in data collection (Walker et al., 2012).

Table 1. Summary data of tuna tagging and recapture. ID 039503 does not have any available tagging and recapture information.

Tagging season	ID	Ref.	FL (cm)	Size class	Tag type	Date of tagging	Time	Tag Lat. (N)	Tag Long. (W)	Recapture Date	Recap Lat. (N)	Recap Long. (W)
2005	0390474	**BET1**	87	Sub-adult	TDR-Mk9	21-09-05	6:03:00	29.183333	-12.35	10-08-06	30.166667	-12.366667
2005	0390491	**BET2**	61	Juvenile	TDR-Mk9	21-09-05	6:18:00	29.183333	-12.35	07-09-06	30.583333	-12.266667
2005	0390503	**BET3**	62	Juvenile	TDR-Mk9	NA	NA	NA	NA	NA	NA	NA

Table 2. Summary data of tuna tagging and pop-up.

Tagging season	ID	Ref.	FL (cm)	Size class	Tag type	Date of tagging	Time	Tag Lat. (N)	Tag Long. (W)	Pop-up date	Pop-up Lat. (N)	Pop-up Long. (W)
2019	84600	**BET4**	187	Adult	Mini PAT	19-09-19	15:05:00	37.62	-25.512	18-01-20	10.75	-30.025
2019	85009	**BET5**	189	Adult	Mini PAT	27-09-19	20:08:00	37.651	-25.391	26-01-20	0.649	-17.6
2020	196132	**BET6**	167	Adult	Mini PAT	16-08-20	14:48:00	37.748	-25.825	15-12-20	44.116	-30.459
2020	196133	**BET7**	162	Adult	Mini PAT	13-08-20	17:40:23	37.699	-25.811	21-10-20	38.953	-28.594
2022	202884	**BET8**	191	Adult	Mini PAT	06-08-22	12:05:00	37.678	-25.291	01-09-22	37.9	-25.1
2022	181756	**BET9**	145	Adult	Mini PAT	14-08-22	12:50:00	37.637	-25.436	08-09-22	34.95	-34.65

3.2. Vertical movement analysis

The time series dataset (see Table 3 for an example) consisted of data collected at high resolution, enabling detailed analysis of the spatiotemporal patterns. This approach allowed for a fine scale understanding of differentiated patterns in vertical habitat use. The datasets were trimmed based on the tagging date and time as well as the pop-up/recapture date and time to ensure data consistency. Time-at-depth (TAD) and time-at-temperature (TAT) matrices were also constructed with ten-meter depth bins and one-degree temperature bins for each dataset.

Table 3. Example of a trimmed time series dataset format for one bigeye tuna used to create R input file.

Datetime	Date	Depth	WaterTemperature	InternalTemperature
2005-09-21 06:07:44	2005-09-21	2.0	21.20	20.80
2005-09-21 06:08:00	2005-09-21	2.0	21.15	20.75
2005-09-21 06:08:16	2005-09-21	2.5	21.20	20.65
2005-09-21 06:08:32	2005-09-21	2.5	21.20	20.65
2005-09-21 06:08:48	2005-09-21	2.5	21.30	20.60
2005-09-21 06:09:04	2005-09-21	2.5	21.20	20.55
2005-09-21 06:09:20	2005-09-21	2.5	21.20	20.50

3.3. Statistical analysis of environmental and biological variables

Minimum, maximum, and mean values for depth, ambient and internal temperatures were extracted and grouped by season (Winter, Spring, Summer, Autumn; see Tables 4-7). The nine individuals were then categorized by region (Azores/Canary Islands and Cabo Verde) and by tagging year. A Kruskal-Wallis test was applied to determine whether significant differences existed across the groups. This test was chosen because it is more appropriate than analysis of variance (ANOVA) when dealing with smaller datasets that do not follow a normal distribution (Guo, Zhong & Zhang, 2013). A p-value below 0.05 ($p < 0.05$) indicates a statistically significant difference, while a p-value equal to or greater than 0.05 ($p \geq 0.05$) suggests no significant difference. Due to incomplete data, the spring season was excluded from the analysis. Ambient temperature, internal temperature, and depth were treated as dependent variables, with region, season, and year as independent variables. All analyses were conducted using the R programming language.

Table 4. Seasonal summary of minimum, maximum, and mean values for internal temperature, ambient temperature, and depth. Data are presented for winter across each individual.

Winter ID ref.	Ambient T. Min (°C)	Internal T. Min (°C)	Depth Min (m)
BET1	7.02	12.1	11.48
BET2	10.68	11.9	0.5
BET3	5.76	10.25	0
BET4	8.45	16.58	0
BET5	7.9	16.16	15
BET6	12.4	19.22	1.5
BET7	NA	NA	NA
BET8	NA	NA	NA
BET9	NA	NA	NA

Winter ID ref.	Ambient T. Max (°C)	Internal T. Max (°C)	Depth Max (m)
BET1	22.36	24.62	915.27
BET2	24.06	24.1	780
BET3	27.59	26.95	1040
BET4	28.1	36.23	513
BET5	28.8	37.06	450.5
BET6	17.9	24.72	341
BET7	NA	NA	NA
BET8	NA	NA	NA
BET9	NA	NA	NA

Winter ID ref.	Ambient T. Mean (°C)	Internal T. Mean (°C)	Depth Mean (m)
BET1	17.35	19.35	148.2
BET2	18.86	19.38	116.66
BET3	20.99	21.88	107.92
BET4	18.15	26.28	140.48
BET5	17.42	25.69	163.18
BET6	16.32	23.15	76.8
BET7	NA	NA	NA
BET8	NA	NA	NA
BET9	NA	NA	NA

Table 5. Seasonal summary of minimum, maximum, and mean values for internal temperature, ambient temperature, and depth. Data are presented for summer across each individual.

Summer ID ref.	Ambient T. Min (°C)	Internal T. Min (°C)	Depth Min (m)
BET1	11.87	15.66	10.32
BET2	8.16	13.85	0
BET3	7	13.6	0
BET4	NA	NA	NA
BET5	NA	NA	NA
BET6	13	19.82	2
BET7	6.9	13.41	0.5
BET8	12.2	20.6	0.5
BET9	11.4	16.88	3

Summer ID ref.	Ambient T. Max (°C)	Internal T. Max (°C)	Depth Max (m)
BET1	23.53	26.18	575.76
BET2	23.77	27.25	1141
BET3	26.95	27.05	1073
BET4	NA	NA	NA
BET5	NA	NA	NA
BET6	24.9	31.72	396.5
BET7	26	32.51	1343.5
BET8	24.4	32.8	471.5
BET9	25.9	31.38	610.5

Summer ID ref.	Ambient T. Mean (°C)	Internal T. Mean (°C)	Depth Mean (m)
BET1	19.51	22.89	113.51
BET2	18.8	21.66	116.66
BET3	20.16	21.05	134.08
BET4	NA	NA	NA
BET5	NA	NA	NA
BET6	21.02	27.85	54.57
BET7	19.95	26.47	155.56
BET8	18.9	27.3	88.89
BET9	19.42	24.91	144.18

Table 6. Seasonal summary of minimum, maximum, and mean values for internal temperature, ambient temperature, and depth. Data are presented for spring across each individual.

Spring ID ref.	Ambient T. Min (°C)	Internal T. Min (°C)	Depth Min (m)	Spring ID ref.	Ambient T. Max (°C)	Internal T. Max (°C)	Depth Max (m)	Spring ID ref.	Ambient T. Mean (°C)	Internal T. Mean (°C)	Depth Mean (m)
BET1	9.29	14.88	11.57	BET1	21.11	24.74	779.81	BET1	18.17	20.96	112.05
BET2	8.92	15.1	0	BET2	24.06	23.55	903.5	BET2	18.99	20.51	75.73
BET3	6.78	10.25	0	BET3	27.59	25.25	883.5	BET3	19.05	19.63	88.89
BET4	NA	NA	NA	BET4	NA	NA	NA	BET4	NA	NA	NA
BET5	NA	NA	NA	BET5	NA	NA	NA	BET5	NA	NA	NA
BET6	NA	NA	NA	BET6	NA	NA	NA	BET6	NA	NA	NA
BET7	NA	NA	NA	BET7	NA	NA	NA	BET7	NA	NA	NA
BET8	NA	NA	NA	BET8	NA	NA	NA	BET8	NA	NA	NA
BET9	NA	NA	NA	BET9	NA	NA	NA	BET9	NA	NA	NA

Table 7. Seasonal summary of minimum, maximum, and mean values for internal temperature, ambient temperature, and depth. Data are presented for autumn across each individual.

Autumn ID ref.	Ambient T. Min (°C)	Internal T. Min (°C)	Depth Min (m)	Autumn ID ref.	Ambient T. Max (°C)	Internal T. Max (°C)	Depth Max (m)	Autumn ID ref.	Ambient T. Mean (°C)	Internal T. Mean (°C)	Depth Mean (m)
BET1	11.59	14.88	11.08	BET1	23.31	26.89	548.42	BET1	21.63	23.45	54.86
BET2	11.64	13.95	0.5	BET2	23.81	27.2	914	BET2	22.22	23.03	49.26
BET3	10.97	13.4	0	BET3	25.78	26.85	763.5	BET3	22.27	22.84	52.99
BET4	5	13.13	0	BET4	26.5	34.63	1486.5	BET4	19.93	28.06	106.23
BET5	9.5	17.76	1.5	BET5	28.6	36.86	590.5	BET5	19.86	28.13	108.14
BET6	7.3	14.12	1.5	BET6	24.8	31.62	1129	BET6	18.07	24.89	108.77
BET7	6.05	12.56	0.5	BET7	26.1	32.61	1488.5	BET7	18.64	25.15	177.68
BET8	NA	NA	NA	BET8	NA	NA	NA	BET8	NA	NA	NA
BET9	12.2	17.68	2.5	BET9	27.2	32.68	578.5	BET9	19.4	24.89	162.45

3.4. Environmental data (temperature and oxygen) extraction

Modelled ambient temperature data throughout the water column were obtained from the global ocean biogeochemistry model outputs provided by the Copernicus Marine Environment Monitoring Service (CMEMS; http://marine.copernicus.eu/) for the period from 2005 to 2006. This database covers the Atlantic Ocean and includes temperature profiles extending from the surface (0 m) to a depth of 2000 m. To address spatial uncertainties, temperature data were averaged over a grid of 1.25° latitude by 0.75° longitude (5 × 3 pixel area) centred on each tuna's geolocation. This method ensured a more conservative representation of ambient temperature at each position.

To determine the horizontal limits of the OMZ, modelled dissolved oxygen concentrations at a depth of 100 m were also extracted from the same CMEMS model. Following the definitions used by Vedor et al. (2021) to analyse horizontal movements, the OMZ area in the ETA was defined as the waters above the OMZ where dissolved oxygen concentrations can drop below 3.5 ml O_2 l^{-1} at depths shallower than 100 m, which is typically where the thermocline is found in this area. This threshold was chosen because studies like Prince et al. (2010) and Stramma et al. (2012) have shown that this DO level can induce stress in large tropical pelagic fishes (Vedor et al., 2021).

3.5. Heat budget model

To explore the thermoregulatory mechanisms of bigeye tuna, a heat budget model (Holland & Sibert, 1994) was adapted and applied. The model indicates that heat loss and gain are proportional to the difference between body and ambient temperatures, as demonstrated in Equation 1:

$$\frac{dTb}{dt} = \lambda\,(Ta - Tb) + \dot{T}m \quad (1)$$

where λ is the whole-body heat transfer coefficient (s^{-1}), $\dot{T}m$ is the rate of temperature change owing to metabolic heat production ($℃s^{-1}$) (Neill, Chang & Dizon, 1976), Ta is the ambient temperature (℃), and Tb is the body (peritoneal cavity) temperature (℃).

In addition, λ can be transformed into Equation 2, as follows Holland and Sibert (1994) and Aoki et al. (2020) where K is the body bulk effect (s^{-1}) and w is the physiological effect (s^{-1}).

$$\lambda = \kappa + w \tag{2}$$

To apportion λ into its components of k and w, the relationships between k and body size were estimated based on the data that recorded cooling after landing by Hino et al. (2021). $\dot{T}m$ and w were also set to 0 in Equations 1 and 2 owing to the fish's death.

K was estimated for each individual following the Equation 3, where BW is body weight in kg (Kitagawa et al., 2006).

$$\kappa = 9.234 \times 10^{-4} \times BW^{-0.554} \tag{3}$$

This suggests that larger individuals experience less heat loss to the surrounding water due to their lower surface-to-volume ratio. As body size increases, the relative surface area exposed to the environment decreases compared to the volume, which reduces the rate of heat exchange. This physical characteristic makes larger fish more efficient at retaining body heat, helping them maintain stable internal temperatures in variable thermal environments (Malte et al., 2007).

As the Equation 3 requires body weight as an input, the fork length (FL) of the fish was converted to body weight (BW) using the length-weight relationships described by Carroceda and Colmenero (2016). The study utilized a non-linear model, which more accurately captures the relationship between length and weight, particularly across a wide range of fish sizes, including larger individuals. The non-linear equation is expressed as:

$$BW = a \times FL^{b} \tag{4}$$

where a and b are parameters estimated from their dataset. This approach allows for precise conversion of fork length measurements into body weight, accounting for the natural variability observed in size-weight dynamics. The specific model applied in this study was:

$$BW = 6.0568 \times 10^{-5} \times FL^{2.79379} \quad (5)$$

Holland and Sibert (1994) reported that the body temperature (Tb) of bigeye tuna remains relatively stable during vertical movements, with no significant differences between warming (ascents) and cooling (descents), and that the $\dot{T}m$ did not differ significantly between these phases. This stability is probably due to the species' thermal inertia, which enables bigeye tuna to maintain consistent internal temperatures despite rapid external changes.

At the end, to calibrate the model parameters specifically for bigeye tuna, three individuals (ID no. 0390474, 0390491 and 0390503) equipped with internal temperature sensors were used. These datasets allowed us to determine the specific values (average values) for all Equation 1. Once identified, Equation 1 was applied to predict the internal temperature (Tb) of six individuals that had only ambient temperature (Ta) values. All model adaptations, predictions, and statistical analyses were performed using the R programming language.

3.6. Equation and model's performance

The performance of the equation and the model was evaluated by comparing the predicted temperatures with the recorded temperatures from the tag. To assess accuracy and precision, several statistical measures were used:

Root Mean Squared Error (RMSE)

RMSE measures the average size of the prediction errors, providing an overall idea of how well the model performs (Hyndman & Koehler, 2006). It is calculated using the formula:

$$RMSE = \sqrt{\frac{1}{n}\sum_{i=1}^{n}(Tpred,i - Tobs,i)^2} \quad (6)$$

where $Tpred,i$ is the predicted temperature, $Tobs,i$ is the observed temperature, and n is the number of observations. A lower RMSE value indicates better model performance.

Mean Absolute Error (MAE)

MAE calculates the average of the absolute differences between the predicted and observed temperatures, offering a straightforward measure of accuracy (Hyndman & Koehler, 2006). The formula is:

$$MAE = \frac{1}{n}\sum_{i=1}^{n} | Tpred, i - Tobs, i |$$

(7)

where $Tpred, i$ is the predicted temperature, $Tobs, i$ is the observed temperature, and n is the total number of observations. A lower MAE value reflects a more accurate model by averaging the absolute errors between predictions and observations.

Pearson Correlation Coefficient (r)

This statistic measures the strength and direction of the relationship between predicted and observed temperatures (Benesty et al., 2009). It is calculated as:

$$r = \frac{\sum_{i=1}^{n}(Tpred, i - \bar{T}pred, i)(Tobs, i - \bar{T}obs, i)}{\sqrt{\sum_{i=1}^{n}(Tpred, i - \bar{T}pred, i)^2 (Tobs, i - \bar{T}obs, i)^2}}$$

(8)

where $\bar{T}pred$ and $\bar{T}obs$ are the averages of the predicted and observed temperatures. Values close to 1 indicate a strong positive correlation, meaning the predictions closely match the observations.

Linear Regression Analysis

Linear regression was used to explore the relationship between predicted and observed temperatures, showing how well the predictions match the actual data (Montgomery, Peck & Vining, 2012). The regression equation is:

$$Tobs, i = \beta 0 + \beta 1\, Tpred, i + \epsilon\, i$$

(9)

where $\beta 0$ is the intercept, $\beta 1$ is the slope, and $\epsilon\, i$ is the error term. The analysis helps evaluate the bias (the difference between the average prediction of the model and the true observed values), the consistency (how well the predictions match observed values), and the overall fit of the model, indicated by how much of the observed temperature variance is explained by the predictions. These statistical measures together provided a comprehensive evaluation of the model's ability to accurately predict temperatures, highlighting its strengths and areas for improvement (James et al., 2021).

4. Results

Between 2005 and 2022, nine bigeye tuna were tagged at two different locations in the North Atlantic Ocean (Tables 1 and 2). Their geo-located tracks (latitude-longitude positions) were successfully obtained and subsequently mapped (Figure 9). Complete archival data were recovered from five individuals (IDs 0390474, 0390491, 0390503, 196133, and 84600) due to the physical recovery of their tags, allowing extraction of high-resolution data at shorter intervals (sixteen and three seconds). This increased the accuracy of the measurements and provided continuous time series data without temporal gaps. The time series for the remaining individuals were sampled at varying intervals (one to seven minutes) and contain some temporal gaps.

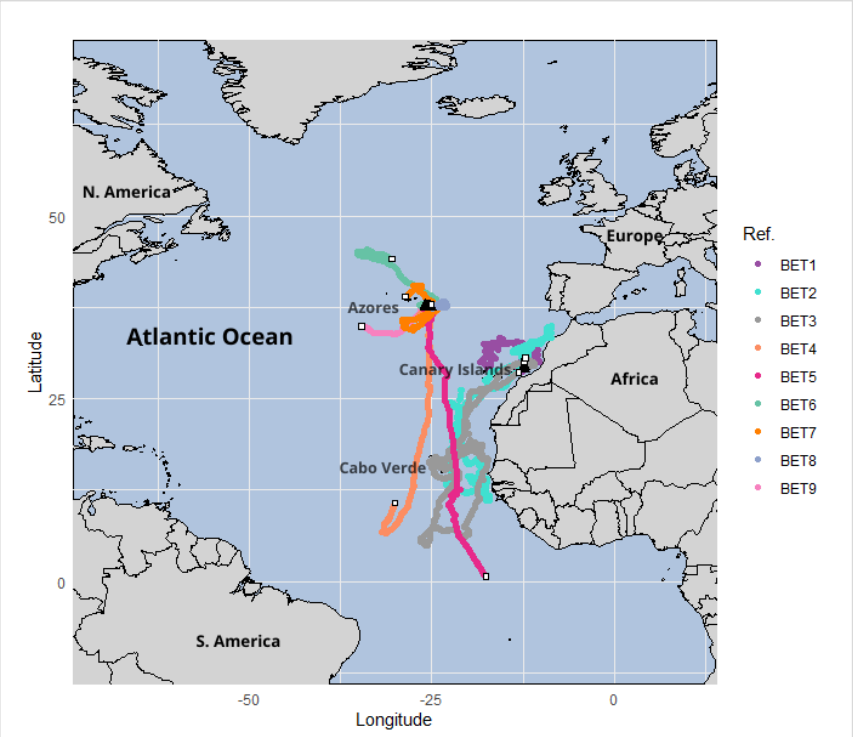

Figure 9. Map showing the general movement patterns of nine geo-located bigeye tuna used in this study. The black triangles represent the tagging sites, and the white quadrilaterals represent the endpoints of each track.

4.1. Data overview

Depth, internal temperature, and ambient temperature data of BET1, BET2 and BET3 were plotted against datetime to explore the temporal patterns and relationships among these variables. These visualizations provided an initial overview of the data and for the purpose of comparison, a specific period was selected: January 20, 2006, at 00:00:00 to January 25, 2006, at 00:00:00. During this period, their data was analysed in detail (Figure 10).

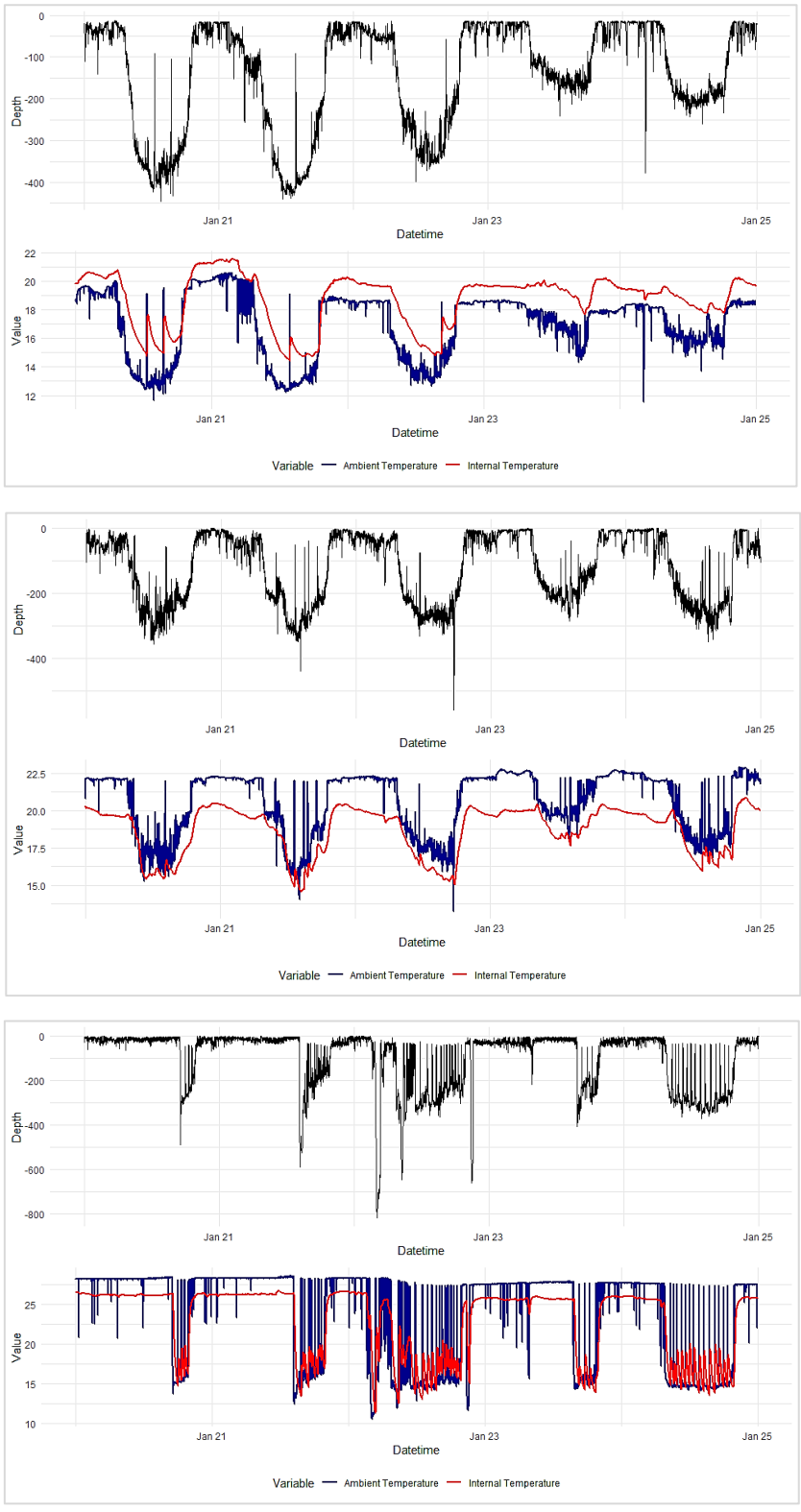

Figure 10. Depth profile (top) and internal (red) and ambient (blue) temperatures for 3 tagged tuna from January 20, 2006, to January 25, 2006. (a) BET1 (b) BET2 (c) BET3.

The data from the first individual (Figure 10, a) showed expected patterns, with internal temperatures consistently higher than ambient temperatures, reflecting normal physiological conditions (Brill & Lutcavage, 2001; Dickson & Graham, 2004). However, in

the other two individuals (Figure 10, b and c), an unusual pattern emerged: the internal temperatures were lower than the ambient temperatures for extended periods. This phenomenon is physiologically improbable for small fish, as internal body temperatures should generally be equal to or higher than the surrounding water temperature, except briefly after events such as deep dives or ingestion of prey (Carey & Teal, 1966).

Upon further investigation with the tag manufacturer, it was determined that this anomaly was associated with a known issue affecting Mk9. In 2008, a problem with the Mk9 sensor stalks was identified and affected tags used between 2003 and 2008. The primary causes of the drift, that could range from 0 to over 4°C, were identified as follows: Defects in the epoxy filling of some tags allowed saltwater to infiltrate and reach the sensor wires, resulting in an increase in the recorded external temperature. Additionally, the thermistors used in the sensor stalks experienced performance degradation due to prolonged exposure to saltwater conditions.

4.2. Ambient temperature data and model performance

This identification of sensor issues set the stage for further analyses and adjustments to ensure the reliability of the data. The next step involved extracting ambient temperature values using the model described in the Materials and Methods section. To assess the model's performance, the ambient temperature data recorded by the BET1' tag - chosen due to its normal patterns where internal temperatures were consistently higher than the ambient temperatures - were compared against the ambient temperatures predicted by the model using the entire available dataset.

The analysis evaluated the model's accuracy through key statistical metrics. The Root Mean Squared Error (RMSE) between the modelled and observed ambient temperatures was 1.59°C, and the Mean Absolute Error (MAE) was 1.28°C. Descriptive statistics revealed a mean recorded temperature of 18.99°C with a standard deviation of 3.04°C, while the modelled temperatures had a slightly lower mean of 18.56°C and a standard deviation of 2.88°C. The Pearson correlation coefficient was strong at 0.906. Linear regression yielded an intercept of 2.933 and a slope of 0.896, with an R-squared value of 0.821, indicating that the model explained approximately 82.1% of the variance in the recorded temperatures. The residual standard error was 1.20°C.

Figure 11 (below) visually compares the recorded (blue line) and modelled (black line) ambient temperatures throughout datetime.

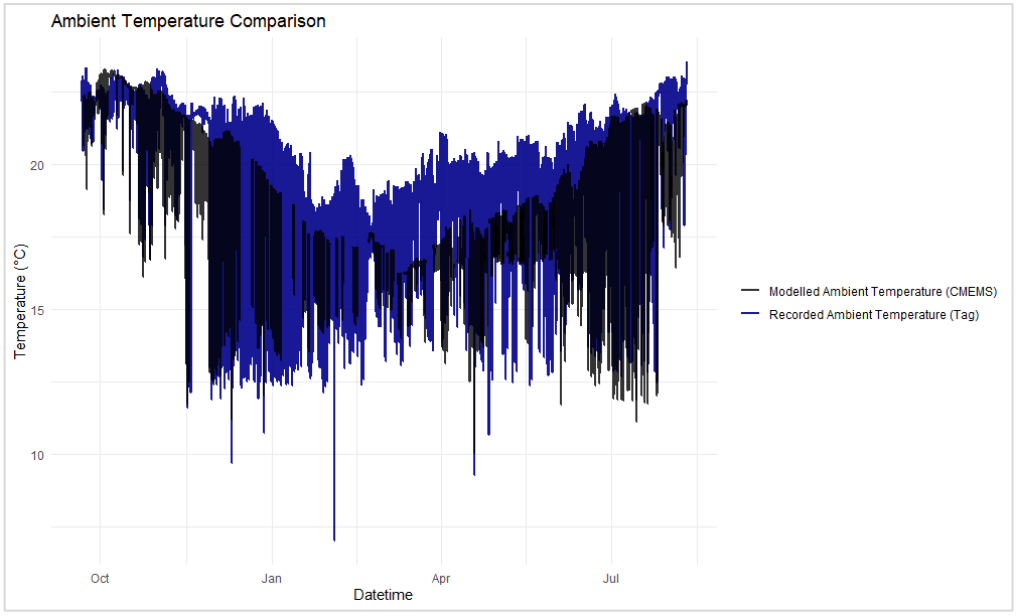

Figure 11. Comparison of recorded ambient temperatures (blue) and modelled ambient temperatures (black) over time.

4.3. Estimation of the body bulk effect (κ) and heat transfer coefficient (λ)

The body weights of the individuals were calculated from fork length using the length-weight relationship defined in Equation 5. For consistency, the calculated body weights (Table 8) were rounded to two decimal places and were crucial for estimating the body bulk effect (κ) according to Equation 3. Since the physiological effect (w) was set to 0 due to the fish's death, λ was directly equated to κ.

Table 8. Fork length (FL) and corresponding estimated body weight (BW) for each tagged bigeye tuna.

ID	FL (cm)	BW (kg)
0390474	87	15.88
0390491	61	5.89
0390503	62	6.16
181756	145	66.17
84600	187	134.68
85009	189	138.74
196132	167	98.19
196133	162	90.19
202884	191	142.88

To determine the rate of temperature change ($\frac{dTb}{dt}$), the ambient temperature and body temperature were extracted by averaging the Ta and Tb measurements from BET1, the only individual with reliable temperature data.

The heat transfer coefficient (λ) for BET1 was calculated to be 0.000199 s^{-1} and the rate of temperature change ($\frac{dTb}{dt}$) to be -0.000496. These values were directly used in the final and reformulated equation to predict the internal body temperature (Tb):

$$Tb = Ta - (\frac{\frac{dTb}{dt}}{\lambda}) \quad (10)$$

4.4. Body temperature prediction and model performance

To evaluate the accuracy of the predictive model for internal temperatures in tagged bigeye tuna, the predicted internal temperatures were compared with the actual recorded temperatures from the tag, just using BET1 data.

The Root Mean Squared Error (RMSE) was 1.34°C, and the Mean Absolute Error (MAE) was 1.07°C. The recorded temperatures had a mean of 21.47°C with a standard deviation of 2.71°C, while the predicted temperatures shared the same mean but exhibited a slightly higher standard deviation of 3.03°C. The Pearson correlation coefficient was 0.897, indicating a strong correlation. Linear regression analysis produced an intercept of 4.310 and a slope of 0.799, suggesting that the predictions are, on average, offset by 4.31°C and that for every unit increase in predicted temperature, the actual temperature rises by 0.799 units. The model's R-squared value of 0.804 indicates that approximately 80.4% of the variance in recorded temperatures is accounted for by the predicted values. The residuals ranged from -4.08°C to 6.39°C, with a standard error of 1.19°C.

Figure 12 visually compares the recorded and predicted internal temperatures over time.

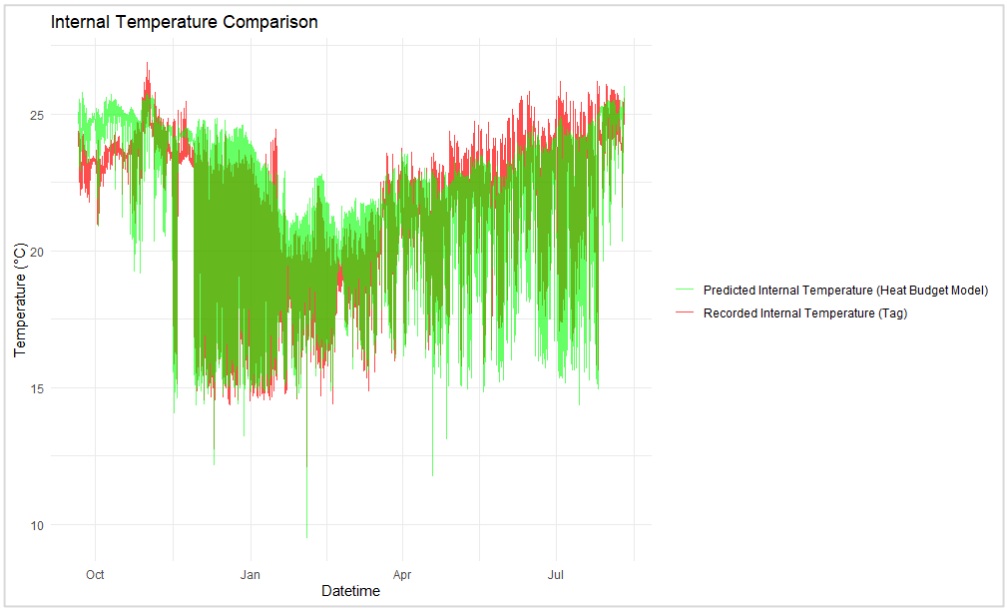

Figure 12. Comparison of recorded internal temperatures (red) and predicted internal temperatures (green) over time.

4.5. Body temperature prediction using modelled ambient temperatures and model performance

The heat budget model was recalibrated using data from three individuals (BET1, BET2, and BET3), this time using estimated ambient temperatures as Ta. This approach allowed for a direct comparison between the calibration using three fish with modelled ambient temperatures and the initial calibration utilizing only BET1 data with recorded values, to determine which method provided more accurate internal temperature predictions.

For each fish, modelled ambient temperatures (Ta) and recorded body temperatures (Tb) were averaged to calculate the rate of temperature change ($\frac{dTb}{dt}$). The heat transfer coefficients (λ) were also determined for each tuna: 0.000199 s^{-1} for BET1, 0.000345 s^{-1} for BET2, and 0.000337 s^{-1} for BET3. The final λ value used in the prediction model was the average of these individual coefficients. With these parameters, Equation 10 was applied to predict the internal body temperature (Tb).

To assess the accuracy of the model, the predicted internal temperatures were compared with the internal temperatures recorded by the tags (Figure 13), and errors were quantified. For BET1, the RMSE was 2.64°C, and the MAE was 2.15°C. The Pearson correlation coefficient was 0.740. Linear regression analysis showed a slope of 0.444, with an R-squared value of 0.547, meaning the model explained 54.7% of the variability in internal

temperature. For BET2, the RMSE was 2.61°C, and the MAE was 2.12°C. The Pearson correlation coefficient was 0.757. The linear regression had a slope of 0.658, and the R-squared value of 0.572 indicated that 57.2% of the variance in internal temperature was accounted for by the model. For BET3, the RMSE was 3.27°C, and the MAE was 2.88°C, with a Pearson correlation coefficient of 0.850. The linear regression slope was 0.468, and the R-squared value was 0.727, showing that the model explained 72.7% of the variability in internal temperature, the highest among the three individuals.

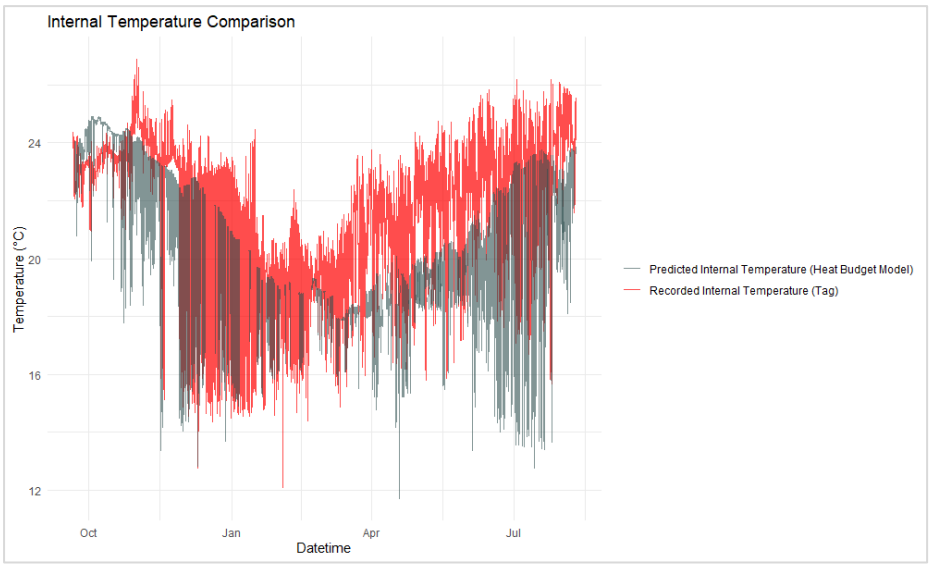

a

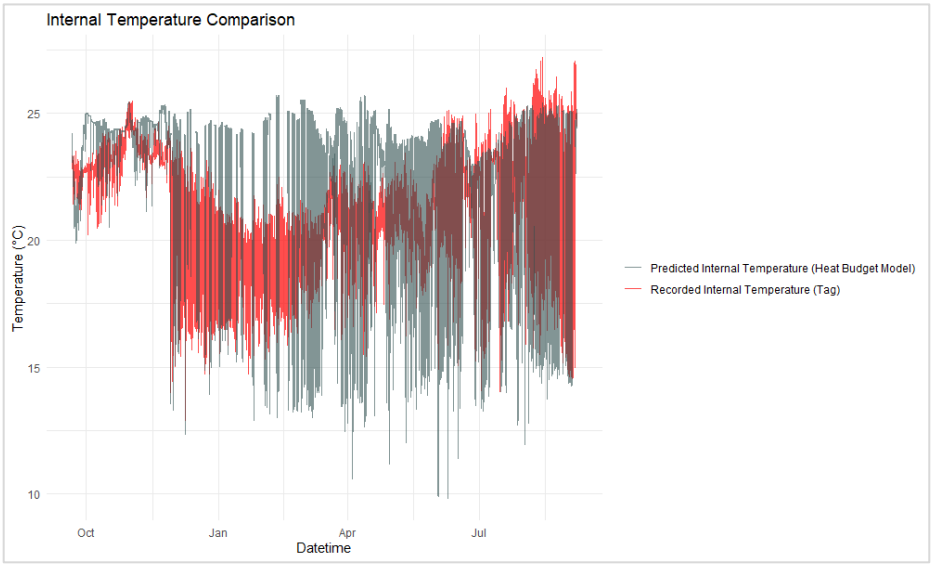

b

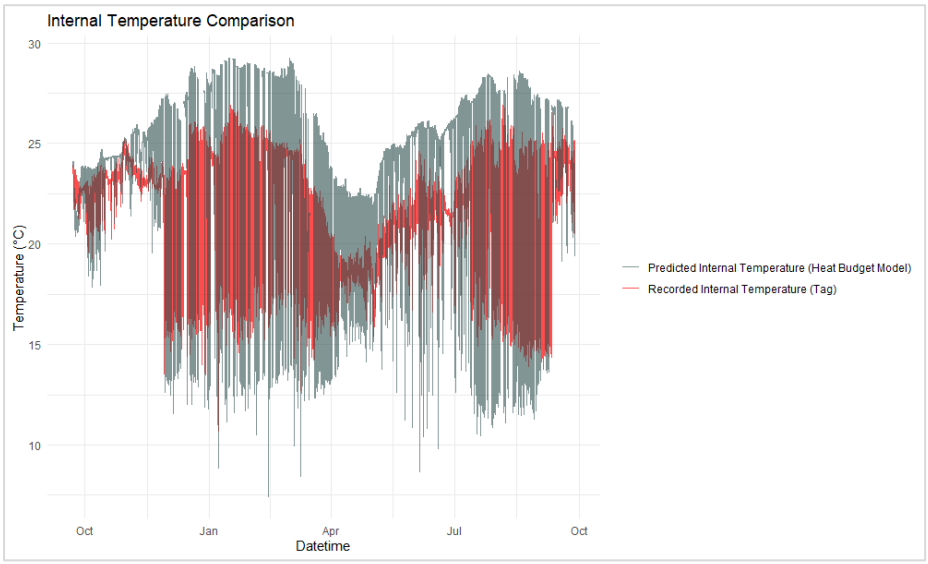

c

Figure 13. Comparison of recorded internal temperatures (red) and predicted internal temperatures (grey) over time. (a) BET1 (b) BET2 (c) BET3.

When considering the three individuals (BET1, BET2, and BET3), the average RMSE was 2.843°C, the MAE was 2.388°C, and the average Pearson correlation coefficient was 0.782. The average linear regression slope across the three individuals was 0.523. Additionally, the average R-squared value was 0.615, meaning that about 61.5% of the variability in the recorded temperatures can be explained by the predicted temperatures.

4.6. Best model

To evaluate which model better predicts internal body temperatures, Model 1 and Model 2 was compared based on their errors and statistical measures. Model 1 used data from BET1, where both ambient and internal temperatures were recorded directly by the tag. In contrast, Model 2 used data from three individuals (BET1, BET2, and BET3), but the ambient temperatures were estimated rather than being recorded directly. Model 1 demonstrated better performance. Specifically, Model 1's RMSE was 1.34°C, which is notably lower than Model 2's average RMSE of 2.84°C. Similarly, Model 1's MAE was 1.07°C, while Model 2 had an average MAE of 2.38°C. The Pearson correlation coefficient for Model 1 was 0.897, higher than Model 2's coefficient of 0.782.

The linear regression analysis shows that Model 1 has an R-squared value of 0.804. This means that about 80.4% of the variability in the recorded temperatures can be explained by the temperatures predicted by this model. On the other hand, Model 2 has a lower R-squared value of 0.727.

Following the selection of the best model and its parameters, and the achievement of the first objective, Equation 1 was used to predict the internal temperatures of BET3 through BET9, thus achieving the second and final objective. A variety of analyses were then conducted to explore the behaviour, responses to ambient variables, habitat preferences, spatial distribution, and movement patterns of all individuals, with the aim of answering the main questions of this study.

4.7. Sea Surface Temperature

A preliminary and exploratory analysis was conducted to examine variations in Sea Surface Temperature (SST) between two groups based on their migration patterns. The first group (Figure 14, a) includes individuals that remained in the higher latitudes of the North Atlantic, particularly around the Canary Islands and the Azores, while the second group (Figure 14, b) consists of tuna that migrated southward toward Cabo Verde or beyond.

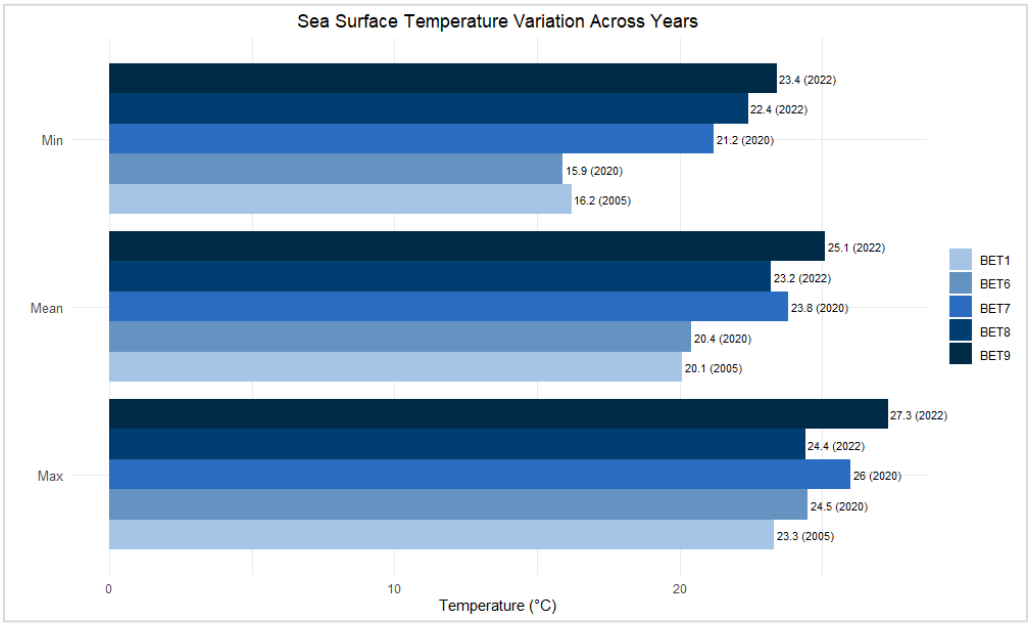

a

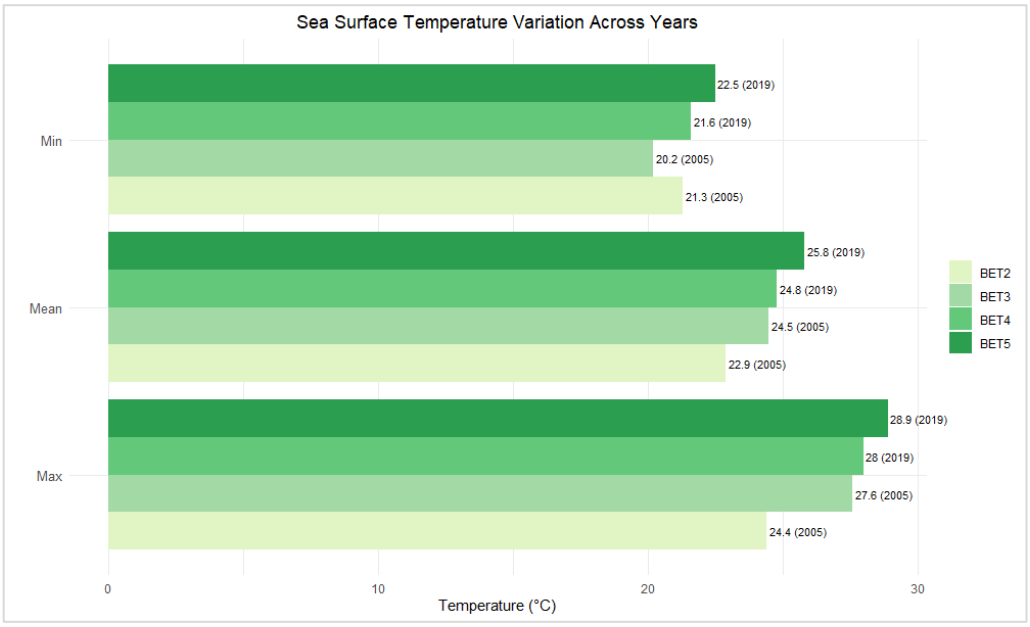

b

Figure 14. Minimum, mean, and maximum sea surface temperature recorded across different years. The y-axis shows SST metrics, and the x-axis represents temperature values (°C), with different colours corresponding to individual tuna ref. (a) Tuna that remained in higher latitude zones throughout the tracking period. (b) Tuna that migrated southward.

The comparison of SST values within each group of tuna highlights significant changes over time, even within similar latitudes. For those that remained in higher latitudes, particularly around the Canary Islands and the Azores, a clear warming trend is evident. BET1, the only tuna recorded in 2005, serves as a reference point for this group. The minimum SST for BET1 was 16.2°C, the mean was 20.1°C, and the maximum reached 23.3°C. These values represent relatively cooler waters from earlier years.

In contrast, the more recent data from BET4-9 (collected in 2019, 2020 and 2022) reveal substantial increases in SST. For instance, the minimum temperature recorded by BET6 in 2020 was 21.2°C, which is 5°C higher than BET1's minimum in 2005. The mean SST also showed a significant increase, reaching 23.8°C, up by 3.7°C compared to 2005. Similarly, the maximum temperature recorded was 26°C, representing a 2.7°C increase from BET1.

This warming trend continued in 2022, with BET9 recording a minimum SST of 23.4°C, marking a substantial rise of 7.2°C compared to 2005, while the mean and maximum temperatures reached 25.1°C and 27.3°C, respectively, both considerably higher than the values recorded by BET1. Overall, the individuals in this group demonstrate that SST has increased considerably, with the most pronounced rise observed in the minimum and maximum temperatures. The increase in SST from 2005 to 2022 reflects a significant shift in the thermal environment of the northern waters.

A similar, though less dramatic, pattern of SST increase is seen in the group of tuna that migrated to lower latitudes, toward Cabo Verde and beyond. In 2005, BET3 recorded a minimum SST of 21.3°C, a mean of 22.9°C, and a maximum of 27.6°C. These values were already higher than those experienced by the tuna that stayed in northern waters during the same period. However, by 2019, BET4 and BET5 both encountered even warmer conditions. The minimum SST recorded by BET4 rose to 22.5°C, a 1.2°C increase compared to BET3 in 2005. Although, those temperatures were not recorded at summer, what could have masked important factors that would have contributed to a more comprehensive analysis and probably even recorded higher values. Similarly, the mean SST increased by 2.9°C, reaching 25.8°C, while the maximum SST peaked at 28.9°C, a 1.3°C rise from 2005. BET5's values were nearly identical, confirming the consistency of the warming trend in this southern region.

4.8. Seasonal patterns

Sea temperature is widely recognized as one of the most critical environmental factors influencing fish behaviour and physiology, as well as a key driver of their seasonal migration patterns and habitat distribution (Tittensor et al., 2010; Kumar, Pillai & Manjusha, 2014). By focusing on a preliminary analysis of the relationships between internal temperature, water temperature, and depth across seasons - excluding spring due to incomplete data - the findings from the Kruskal-Wallis test are presented below.

Although most of the results were not statistically significant and the sample was small, they still revealed patterns that provide insight into the environmental conditions the tuna experienced in different seasons. Starting with water temperature, the analysis showed no significant differences across years or regions in winter and summer. For winter, the lack of variation in temperature by year or region suggests a certain consistency in the environment during this season, regardless of the year or location. Similarly, in summer, the water temperature remained stable, showing no detectable shifts across years or regions. However, the lack of summer data for the two individuals that migrated south in 2019 (BET4 and BET5), who experienced higher temperatures, might have hidden important details that could have made the analysis more complete. As the analysis moved into autumn, a subtle shift began to emerge. Although not statistically significant, the results suggested some variability, with both year and region approaching significance.

A similar pattern emerged for internal temperature. Like water temperature, the tuna's internal temperature remained stable during winter and summer, showing no significant differences across years or regions. In both seasons, the internal temperature closely mirrored the surrounding environmental conditions, regardless of the year or location. However, autumn told a different story. The test results for this season nearly reached significance, suggesting there might be subtle variations in internal temperature, possibly linked to changes in the environment or the tuna's behaviour during this period.

The depth data followed a similar pattern. In winter and summer, depth did not vary significantly by either year or region, indicating that the tuna consistently used similar depths during these seasons. Yet again, autumn showed more variability. Though not significant, the results indicated that both year and region could play a role in how deep the tuna dive during this season.

Detailed monthly movement patterns of all individuals are provided in the Supplementary Materials (Figure S1), illustrating their seasonal distribution.

4.9. Ambient temperature, internal temperature and depth preferences

Bigeye tuna habitat selection and preferences are influenced by various factors, including physiological limitations (Brill et al., 1994), biotic interactions and abiotic oceanographic conditions (Marcinek et al., 2001). To explore these influences, vertical profiles of each deployment were generated, such as time-at-depth and time-at-temperature.

a

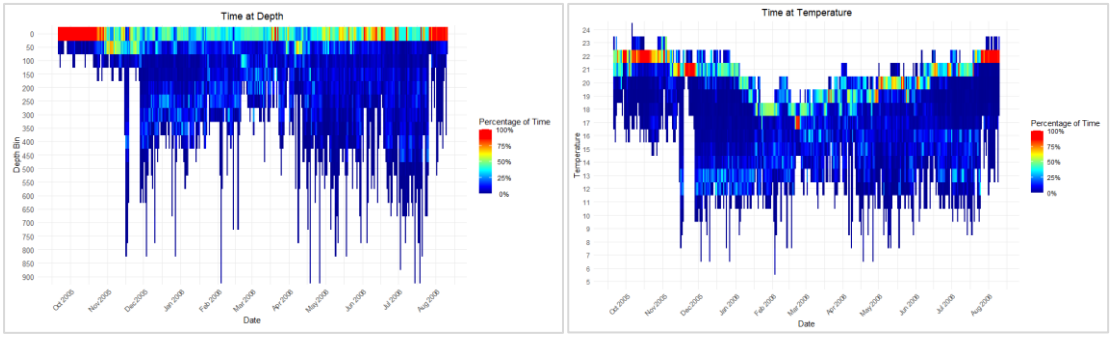

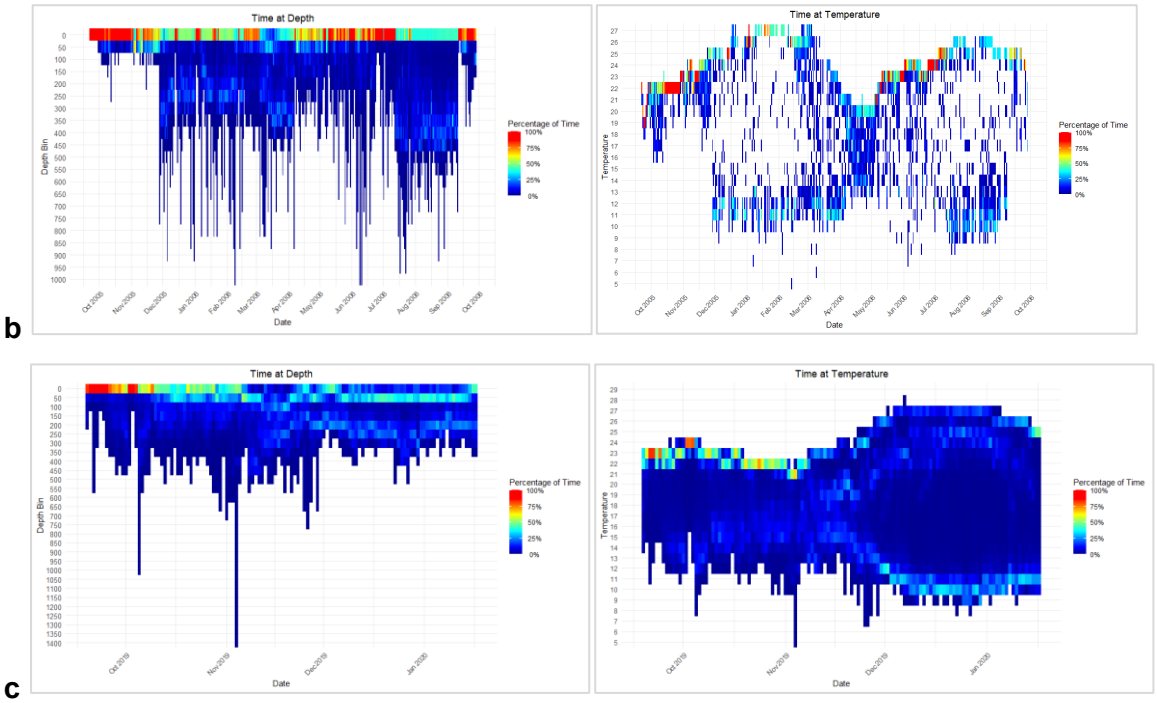

Figure 15. Time spent at different depths (left) and temperatures (right). In the depth graphs, the y-axis shows depth bins (in meters), while in the temperature graphs, the y-axis shows temperature bins (in degrees). The x-axis in both represents the date. The colour scale indicates the percentage of time tuna spent at each depth or temperature bin, with red representing 100% of the time and dark blue indicating 0%. (a) BET1, (b) BET3, (c) BET4.

Bigeye tuna exhibit distinct preferences for ambient water temperatures, which are closely linked to their vertical movement patterns. It is also hypothesized that these vertical excursions enable the tuna to rewarm after spending approximately an hour in colder deep water (Schaefer and Fuller, 2002). Studies show that they typically remain in deeper waters during the day, where ambient temperatures can drop to around 10°C (Musyl et al., 2003; Hanamoto, 1987). At night, they ascend to the surface, where the water is warmer, generally between 20°C and 25°C (Josse et al., 1998). In this study, the lowest ambient temperature recorded was 5°C for BET4, while the highest was 28.8°C for BET5. In comparison, Evans et al. (2008) reported a minimum of 2.5°C and a maximum of 31.9°C for the same species, and Aoki et al. (2020) recorded a maximum of 32.2°C. For optimal conditions, Bigeye tuna is known to prefer a broader and cooler temperature range of 14.7°C to 23.2°C. In contrast, yellowfin tuna thrives in warmer temperatures between 20.3°C and 25.5°C, while skipjack tuna favor even warmer temperatures, ranging from 19.3°C to 27.9°C (Norelli, Die & Moffat, 2022).

Individuals such as BET3 and BET4 (Figure 15, b and c) and BET5 and BET2 (see Figure S2, a and b) exhibited a clear trend of spending more time in cooler waters during their southern migrations compared to those that remained in higher latitudes (see Figure 15, a). Initially, while in the Azores and Canary Islands region, they primarily occupied warmer

waters. However, as they migrated southward, especially near Cabo Verde, a noticeable shift toward cooler waters occurred. This trend was even more pronounced in recent years, as demonstrated by BET4 and BET5, who were tagged in 2019. In contrast, individuals from 2005 who followed similar migration paths occupied warmer waters. Figure 16 highlights these changes through the most frequently used temperature bins, reflecting variations in habitat preference by latitude (see Figure S3 in Supplementary Materials for details on other individuals).

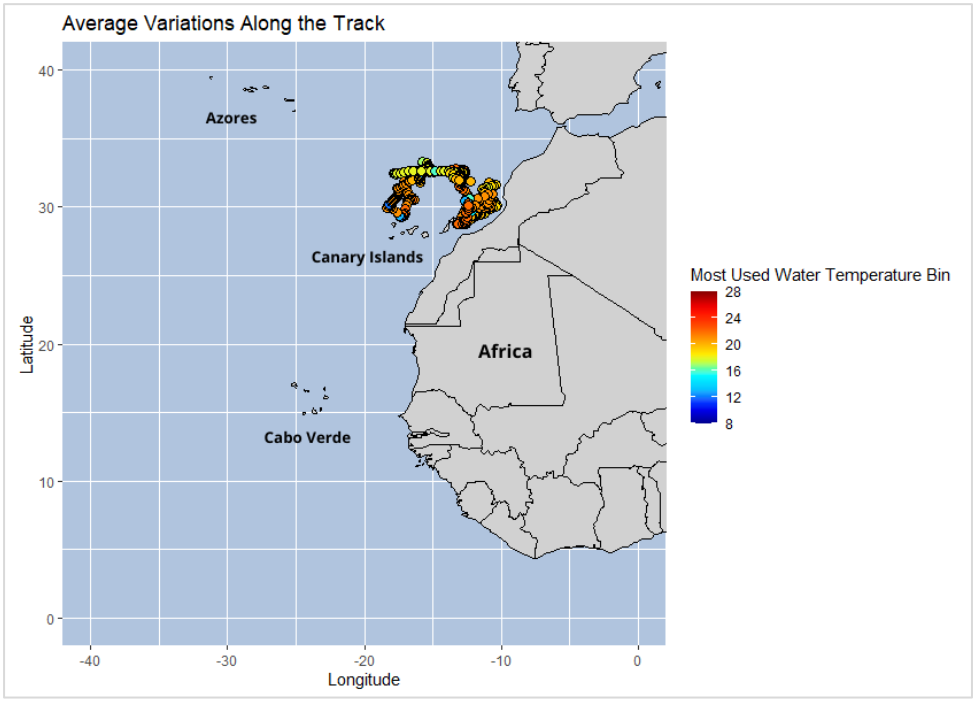

a

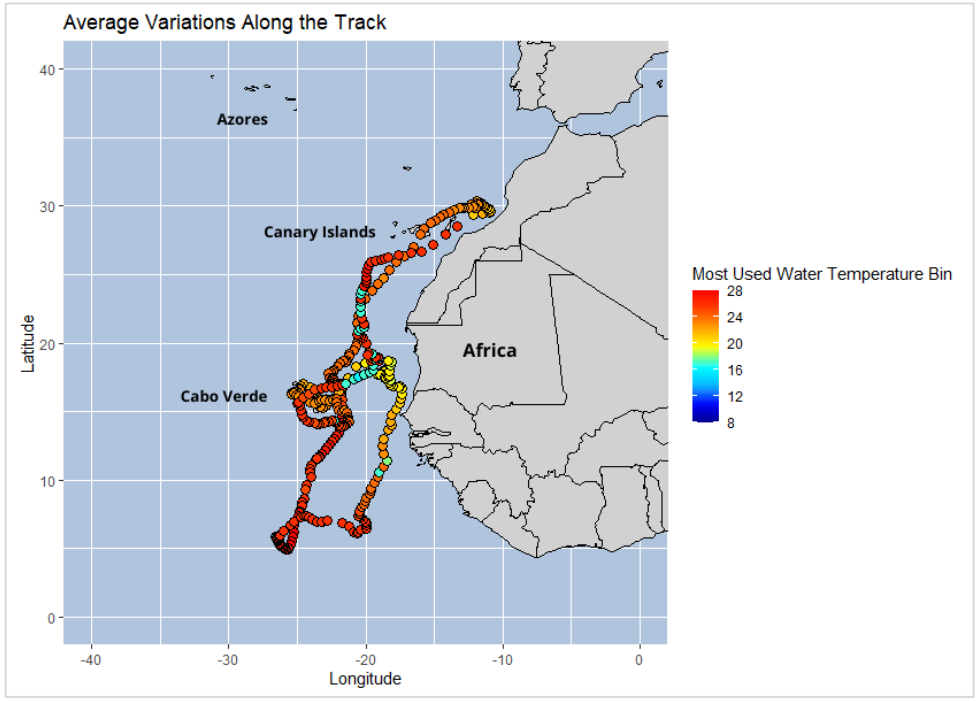

b

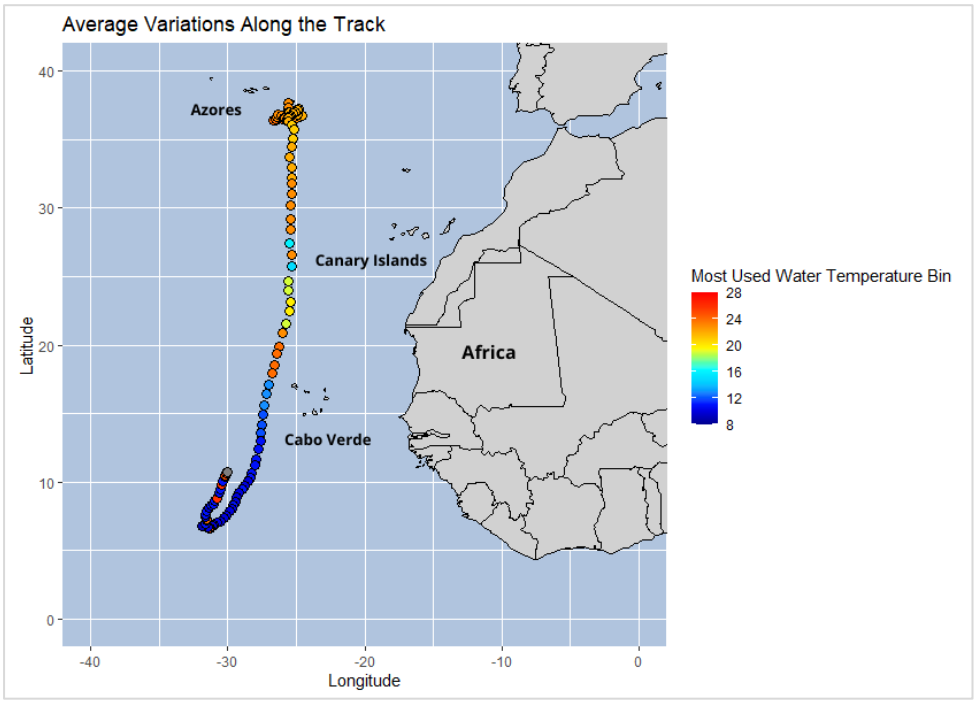

c

Figure 16. Average variations in most used ambient temperature bins along the track. The colour scale represents the water temperature (°C), with warmer temperatures in red and cooler temperatures in yellow. (a) BET1 (b) BET3 (c) BET4

Depth patterns were also analysed. Bigeye tuna frequently exhibit deep-diving behaviour, diving beyond 500 meters (Evans et al., 2008). The deepest dive reported at this study was 1485.5 m. Leroy et al. (2009) also reported a deep diving of maximum of 1498 m and Schaefer & Fuller (2010) reported another of 1902 m. Possibly, these extremely deep dives were made for predator avoidance (Schaefer & Fuller, 2002), to hunt for deep-sea squids (Roper et al., 1984) or mesopelagic fish (Maynard et al., 1975).

While the depth-use patterns show limited variation (Figure 15; see Figure S2 for other individuals), BET4 notably spent more time in waters around 50 and 100 meters deep during its southward migration. This observation is significant, as colder temperatures experienced by it in this region are typically found at greater depths. To provide further insight into this observation, Figure 17 shows water temperatures at a depth of 100 m at different regions, and a black line highlighting the limits of the OMZ (see Figure S4 for other individuals).

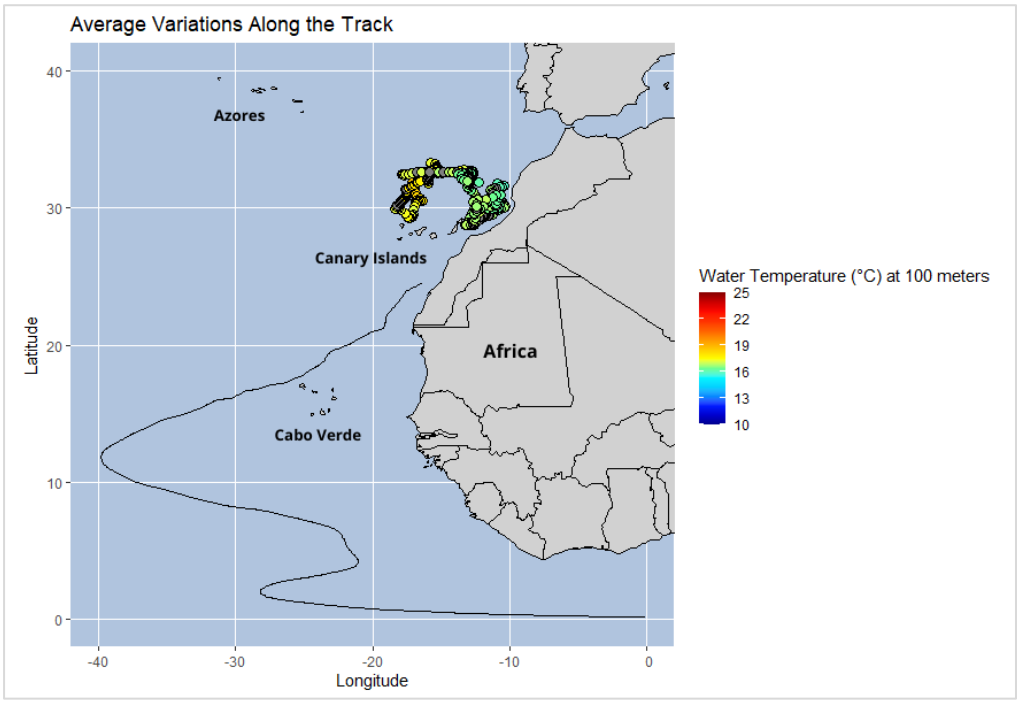
Average Variations Along the Track
Azores
Canary Islands
Africa
Cabo Verde
Latitude
Longitude
40
30
20
10
0
-40
-30
-20
-10
0
Water Temperature (°C) at 100 meters
25
22
19
16
13
10

a

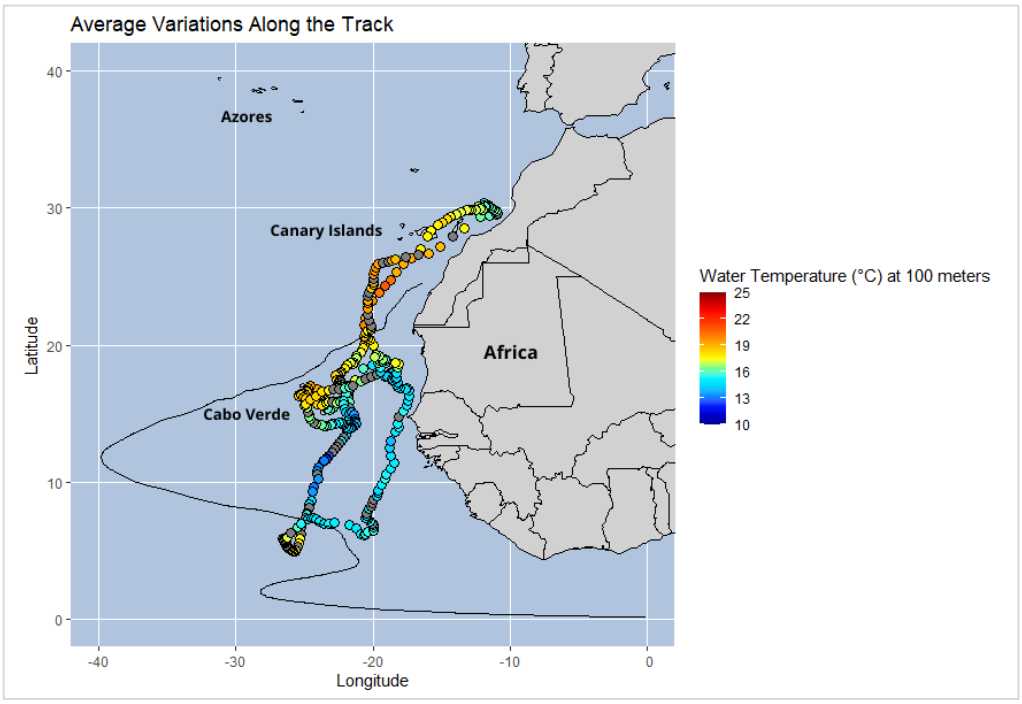
Average Variations Along the Track
Azores
Canary Islands
Africa
Cabo Verde
Latitude
Longitude
40
30
20
10
0
-40
-30
-20
-10
0
Water Temperature (°C) at 100 meters
25
22
19
16
13
10

b

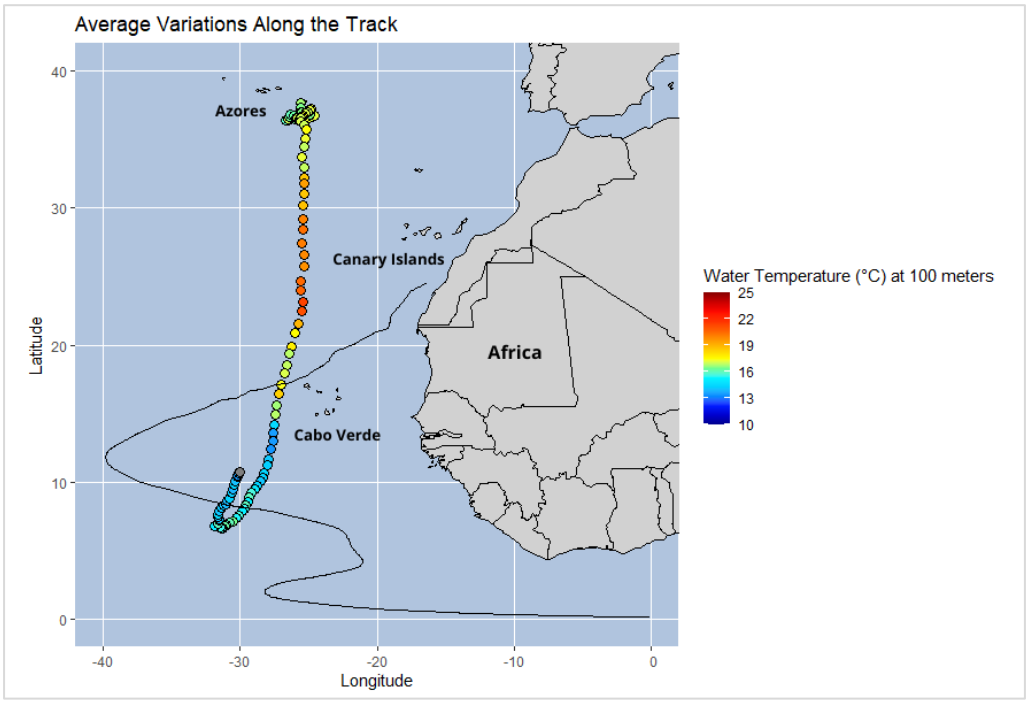

c

Figure 17. Average water temperature variations at a depth of 100 meters along the track overlaid with the OMZ limits obtained from modelled dissolved oxygen concentrations (at 100 m). The colour scale represents water temperature (°C), with warmer temperatures shown in red and cooler temperatures in blue. (a) BET1 (b) BET3 (c) BET4.

These graphs offer valuable insights into temperature variations at a depth of 100 meters across different regions. Around the Canary Islands and the Azores, ambient temperatures at this depth are generally warmer, as shown in the northern part of the figure. In contrast, in the Cabo Verde region and further south, temperatures drop significantly at the same depth. This notable decrease in temperature in the southern regions is clearly visualized on the map and further highlights the variations experienced by BET2, BET3, BET4, and BET5 during their migration southward.

Since internal temperatures are closely dependent on ambient water temperatures (Dagorn et al., 2000; Schaefer & Fuller, 2002), Figure 18 illustrates this relationship by analysing the most frequently used internal temperature bins.

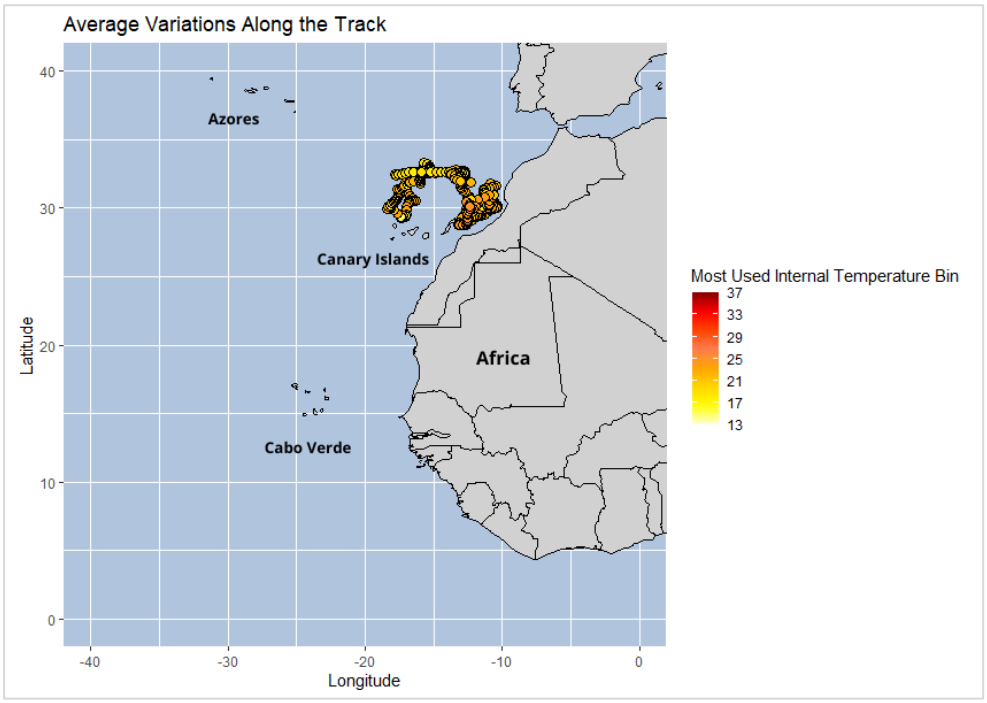
Average Variations Along the Track
Azores
Canary Islands
Africa
Cabo Verde
Latitude
Longitude
Most Used Internal Temperature Bin
37
33
29
25
21
17
13
40
30
20
10
0
-40
-30
-20
-10
0

a

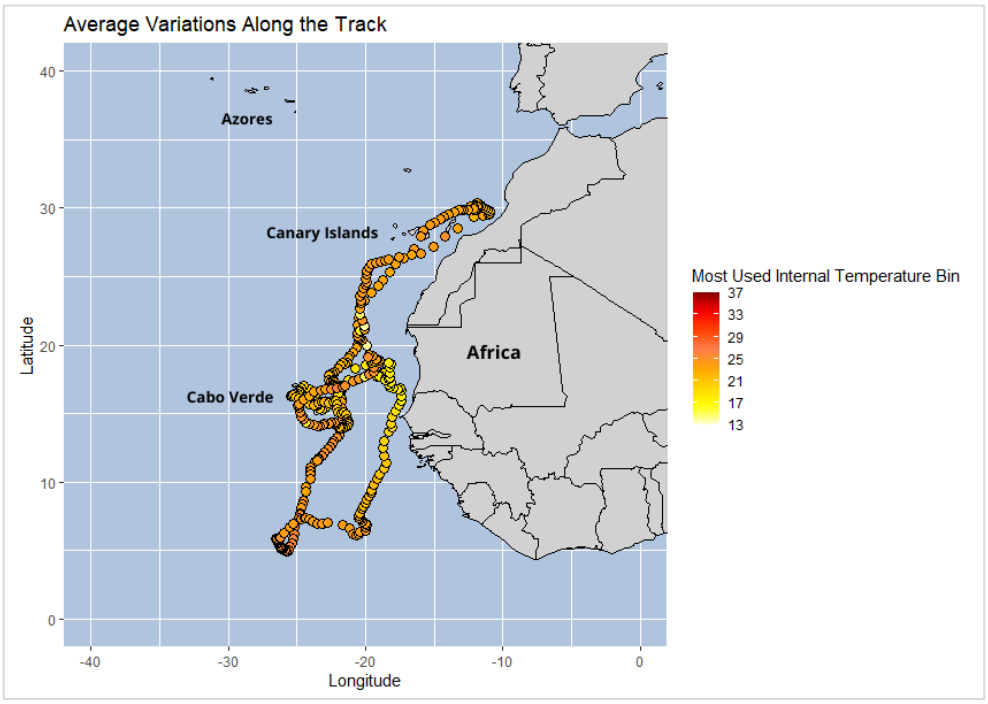
Average Variations Along the Track
Azores
Canary Islands
Africa
Cabo Verde
Latitude
Longitude
Most Used Internal Temperature Bin
37
33
29
25
21
17
13
40
30
20
10
0
-40
-30
-20
-10
0

b

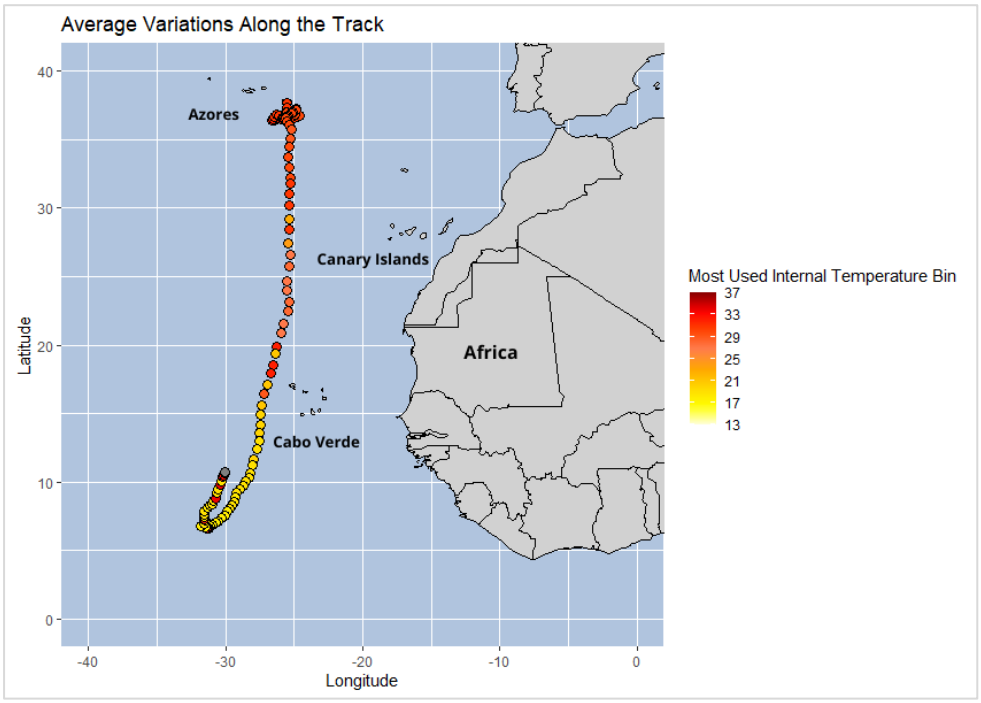

c

Figure 18. Average variations in most used internal temperature bins along the track. The colour scale represents the internal body temperature (°C), with warmer internal temperatures in red and cooler internal temperatures in yellow. (a) BET1 (b) BET3 (c) BET4.

It is particularly notable that the internal temperature variations mirrored the surrounding environmental conditions. The lowest internal temperature experienced in this study was 10.25°C for BET3, and the highest was 37.06°C for BET5 (FL 61-191 cm). See Figure S5 in Supplementary Materials for data on other individuals.

5. Discussion

The faulty external temperature readings for BET2 and BET3, where recorded water temperatures were higher than expected and seemed to occur particularly in regions with significant temperature fluctuations. For example, these two individuals migrated southward into warmer waters, while the individual with accurate readings stayed near the Canary Islands throughout the study. This suggests that sensor drift may have been exacerbated by the environmental conditions encountered during southern migrations.

Regarding ambient temperature data and model performance, the RMSE between modelled and recorded ambient temperatures was 1.59°C, indicating a moderate discrepancy between predicted and actual values. The MAE of 1.28°C reflected the average error magnitude. Descriptive statistics indicated that the model generally underestimated both ambient temperature and its variability. A Pearson correlation coefficient of 0.906 demonstrated a strong positive relationship between recorded and modelled temperatures, showing that the model captured overall temperature trends. However, the linear regression analysis revealed a slight bias, with predicted temperatures consistently deviating from actual measurements. The residual standard error of 1.20°C reflected the typical deviation of the residuals from the regression line, while the R-squared value of 0.821 suggested that about 82.1% of the recorded temperature variability could be explained by the modelled temperatures. As illustrated in Figure 11, although the model generally aligns with observed data, discrepancies, particularly during rapid temperature changes, are evident.

The application of the heat exchange model for predicting internal temperature in tuna species to assess their thermal biology has been extensively utilized and tested in previous studies (Holland & Sibert, 1994; Kitagawa et al., 2001; Kitagawa et al., 2006; Aoki et al., 2020; Hino et al., 2021; Kitagawa et al., 2022). In this study, for body temperature prediction and equation performance, the RMSE was 1.34°C, meaning the predictions differed from actual temperatures by this amount on average. The MAE of 1.07°C similarly reflected a consistent, though small, error in temperature estimates. The average recorded temperature was 21.47°C with a standard deviation of 2.708°C, while the average predicted temperature was also 21.47°C but with a slightly higher standard deviation of 3.03°C. This suggests that, while the model accurately estimates the average temperature, it shows higher variability compared to the actual data. A Pearson correlation coefficient of 0.897 indicated a strong positive relationship between predicted and actual temperatures, demonstrating that the model effectively tracks temperature trends. The linear regression

analysis showed that, on average, the equation's predictions were offset by approximately 4.31°C from actual temperatures, while the slope of 0.799 suggests that for every unit increase in predicted temperature, actual temperature increased by 0.799 units, indicating a slight underestimation of the magnitude of temperature changes. The R-squared value of 0.804 indicated that 80.4% of the variance in recorded temperatures could be explained by predicted values, showing a good model fit. Residuals with a standard error of 1.19°C highlighted notable deviations, particularly during rapid temperature changes, as confirmed by Figure 12.

In terms of body temperature prediction using modelled ambient temperatures, BET1's RMSE and MAE values indicated moderate prediction errors (see Figure 13, a). The Pearson correlation coefficient of 0.740 pointed to a moderately strong positive relationship between modelled and recorded temperatures, while the linear regression slope of 0.444 and R-squared value of 0.547 indicated that about 54.7% of internal temperature variability was explained by the model. For BET2, RMSE and MAE values demonstrated slightly improved accuracy compared to BET1 (see Figure 13, b), with a Pearson correlation coefficient of 0.757 reflecting a stronger correlation. The slope of 0.658 and R-squared value of 0.572 showed that 57.2% of the variance in internal temperature was accounted for by the predicted values. BET3's RMSE and MAE values, however, reflected higher errors compared to BET1 and BET2 (see Figure 13, c), though the Pearson correlation coefficient of 0.850 pointed to a strong positive correlation. The slope of 0.468 and R-squared value of 0.727 indicated that 72.7% of internal temperature variability was explained by the model, the highest among the three individuals. Considering the three individuals, the average Pearson correlation coefficient of 0.782 indicated a generally strong positive relationship between predicted and recorded temperatures. The average linear regression slope of 0.523 suggested that, for every unit increase in predicted temperature, actual temperature increased by approximately 0.523 units. With an average R-squared value of 0.615, the model explained about 61.5% of internal temperature variability, indicating a moderate fit with significant explanatory power.

The consistency observed in the mean error metrics for the first two datasets suggests that averaging their values provides a reliable representation of model performance, demonstrating stability. However, the variation in the third dataset highlights that model accuracy may vary depending on specific data characteristics. Overall, Model 1 demonstrated superior performance, with lower RMSE and MAE values, a higher Pearson correlation coefficient, and a better fit as reflected by its higher R-squared value. Model 1 explained 80.4% of the variability in recorded temperatures, whereas Model 2's R-squared

value of 0.727, though positive, accounted for less variability. These results indicate that Model 1 is more reliable for predicting internal temperatures, providing a better fit to the data.

The comparison of SST values within the tuna groups revealed significant temporal changes, even within similar latitudes. For those that remained in higher latitudes, particularly around the Canary Islands and the Azores, a clear warming trend was evident. A similar, though less pronounced, SST increase was observed in the group that migrated toward Cabo Verde. Its SST values were already higher than those experienced by the 2005s tuna. While the SST increase in the lower-latitude group was less dramatic than in the northern group, it remains significant, particularly in average temperatures, underscoring the broader trend of ocean warming. The northern group experienced a sharper rise in SST, especially in minimum and maximum values, suggesting that environmental changes in the north are occurring at a faster rate. Reports from NOAA and WMO reported similar findings, highlighting that the rapid warming of the North Atlantic Ocean is also contributing to marine heatwaves. This warming is likely driven by its circulation changes that are also strongly tied to atmospheric circulation changes (Polyakov et al., 2005; Woollings et al., 2012; Lapointe et al., 2020).

Regarding seasonal patterns, although the analysis did not reveal strong statistical differences, subtle trends observed in autumn across water temperature, internal temperature, and depth required attention. These results suggest that, while conditions remain relatively stable for tuna in winter and summer, autumn may represent a transitional period, especially in diving behaviour, potentially in response to cooling surface temperatures and the shifting thermocline (Kitagawa et al., 2007). While the data is not conclusive, it highlights the need for further investigation into how these factors interact during this season. Additionally, other study has also observed that tuna behaviour adapts to seasonal changes and varying oceanographic conditions (Hino et al., 2018).

The observed behaviour patterns in this study and the significant temperature changes are likely linked to the thermocline, where rapid decreases in temperature create sudden environmental changes. In the Eastern Tropical Atlantic, the thermocline typically occurs at depths of 50 to 100 meters, and becomes notably sharper above the OMZ, areas where the vertical distribution of bigeye tuna frequently overlaps (Schaefer et al., 2007; Schaefer and Fuller, 2009). Other studies also reported thermocline effects on the vertical migration of tuna. Houssard et al. (2017) observed that bigeye tuna expands its vertical habitat in areas where deeper thermoclines occur, which allows it to access higher trophic prey. In the North

Atlantic, Brill et al. (2002) found that bluefin tuna remained close to the surface in strong thermoclines, while in weaker thermoclines it changed its diel vertical behaviour, probably due to foraging. Additionally, Bauer et al. (2017) concluded that changing between surface-oriented behaviour and deep diving behaviour in the same tuna species in the Mediterranean was induced by a shift in the thermal stratification.

Humphries et al. (2024) demonstrated in their study that focused on the Eastern Pacific, that bigeye tuna continued foraging at depth despite hypoxic and cold conditions, highlighting their resilience in such environments. This is further supported by Hino et al. (2019), who found that as bigeye tuna grow, they may develop enhanced endothermic and thermoregulatory abilities. Larger individuals are known to require fewer thermoregulatory ascents, allowing them to remain at depth longer; while small fish cool faster and are more susceptible to the physiological effects of rapid temperature oscillations, which may explain why BET2 and BET3, being smaller than the others, spent a significant amount of time in warmer surface waters, possibly avoiding the sharp thermocline. However, while cold tolerance increases with size (which could also explain the fact that BET4 and BET5 spent a lot of time at colder waters and close to the sharp thermocline), larger fish also have higher oxygen demands. This highlights the complex interaction between size, temperature, oxygen availability, and vertical distribution.

Tunas, in general, with their high metabolic oxygen demands, are particularly sensitive to these low-oxygen environments. Other marine predators, such as ectothermic blue sharks, also are affected by low DO levels (Vedor et al., 2021). Although bigeye tuna has evolved adaptations such as haemoglobin with a higher affinity for oxygen compared to yellowfin or skipjack tuna (Lowe, Brill & Cousins, 2000; Mislan et al., 2017), their ability to withstand hypoxic conditions is limited.

Humphries et al. (2024) also observed that bigeye tuna exhibited a significant increase in upward vertical excursions in low-oxygen areas, compared to regions with higher DO availability. These vertical movements likely help to restore oxygen levels and regulate body temperature. The increased frequency of such excursions means that they spend more time in shallower waters, making them more susceptible to capture by longlines and purse seines, as their vertical movements overlap with fishing gear depths – ranging from 100 to 300 meters (Ward & Myers, 2005; Bigelow et al., 2006). This pattern is further supported by studies showing that tunas, when encountering OMZs, tend to shift their vertical movements to shallower depths (Song et al., 2009; Potier et al., 2014) and supported by this study, as similar behaviour was observed for BET4 and BET5, with both individuals spending

significant time at depths of 50 to 100 meters with fewer long dives, likely to avoid the OMZ core. This aggregation, rather than closer to the surface where oxygen concentrations are likely higher, may also be attributed to elevated surface temperatures. In this area and in this period, SSTs ranged around 26–29°C.

Collins et al. (2010) emphasized that future projections suggest global warming may also impact the physical characteristics of the thermocline, making it shallower with sharper gradients. Given that fish movements are linked to the thermocline, this could lead to a reduction in the vertical habitat available to marine species. Consequently, such individuals can get trap into these areas, gaining one more reason to became more susceptible to fishing exploitation.

Vedor et al. (2021) demonstrated that some of the most significant fishing hotspots are concentrated above the ETA OMZ. These regions of concentrated fishing effort emerge as vessels continuously set longlines in specific areas rather than having to interrupt fishing by travelling for days between hotspots (Queiroz et al., 2016). As fishing pressure within OMZ zones grows, the deployment of baited longline hooks is expected to increase too, intensifying the overall fishing impact (Prince & Goodyear, 2006).

6. Conclusion

This study successfully tracked the movements of nine bigeye tuna tagged between 2005 and 2022 in the North Atlantic Ocean, providing valuable insights into their spatial distribution and behaviour. The initial analysis of depth, internal, and ambient temperature data from individuals BET1, BET2, and BET3 emphasized the importance of data validation, particularly in ecological studies reliant on tagging technologies. Sensor inaccuracies, such as those identified here, can significantly affect the reliability of ecological conclusions, underscoring the need for rigorous quality control in tagging technologies.

After the extraction of modelled data, the evaluation of the water temperature model showed that while it captured general temperature trends, it underestimated actual values during periods of rapid change. A Pearson correlation coefficient of 0.906 reflects its overall accuracy, though consistent biases were noted, especially during rapid temperature changes. Similarly, the heat budget model used to predict internal temperatures and first based only on data from BET1, performed well, effectively capturing average temperatures for both predicted and recorded values at 21.47°C. However, it also exhibited underestimation.

Recalibrating the equation using modelled ambient temperatures provided a more comprehensive evaluation across additional individuals. While moderate prediction errors were noted, the model captured general temperature trends, though individual variability remained a factor. Consistent error metrics for BET1 and BET2 suggest reliable performance using average values, but the higher variability seen in BET3 indicates individual characteristics can impact model accuracy.

When comparing Model 1 (using data from BET1) and Model 2 (averaging data from BET1-3), Model 1 outperformed, with a lower RMSE of 1.34°C and MAE of 1.07°C, whereas Model 2's RMSE increased to 2.843°C. These findings further highlight the need for refining predictive models and the necessity of developing models that account for individual-specific factors to improve reliability and accuracy in future studies.

The analysis of SSTs variations also provided key insights into thermal dynamics, particularly when comparing different migration patterns. Both groups experienced significant warming, with a more pronounced increase in the northern group, highlighting the rapid environmental changes in the North Atlantic. This warming underscore the

possible influence of rising ocean temperatures on fish behaviour and distribution and may have implications for habitat suitability and migration patterns in the future.

Seasonal patterns in internal temperature, water temperature, and depth across different regions and years pointed to autumn as a potential transitional period, requiring further investigation into how these seasonal shifts effectively influence tuna behaviour. It's important to highlight that spring was excluded from the analysis due to missing data, which might have hidden critical insights. Additionally, the absence of summer data for the two individuals that migrated south in 2019 (BET4 and BET5), who recorded higher temperatures, could also have masked important factors that would have contributed to a more comprehensive analysis.

Southward migration resulted in increased time spent in cooler waters, particularly near Cabo Verde, where ETA OMZ and a sharper thermocline are present. Recent migrations also indicated cooler temperature trends in this zone compared to those observed in 2005, especially for BET4, tagged in 2019, that spent a lot of time in temperature bins of 8-12°C. In contrast, tuna in higher latitudes primarily occupied warmer waters. Additionally, ambient temperatures at a depth of 100 meters were higher in Canary Islands and Azores region than around Cabo Verde. On top of that, internal temperature was closely linked to these ambient conditions, mirroring these patterns, with the lowest recorded internal temperature being 10.25°C. All these variations suggest that environmental conditions influence tuna habitat use.

Additionally, this study highlights the complex interaction between temperature, oxygen availability, and vertical distribution, particularly with expanding OMZs. As these fish adapt to its environments, especially bigeye tuna that has evolved adaptations such as haemoglobin with a higher affinity for oxygen, it demonstrates resilience in foraging at depth, even in low-oxygen and cold conditions. However, the expansion of OMZs due to climate-driven deoxygenation can present significant vulnerabilities. Larger individuals, while exhibiting better thermoregulatory abilities, have higher oxygen demands, prompting them to seek warmer, oxygen-rich waters - a behaviour that increases its risk from fishing pressure. Also, the identification of significant fishing hotspots above OMZs in other studies, along with observed increases in upward vertical movements of bigeye tuna in low-oxygen regions found by Humphries et al. (2024), underscores the importance of improving fisheries management strategies to address expanding OMZs and their effects on larger species.

Future research should prioritize dissolved-oxygen sensing archival tag, like the DOME archival tag (Da Costa et al., 2024), that can measure dissolved oxygen levels in situ, allowing a clearer understanding of the specific oxygen conditions fish encounter and their actual tolerances and preferences, highlighting also the need for precise calibration and validation of tagging tools, rather than relying on modelled DO or ambient temperature data derived from ocean-environmental databases. Actual concentrations of those variables in real habitats may therefore differ from interpolated values and used model predictions can underestimate values, as found by Oschlies et al. (2018) and Da costa et al. (2024). Filling these gaps can significantly enhance the understanding of the impact of expanding OMZs and the rise of ocean temperatures on bigeye tuna populations and other marine ecosystems.

To conclude, this study found that climate change-induced temperature increases can directly and indirectly influence the behaviour, thermoregulation, and habitat use patterns of bigeye tuna. These findings enhance predictions of how future warming scenarios may affect this and other endothermic species. Moreover, understanding the interactions between fish, fisheries, and climate change is crucial for sustaining tuna populations in the 21st century, highlighting the need for targeted conservation measures to protect these top marine predators, which play a vital role in marine ecosystems (Lehodey et al., 2011; Hobday et al., 2013; Brill & Hobday, 2017). Effective strategies may include reducing longline soak times to minimize bycatch and lower mortality rates of non-target species, including juvenile individuals; limiting fishing activity in known aggregation hotspots, particularly above expanding OMZs; implementing seasonal fishing closures based on scientific assessments of species' seasonal patterns; adopting modifications to fishing gear, such as using circle and weak hooks; reinforcing data reporting for clearer stock assessments; and investing in bio-logging to better understand species' movements and behaviour. These approaches will help develop precise conservation strategies to promote population growth and ensure sustainability.

7. References

1. Aoki, Y., Aoki, A., Ohta, I., & Kitagawa, T. (2020). Physiological and behavioural thermoregulation of juvenile yellowfin tuna Thunnus albacares in subtropical waters. *Marine Biology*, *167*(6), 71.

2. Ariz, J., Delgado, A., Fonteneau, A., Gonzales Costas, F., & Pallares, P. (1992). Logs and tunas in the eastern tropical Atlantic: A review of present knowledge and uncertainties. In *Proceedings of the international workshop on fishing for tunas associated with floating objects, La Jolla, CA* (pp. 21-65).

3. Arrizabalaga, H., Dufour, F., Kell, L., Merino, G., Ibaibarriaga, L., Chust, G., Irigoien, X., Santiago, J., Murua, H., Fraile, I., Chifflet, M., Goikoetxea, N., Sagarminaga, Y., Aumont, O., Bopp, L., Herrera, M., Marc Fromentin, J., & Bonhomeau, S. (2015). Global habitat preferences of commercially valuable tuna. *Deep Sea Research Part II: Topical Studies in Oceanography*, *113*, 102-112.

4. Aspillaga, E., Bartumeus, F., Starr, R. M., López-Sanz, À., Linares, C., Díaz, D., Garrabou, J., Zabala, M., & Hereu, B. (2017). Thermal stratification drives movement of a coastal apex predator. *Scientific Reports*, *7*(1), 526.

5. Bauer, R. K., Fromentin, J.-M., Demarcq, H., & Bonhommeau, S. (2017). Habitat use, vertical and horizontal behaviour of Atlantic bluefin tuna (Thunnus thynnus) in the Northwestern Mediterranean Sea in relation to oceanographic conditions. *Deep Sea Research Part II: Topical Studies in Oceanography*, *141*, 248-261.

6. Benesty, J., Chen, J., Huang, Y., & Cohen, I. (2009). Pearson Correlation Coefficient. In I. Cohen, Y. Huang, J. Chen, & J. Benesty. *Noise Reduction in Speech Processing* (pp. 1-4). Springer Berlin Heidelberg.

7. Bernal, D., Brill, R. W., Dickson, K. A., & Shiels, H. A. (2017). Sharing the water column: physiological mechanisms underlying species-specific habitat use in tunas. *Reviews in Fish Biology and Fisheries*, *27*(4), 843-880.

8. Bernal, D., Sepulveda, C., & Graham, J. B. (2012). Water temperature and heat transfer in the endothermic bigeye thresher shark (Alopias superciliosus). *Journal of Fish Biology*, 80(5), 1360-1375.

9. Bigelow, K., Musyl, M. K., Poisson, F., & Kleiber, P. (2006). Pelagic longline gear depth and shoaling. *Fisheries Research*, *77*(2), 173-183.

10. Block, B. A., Booth, D. T., & Carey, F. G. (1992). Depth and temperature of the blue marlin, Makaira nigricans, observed by acoustic telemetry. *Marine Biology*, *114*(2), 175-183.

11. Block, B. A., Jonsen, I. D., Jorgensen, S. J., Winship, A. J., Shaffer, S. A., Bograd, S. J., Hazen, E. L., Foley, D. G., Breed, G. A., Harrison, A. L., Ganong, J. E., Swithenbank, A., Castleton, M., Dewar, H., Mate, B. R., Shillinger, G. L., Schaefer, K. M., Benson, S. R., Weise, M. J., . . . Costa, D. P. (2011). Tracking apex marine predator movements in a dynamic ocean. *Nature*, *475*(7354), 86-90.

12. Breitburg, D., Levin, L. A., Oschlies, A., Grégoire, M., Chavez, F. P., Conley, D. J., Garçon, V., Gilbert, D., Gutiérrez, D., Isensee, K., Jacinto, G. S., Limburg, K. E., Montes, I., Naqvi, S. W. A., Pitcher, G. C., Rabalais, N. N., Roman, M. R., Rose, K. A., Seibel, B. A., . . . Zhang, J. (2018). Declining oxygen in the global ocean and coastal waters. *Science*, *359*(6371), eaam7240.

13. Brierley, A. S. (2014). Diel vertical migration. *Current Biology*, 24(22), R1074-R1076.

14. Brill, R. W. (1994). A review of temperature and oxygen tolerance studies of tunas pertinent to fisheries oceanography, movement models and stock assessments. *Fisheries Oceanography*, *3*(3), 204-216.

15. Brill, R. W., & Hobday, A. J. (2017). Tunas and their fisheries: safeguarding sustainability in the twenty-first century. *Reviews in Fish Biology and Fisheries*, *27*(4), 691-695.

16. Brill, R. W., & Lutcavage, M. E. (2001). Understanding environmental influences on movements and depth distributions of tunas and billfishes can significantly improve population assessments. In *American Fisheries Society Symposium* (pp. 179-198).

17. Brill, R., Bigelow, K., Musyl, M., Fritsches, K., & Warrant, E. (2005). Bigeye tuna (Thunnus obesus) behavior and physiology and their relevance to stock assessments and fishery biology. *Collect. Vol. Sci. Pap. ICCAT*, *57*.

18. Brill, R., Lutcavage, M., Metzger, G., Bushnell, P., Arendt, M., Lucy, J., Watson, C., & Foley, D. (2002). Horizontal and vertical movements of juvenile bluefin tuna (Thunnus thynnus), in relation to oceanographic conditions of the western North Atlantic, determined with ultrasonic telemetry. *Fishery Bulletin*, *100*, 155-167.

19. Brown, B. E. (1997). Coral bleaching: causes and consequences. *Coral Reefs*, *16*(1), S129-S138.

20. Burrows, M. T., Schoeman, D. S., Buckley, L. B., Moore, P., Poloczanska, E. S., Brander, K. M., Brown, C., Bruno, J. F., Duarte, C. M., Halpern, B. S., Holding, J., Kappel, C. V., Kiessling, W., O'Connor, M. I., Pandolfi, J. M., Parmesan, C., Schwing, F. B., Sydeman, W. J., & Richardson, A. J. (2011). The pace of shifting climate in marine and terrestrial ecosystems. *Science*, *334*(6056), 652-655.

21. Carey, F. G., & Teal, J. M. (1966). Heat conservation in tuna fish muscle. *Proceedings of the National Academy of Sciences*, *56*(5), 1464-1469.

22. Carey, F. G., Kanwisher, J. W., & Stevens, E. D. (1984). Bluefin Tuna Warm Their Viscera During Digestion. *Journal of Experimental Biology*, *109*(1), 1-20.

23. Carroceda, A., & Colmenero, C. (2016). Size-weight relationships of the bigeye tuna (*Thunnus obesus*) from North Atlantic areas using linear and non-linear fits. *Collective Volume of Scientific Papers ICCAT*, 72(2), 472-484.

24. Chan, F., Barth, J. A., Lubchenco, J., Kirincich, A., Weeks, H., Peterson, W. T., & Menge, B. A. (2008). Emergence of Anoxia in the California Current Large Marine Ecosystem. *Science*, *319*(5865), 920-920.

25. Cheng, L., Abraham, J., Hausfather, Z., & Trenberth, K. E. (2019). How fast are the oceans warming? *Science*, *363*(6423), 128-129.

26. Cheng, L., Zhu, J., Abraham, J., Trenberth, K. E., Fasullo, J. T., Zhang, B., Yu, F., Wan, L., Chen, X., & Song, X. (2019). 2018 Continues Record Global Ocean Warming. *Advances in Atmospheric Sciences*, *36*(3), 249-252.

27. Chung, H., Lee, J., & Lee, W. Y. (2021). A Review: Marine Bio-logging of Animal Behaviour and Ocean Environments. *Ocean Science Journal*, *56*(2), 117-131.

28. Clarke, A., & Pörtner, H. O. (2010). Temperature, metabolic power and the evolution of endothermy. *Nature*, 463(7282), 1022-1025.

29. Collins, M., An, S.I., Cai, W., Ganachaud, A., Guilyardi, E., Jin, F.F., Jochum, M., Lengaigne, M., Power, S., Timmermann, A., Vecchi, G., & Wittenberg, A. (2010). The impact of global warming on the tropical Pacific Ocean and El Niño. *Nature Geoscience*, *3*(6), 391-397.

30. Cooke, S. J., & O'Connor, C. M. (2010). Making conservation physiology relevant to policy makers and conservation practitioners. *Conservation Letters*, *3*(3), 159-166.

31. Cooke, S. J., Hinch, S. G., Wikelski, M., Andrews, R. D., Kuchel, L. J., Wolcott, T. G., & Butler, P. J. (2004). Biotelemetry: a mechanistic approach to ecology. *Trends in Ecology & Evolution*, *19*(6), 334-343.

32. Cutler, B., & Haesemeyer, M. (2024). Vertebrate behavioral thermoregulation: knowledge and future directions. *Neurophotonics*, *11*(3), 033409.

33. da Costa, I., Sims, D. W., Loureiro, B., Waller, M. J., Womersley, F. C., Loveridge, A., Humphries, N. E., Southall, E. J., Vedor, M., Mucientes, G., Prendergast, S., Fontes, J., Afonso, P., Macena, B. C. L., Watanabe, Y. Y., & Queiroz, N. (2024). Measuring deoxygenation effects on marine predators: A new animal-attached archival tag recording in situ dissolved oxygen, temperature, fine-scale movements and behaviour. *Methods in Ecology and Evolution*, *15*(8), 1360-1379.

34. da Silva, G. B., Hazin, H. G., Hazin, F. H. V., & Vaske-Jr, T. (2019). Diet composition of bigeye tuna (Thunnus obesus) and yellowfin tuna (Thunnus albacares) caught on aggregated schools in the western equatorial Atlantic Ocean. *Journal of Applied Ichthyology*, *35*(5), 1111-1118.

35. Dagorn, L., Josse, E., Bach, P., & Bertrand, A. (2000). Modeling tuna behaviour near floating objects: from individuals to aggregations. *Aquatic Living Resources*, *13*(4), 203-211.

36. Deutsch, C., Ferrel, A., Seibel, B., Pörtner, H. O., & Huey, R. B. (2015). Ecophysiology. Climate change tightens a metabolic constraint on marine habitats. *Science*, *348*(6239), 1132–1135.

37. Diaz, R. J., & Rosenberg, R. (2008). Spreading dead zones and consequences for marine ecosystems. *Science, 321*(5891), 926–929.

38. Dickson, K. A., & Graham, J. B. (2004). Evolution and consequences of endothermy in fishes. *Physiological and biochemical zoology*, *77*(6), 998–1018.

39. Dickson, K. A., & Graham, J. B. (2004). Evolution and consequences of endothermy in fishes. *Physiological and Biochemical Zoology*, 77(6), 998-1018.

40. Ekau, W., Auel, H., Pörtner, H. O., & Gilbert, D. (2010). Impacts of hypoxia on the structure and processes in pelagic communities (zooplankton, macro-invertebrates and fish). *Biogeosciences*, *7*(5), 1669-1699.

41. Erdaide, O., Lekube, X., Olsen, R. L., Ganzedo, U., & Martinez, I. (2016). Comparative study of muscle proteins in relation to the development of yake in three tropical tuna species yellowfin (Thunnus albacares), big eye (Thunnus obesus) and skipjack (Katsuwonus pelamis). *Food chemistry*, *201*, 284–291.

42. Evans, K., Langley, A., Clear, N. P., Williams, P., Patterson, T., Sibert, J., Hampton, J., & Gunn, J. S. (2008). Behaviour and habitat preferences of bigeye tuna (Thunnus obesus) and their influence on longline fishery catches in the western Coral Sea. *Canadian Journal of Fisheries and Aquatic Sciences*, *65*(11), 2427-2443.

43. FAO, IFAD, UNICEF, WFP, & WHO. (2018). The state of food security and nutrition in the world 2018: Building climate resilience for food security and nutrition. Rome, Italy: *FAO*.

44. Farrell, A. P. (2002). Cardiorespiratory performance in salmonids during exercise at high temperatures: Insights into cardiovascular design limitations in fishes. *Comparative Biochemistry and Physiology Part A: Molecular & Integrative Physiology*, 132(4), 797-810.

45. Galland, G. R. (2018). FAD management objectives should be defined and implemented at ICCAT. *Collect. Vol. Sci. Pap. ICCAT*, *74*(5), 2214-2218.

46. Gilly, W. F., Beman, J. M., Litvin, S. Y., & Robison, B. H. (2013). Oceanographic and biological effects of shoaling of the oxygen minimum zone. *Annual review of marine science*, *5*, 393–420.

47. Grady, J. M., Enquist, B. J., Dettweiler-Robinson, E., Wright, N. A., & Smith, F. A. (2014). Evidence for mesothermy in dinosaurs. *Science*, 344(6189), 1268-1272.

48. Greene, C. H., Block, B. A., Welch, D., Jackson, G., Lawson, G. L., & Rechisky, E. L. (2009). Advances in conservation oceanography: new tagging and tracking technologies and their potential for transforming the science underlying fisheries management. *Oceanography*, *22*(1), 210-223.

49. Gruber, N., Boyd, P. W., Frölicher, T. L., & Vogt, M. (2021). Biogeochemical extremes and compound events in the ocean. *Nature*, *600*(7889), 395–407.

50. Guo, S., Zhong, S., & Zhang, A. (2013). Privacy-preserving Kruskal-Wallis test. *Computer methods and programs in biomedicine*, *112*(1), 135–145.

51. Hall, M. A., Alverson, D. L., & Metuzals, K. I. (2000). By-Catch: Problems and Solutions. *Marine Pollution Bulletin*, 41(1), 204-219.

52. Hanamoto, E. (1987). Effect of oceanographic environment on bigeye tuna distribution. *Bull.Jap.Soc.Fish.Oceanogr.,* 51(3):203–16.

53. Hays, G. C. (2003). A review of the adaptive significance and ecosystem consequences of zooplankton diel vertical migrations. *Hydrobiologia*, 503(1-3), 163-170.

54. Hazen, E. L., Jorgensen, S., Rykaczewski, R. R., Bograd, S. J., Foley, D. G., Jonsen, I. D., Shaffer, S. A., Dunne, J. P., Costa, D. P., Crowder, L. B., & Block, B. A. (2013). Predicted habitat shifts of Pacific top predators in a changing climate. *Nature Climate Change*, *3*(3), 234-238.

55. Herbing, I. H. (2002). Effects of temperature on larval fish swimming performance: the importance of physics to physiology. *Journal of Fish Biology*, *61*(4), 865-876.

56. Heylen, B.C.; Nachtsheim, D.A. (2018). Bio-telemetry as an essential tool in movement ecology and marine conservation, *in*: Jungblut, S. *et al. YOUMARES 8 – Oceans Across Boundaries: Learning from each other: Proceedings of the 2017 conference for YOUng MARine RESearchers in Kiel, Germany.* pp. 83-107.

57. Hino, H., Kitagawa, T., Matsumoto, T., Aoki, Y., & Kimura, S. (2019). Changes to vertical thermoregulatory movements of juvenile bigeye tuna (Thunnus obesus) in the northwestern Pacific Ocean with time of day, seasonal ocean vertical thermal structure, and body size. *Fisheries Oceanography*, *28*(4), 359-371.

58. Hino, H., Kitagawa, T., Matsumoto, T., Aoki, Y., & Kimura, S. (2021). Development of behavioral and physiological thermoregulatory mechanisms with body size in juvenile bigeye tuna Thunnus obesus. *Fisheries Oceanography*, *30*(3), 219-231.

59. Hobday, A. J., Young, J. W., Abe, O., Costa, D. P., Cowen, R. K., Evans, K., Gasalla, M. A., Kloser, R., Maury, O., & Weng, K. C. (2013). Climate impacts and oceanic top predators: moving from impacts to adaptation in oceanic systems. *Reviews in Fish Biology and Fisheries*, *23*(4), 537-546.

60. Holbrook, N. J., Sen Gupta, A., Oliver, E. C. J., Hobday, A. J., Benthuysen, J. A., Scannell, H. A., Smale, D. A., & Wernberg, T. (2020). Keeping pace with marine heatwaves. *Nature Reviews Earth & Environment*, *1*(9), 482-493.

61. Holland, K. N., Brill, R. W., Chang, R. K., Sibert, J. R., & Fournier, D. A. (1992). Physiological and behavioural thermoregulation in bigeye tuna (Thunnus obesus). *Nature*, *358*(6385), 410–412.

62. Houssard, P., Lorrain, A., Tremblay-Boyer, L., Allain, V., Graham, B. S., Menkes, C. E., Pethybridge, H., Couturier, L. I. E., Point, D., Leroy, B., Receveur, A., Hunt, B. P. V., Vourey, E., Bonnet, S., Rodier, M., Raimbault, P., Feunteun, E., Kuhnert, P. M., Munaron, J.-M., . . . Letourneur, Y. (2017). Trophic position increases with thermocline depth in yellowfin and bigeye tuna across the Western and Central Pacific Ocean. *Progress in Oceanography*, *154*, 49-63.

63. Hubbs, C. L. (1948). Changes in the fish fauna of western North America correlated with changes in ocean temperature. *Journal of Marine Research* 7, (3).

64. Huey, R. B., & Kingsolver, J. G. (2019). Climate warming, resource availability, and the metabolic meltdown of ectotherms. *The American Naturalist*, 193(2), E91-E102.

65. Humphries, N. E., Fuller, D. W., Schaefer, K. M., & Sims, D. W. (2024). Highly active fish in low oxygen environments: vertical movements and behavioural responses of bigeye and yellowfin tunas to oxygen minimum zones in the eastern Pacific Ocean. *Marine Biology*, *171*(2), 55.

66. Hussey, N. E., Kessel, S. T., Aarestrup, K., Cooke, S. J., Cowley, P. D., Fisk, A. T., Harcourt, R. G., Holland, K. N., Iverson, S. J., Kocik, J. F., Mills Flemming, J. E., & Whoriskey, F. G. (2015). Ecology. Aquatic animal telemetry: A panoramic window into the underwater world. *Science, 348*(6240), 1255642.

67. Hyndman, R. J., & Koehler, A. B. (2006). Another look at measures of forecast accuracy. *International Journal of Forecasting*, *22*(4), 679-688.

68. Intergovernmental Panel on Climate Change (IPCC). (2023). Summary for Policymakers. In *Climate Change 2021 – The Physical Science Basis: Working Group I Contribution to the Sixth Assessment Report of the Intergovernmental Panel on Climate Change* (pp. 3–32). Cambridge University Press.

69. James, G., Witten, D., Hastie, T. & Tibshirani, R. (2021). An Introduction to Statistical Learning. 2. *Springer*.

70. Johnson, G. C., & Lyman, J. M. (2020). Warming trends increasingly dominate global ocean. *Nature Climate Change*, *10*(8), 757-761.

71. Josse, E., Bach, P., & Dagorn, L. (1998). Simultaneous observations of tuna movements and their prey by sonic tracking and acoustic surveys. *Hydrobiologia*, *371*(0), 61-69.

72. Karstensen, J., Fiedler, B., Schütte, F., Brandt, P., Körtzinger, A., Fischer, G., Zantopp, R., Hahn, J., Visbeck, M., & Wallace, D. (2015). Open ocean dead zones in the tropical North Atlantic Ocean. *Biogeosciences*, *12*(8), 2597-2605.

73. Kawamura, G., Nishimura, W., Ueda, S., & Nishi, T. (1981). Vision in tunas and marlins. *南海研紀要*, *2*(1), 3-47.

74. Keeling, R. F., Körtzinger, A., & Gruber, N. (2010). Ocean deoxygenation in a warming world. *Annual Review of Marine Science*, *2*, 199-229.

75. Kessouri, F., McWilliams, J. C., Bianchi, D., Sutula, M., Renault, L., Deutsch, C., Feely, R. A., McLaughlin, K., Ho, M., Howard, E. M., Bednaršek, N., Damien, P., Molemaker, J., & Weisberg, S. B. (2021). Coastal eutrophication drives acidification, oxygen loss, and ecosystem change in a major oceanic upwelling system. *Proceedings of the National Academy of Sciences of the United States of America*, *118*(21), e2018856118.

76. Kitagawa, T., Abe, T. K., Kubo, K., Fujioka, K., Fukuda, H., & Tanaka, Y. (2022). Rapid endothermal development of juvenile pacific bluefin tuna. *Frontiers in physiology*, *13*, 968468.

77. Kitagawa, T., Boustany, A. M., Farwell, C. J., Williams, T. D., Castleton, M. R., & Block, B. A. (2007). Horizontal and vertical movements of juvenile bluefin tuna (Thunnus orientalis) in relation to seasons and oceanographic conditions in the eastern Pacific Ocean. *Fisheries Oceanography*, *16*(5), 409-421.

78. Kitagawa, T., Kimura, S., Nakata, H., & Yamada, H. (2006). Thermal adaptation of pacific bluefin tuna Thunnus orientalis to temperate waters. *Fisheries Science*, *72*(1), 149-156.

79. Kitagawa, T., Kimura, S., Nakata, H., & Yamada, H. (2007). Why do young Pacific bluefin tuna repeatedly dive to depths through the thermocline? *Fisheries Science*, *73*(1), 98-106.

80. Kitagawa, T., Nakata, H., Kimura, S., & Tsuji, S. (2001). Thermoconservation mechanisms inferred from peritoneal cavity temperature in free-swimming Pacific bluefin tuna Thunnus thynnus orientalis. *Marine Ecology Progress Series*, *220*, 253-263.

81. Klimley, A. P., Butler, S. B., Nelson, D. R., & Stull, A. T. (1988). Diel movements of scalloped hammerhead sharks, Sphyrna lewini Griffith and Smith, to and from a seamount in the Gulf of California. *Journal of Fish Biology*, *33*(5), 751-761.

82. Kohler, N. E., & Turner, P. A. (2001). Shark Tagging: a review of conventional methods and studies. *environmental biology of fishes*, *60*(1), 191-224.

83. Kuhlbrodt, T., Swaminathan, R., Ceppi, P., & Wilder, T. (2024). A Glimpse into the Future: the 2023 ocean temperature and sea ice extremes in the context of longer-term climate change. *Bulletin of the American Meteorological Society*, *105*(3), E474-E485.

84. Kumar, P. S., Pillai, G. N., & Manjusha, U. (2014). El Nino Southern Oscillation (ENSO) impact on tuna fisheries in Indian Ocean. *SpringerPlus*, *3*(1), 591.

85. Kurz A. (2008). Physiology of thermoregulation. *Best practice & research. Clinical anaesthesiology*, *22*(4), 627–644.

86. Lam, C. H., Galuardi, B., & Lutcavage, M. E. (2014). Movements and oceanographic associations of bigeye tuna (Thunnus obesus) in the Northwest Atlantic. *Canadian Journal of Fisheries and Aquatic Sciences*, *71*(10), 1529-1543.

87. Lapointe, F., Bradley, R. S., Francus, P., Balascio, N. L., Abbott, M. B., Stoner, J. S., St-Onge, G., De Coninck, A., & Labarre, T. (2020). Annually resolved Atlantic Sea surface temperature variability over the past 2,900 y. *Proceedings of the National Academy of Sciences*, *117*(44), 27171-27178.

88. Legendre, L. J., & Davesne, D. (2020). The evolution of mechanisms involved in vertebrate endothermy. *Philosophical Transactions of the Royal Society B*, *375*(1793), 20190136.

89. Lehodey, P., Hampton, J., Brill, R. W., Nicol, S., Senina, I., Calmettes, B., ... & Sibert, J. (2011). Vulnerability of oceanic fisheries in the tropical Pacific to climate change. *Vulnerability of tropical Pacific fisheries and aquaculture to climate change*, 433-492.

90. Leroy, B., Itano, D. G., Usu, T., Nicol, S. J., Holland, K. N., & Hampton, J. (2009). Vertical behavior and the observation of FAD effects on tropical tuna in the warm-pool of the western Pacific Ocean. *Tagging and tracking of marine animals with electronic devices*, 161-179.

91. Li, G., Cheng, L., Zhu, J., Trenberth, K. E., Mann, M. E., & Abraham, J. P. (2020). Increasing ocean stratification over the past half-century. *Nature Climate Change*, *10*(12), 1116-1123.

92. Lowe, T. E., Brill, R. W., & Cousins, K. L. (2000). Blood oxygen-binding characteristics of bigeye tuna (Thunnus obesus), a high-energy-demand teleost that is tolerant of low ambient oxygen. *Marine Biology*, *136*, 1087-1098.

93. Malte, H., Larsen, C., Musyl, M., & Brill, R. (2007). Differential heating and cooling rates in bigeye tuna (Thunnus obesus Lowe): a model of non-steady state heat exchange. *Journal of Experimental Biology*, *210*(15), 2618-2626.

94. Marcinek, D. J., Bonaventura, J., Wittenberg, J. B., & Block, B. A. (2001). Oxygen affinity and amino acid sequence of myoglobins from endothermic and ectothermic fish. *American Journal of Physiology-Regulatory, Integrative and Comparative Physiology*, *280*(4), R1123-R1133.

95. Matsumoto, T., Kitagawa, T., & Kimura, S. (2013). Vertical behavior of bigeye tuna (Thunnus obesus) in the northwestern Pacific Ocean based on archival tag data. *Fisheries Oceanography*, *22*(3), 234-246.

96. Maunder, M. N., Sibert, J. R., Fonteneau, A., Hampton, J., Kleiber, P., & Harley, S. J. (2006). Interpreting catch per unit effort data to assess the status of individual stocks and communities. *Ices Journal of marine science*, *63*(8), 1373-1385.

97. Maynard, S. D. (1975). Mesopelagic micronekton in Hawaiian waters: faunal composition, standing stock, and diel vertical migration. *Fish. Bull.*, *73*, 726-736.

98. McCauley, D. J., Pinsky, M. L., Palumbi, S. R., Estes, J. A., Joyce, F. H., & Warner, R. R. (2015). Marine defaunation: animal loss in the global ocean. *Science*, *347*(6219), 1255641.

99. McCormick, M. I., & Molony, B. W. (1995). Influence of water temperature during the larval stage on size, age and body condition of a tropical reef fish at settlement. *Marine ecology progress series, 118*(1), 59-68.

100. Mellor, G. L., & Durbin, P. A. (1975). The structure and dynamics of the ocean surface mixed layer. *J. Phys. Oceanogr*, *5*(4), 718-728.

101. Metcalfe, J. D., & Arnold, G. P. (1997). Tracking fish with electronic tags. *Nature*, *387*(6634), 665-666.

102. Mislan, K. A. S., Deutsch, C. A., Brill, R. W., Dunne, J. P., & Sarmiento, J. L. (2017). Projections of climate-driven changes in tuna vertical habitat based on species-specific differences in blood oxygen affinity. *Global Change Biology*, *23*(10), 4019-4028.

103. Montgomery, D. C., Peck, E. A., & Vining, G. G. (2021). Introduction to linear regression analysis. *John Wiley & Sons*.

104. Musyl, M. K., Brill, R. W., Boggs, C. H., Curran, D. S., Kazama, T. K., & Seki, M. P. (2003). Vertical movements of bigeye tuna (Thunnus obesus) associated with islands, buoys, and seamounts near the main Hawaiian Islands from archival tagging data. *Fisheries Oceanography*, *12*(3), 152-169.

105. Nagelkerken, I., & Connell, S. D. (2015). Global alteration of ocean ecosystem functioning due to increasing human CO2 emissions. *Proceedings of the National Academy of Sciences*, 112(43), 13272-13277.

106. Neill, W. H., Chang, R. K., & Dizon, A. E. (1976). Magnitude and ecological implications of thermal inertia in skipjack tuna, Katsuwonus pelamis (Linnaeus). *Environmental Biology of Fishes*, 1, 61-80.

107. NOAA. (2024). Annual 2023 global climate report. https://www.ncei.noaa.gov/access/monitoring/monthly-report/global/202313.

108. Nordstrom, C. A., Battaile, B. C., Cotte, C., & Trites, A. W. (2013). Foraging habitats of lactating northern fur seals are structured by thermocline depths and submesoscale fronts in the eastern Bering Sea. *Deep Sea Research Part II: Topical Studies in Oceanography*, *88*, 78-96.

109. Norelli, A. P., Die, D. J., & Moffat, B. T. (2022). A systematic review of tropical tuna preferences for movement models. *ICCAT*, 79(1), 261-293.

110. Okuyama, J., Kataoka, K., Kobayashi, M., Abe, O., Yoseda, K., & Arai, N. (2012). The regularity of dive performance in sea turtles: a new perspective from precise activity data. *Animal Behaviour*, 84(2), 349-359.

111. Olson, R. J., Young, J. W., Ménard, F., Potier, M., Allain, V., Goñi, N., Logan, J. M., & Galván-Magaña, F. (2016). Bioenergetics, Trophic Ecology, and Niche Separation of Tunas. *Advances in marine biology*, *74*, 199–344.

112. Oschlies, A., Brandt, P., Stramma, L., & Schmidtko, S. (2018). Drivers and mechanisms of ocean deoxygenation. *Nature Geoscience*, 11(7), 467–473.

113. Parmesan, C. (2006). Ecological and evolutionary responses to recent climate change. *Annu. Rev. Ecol. Evol. Syst.*, *37*(1), 637-669.

114. Paulmier, A., & Ruiz-Pino, D. (2009). Oxygen minimum zones (OMZs) in the modern ocean. *Progress in oceanography*, 80(3-4), 113-128.

115. Pauly, D., Christensen, V., Dalsgaard, J., Froese, R., & Torres Jr, F. (1998). Fishing down marine food webs. *Science*, 279(5352), 860-863.

116. Polovina, J., Abécassis, M., Howell, E., & Woodworth-Jefcoats, P. (2009). Increases in the Relative Abundance of Mid-Trophic Level Fishes Concurrent with Declines in Apex Predators in the Subtropical North Pacific, 1996–2006. *Fishery Bulletin*, *107*.

117. Polyakov, I. V., Bhatt, U. S., Simmons, H. L., Walsh, D., Walsh, J. E., & Zhang, X. (2005). Multidecadal variability of North Atlantic temperature and salinity during the twentieth century. *Journal of Climate*, 18(21), 4562-4581.

118. Potier, M., Bach, P., Ménard, F., & Marsac, F. (2014). Influence of mesoscale features on micronekton and large pelagic fish communities in the Mozambique Channel. *Deep Sea Research Part II: Topical Studies in Oceanography*, 100, 184-199.

119. Potier, M., Marsac, F., Cherel, Y., Lucas, V., Sabatié, R., & Maury, O. (2014). Forage fauna in the diet of three large pelagic fish (yellowfin tuna, Thunnus albacares, swordfish, Xiphias gladius, and sailfish, Istiophorus platypterus) in the western Indian Ocean. *Fishery Bulletin*, 112(2-3), 252-257.

120. Prince, E. D., & Goodyear, C. P. (2006). Hypoxia-based habitat compression of tropical pelagic fishes. *Fisheries Oceanography*, 15(6), 451-464.

121. Queiroz, N., Humphries, N. E., Mucientes, G., Hammerschlag, N., Lima, F. P., Scales, K. L., ... & Sims, D. W. (2016). Ocean-wide tracking of pelagic sharks reveals extent of overlap with longline fishing hotspots. *Proceedings of the National Academy of Sciences*, 113(6), 1582-1587.

122. Rogan, E., & Mackey, M. (2007). Megafauna bycatch in drift nets for albacore tuna (Thunnus alalunga) in the NE Atlantic. *Fisheries Research*, 86(1), 6-14.

123. Roper, C. F., Sweeney, M. J., & Nauen, C. E. (1984). FAO species catalogue: Vol. 3. Cephalopods of the world. An annotated and illustrated catalogue of species of interest to fisheries. *FAO fisheries Synopsis*, (3).

124. Sato, K., Charrassin, J. B., Bost, C. A., & Naito, Y. (2004). Why do macaroni penguins choose shallow body angles that result in longer descent and ascent durations?. *Journal of Experimental Biology*, 207(23), 4057-4065.

125. Schaefer, K. M., & Fuller, D. W. (2002). Movements, behavior, and habitat selection of bigeye tuna (Thunnus obesus) in the eastern equatorial Pacific, ascertained through archival tag data. *Marine Biology*, 140(2), 383–393.

126. Schaefer, K. M., & Fuller, D. W. (2010). Vertical movements, behavior, and habitat of bigeye tuna (Thunnus obesus) in the equatorial eastern Pacific Ocean, ascertained from archival tag data. *Marine Biology*, 157, 2625-2642.

127. Seibel, B. A. (2011). Critical oxygen levels and metabolic suppression in oceanic oxygen minimum zones. *The Journal of Experimental Biology*, 214(2), 326-336.

128. Sethi, S. A., Branch, T. A., & Watson, R. (2010). Global fishery development patterns are driven by profit but not trophic level. *Proceedings of the National Academy of Sciences*, 107(27), 12163-12167.

129. Shepard, D. B., Kuhns, A. R., Dreslik, M. J., & Phillips, C. A. (2008). Roads as barriers to animal movement in fragmented landscapes. *Animal conservation*, 11(4), 288-296.

130. Sims, D. W., Southall, E. J., Humphries, N. E., Hays, G. C., Bradshaw, C. J., Pitchford, J. W., ... & Metcalfe, J. D. (2008). Scaling laws of marine predator search behaviour. *Nature*, *451*(7182), 1098-1102.

131. Sogard, S. M., & Olla, B. L. (1993). Effects of light, thermoclines and predator presence on vertical distribution and behavioral interactions of juvenile walleye pollock, Theragra chalcogramma Pallas. *Journal of Experimental Marine Biology and Ecology*, 167(2), 179-195.

132. Song, L., Zhou, J., Zhou, Y., Nishida, T., Jiang, W., & Wang, J. (2009). Environmental preferences of bigeye tuna, Thunnus obesus, in the Indian Ocean: an application to a longline fishery. *Environmental Biology of Fishes*, 85, 153-171.

133. Stevens et al. (2011) The Retia. *Encyclopedia of fish physiology: from genome to environment 2*: 1119-1131.

134. Stevenson, R. D. (1985). The relative importance of behavioral and physiological adjustments controlling body temperature in terrestrial ectotherms. *The American Naturalist*, 126(3), 362-386.

135. Stramma, L., Brandt, P., Schafstall, J., Schott, F., Fischer, J., & Körtzinger, A. (2008). Oxygen minimum zone in the North Atlantic south and east of the Cape Verde Islands. *Journal of Geophysical Research: Oceans*, *113*(C4).

136. Stramma, L., Johnson, G. C., Sprintall, J., & Mohrholz, V. (2008). Expanding oxygen-minimum zones in the tropical oceans. *Science*, *320*(5876), 655–658.

137. Stramma, L., Prince, E. D., Schmidtko, S., Luo, J., Hoolihan, J. P., Visbeck, M., ... & Körtzinger, A. (2012). Expansion of oxygen minimum zones may reduce available habitat for tropical pelagic fishes. *Nature Climate Change*, 2(1), 33-37.

138. Takahashi, M., McCormick, M. I., Munday, P. L., & Jones, G. P. (2012). Influence of seasonal and latitudinal temperature variation on early life-history traits of a coral reef fish. *Marine and Freshwater Research,* 63(10), 856-864.

139. Thiem, H. (2024). For more than a year, the North Atlantic has been running a fever. NOAA Climate.gov. https://www.climate.gov/news-features/featured-images/more-year-north-atlantic-has-been-running-fever.

140. Thirumalai, K., McCave, I. N., Hall, I. R., & Middleton, J. (2023). A 3000-year perspective on North Atlantic Ocean warming. *Nature Geoscience*, 16(2), 123–130.

141. Thomas, C. D., Cameron, A., Green, R. E., Bakkenes, M., Beaumont, L. J., Collingham, Y. C., Erasmus, B. F., De Siqueira, M. F., Grainger, A., Hannah, L., Hughes, L., Huntley, B., Van Jaarsveld, A. S., Midgley, G. F., Miles, L., Ortega-Huerta, M. A., Peterson, A. T., Phillips, O. L., & Williams, S. E. (2004). Extinction risk from climate change. *Nature*, *427*(6970), 145–148.

142. Tittensor, D. P., Mora, C., Jetz, W., Lotze, H. K., Ricard, D., Berghe, E. V., & Worm, B. (2010). Global patterns and predictors of marine biodiversity across taxa. *Nature*, 466(7310), 1098-1101.

143. Vedor, M., Queiroz, N., Mucientes, G., Couto, A., Costa, I. D., Santos, A. D., ... & Sims, D. W. (2021). Climate-driven deoxygenation elevates fishing vulnerability for the ocean's widest ranging shark. *Elife*, 10, e62508.

144. Walker, K. A., Trites, A. W., Haulena, M., & Weary, D. M. (2012). A review of the effects of different marking and tagging techniques on marine mammals. *Wildlife Research*, *39*(1), 15-30.

145. Wang, X.-Y., & Xie, J. (2019). Evaluation of water dynamics and protein changes in bigeye tuna (Thunnus obesus) during cold storage. *LWT*, *108*, 289-296.

146. Ward, P., & Myers, R. A. (2005). Inferring the depth distribution of catchability for pelagic fishes and correcting for variations in the depth of longline fishing gear. *Canadian Journal of Fisheries and Aquatic Sciences*, 62(5), 1130-1142.

147. Ward, P., & Myers, R. A. (2005). Shifts in open-ocean fish communities coinciding with the commencement of commercial fishing. *Ecology*, 86(4), 835-847.

148. Watanabe, Y. Y., & Takahashi, A. (2013). Linking animal-borne video to accelerometers reveals prey capture variability. *Proceedings of the National Academy of Sciences*, 110(6), 2199-2204.

149. Wegner, N. C., Snodgrass, O. E., Dewar, H., & Hyde, J. R. (2015). Animal physiology. Whole-body endothermy in a mesopelagic fish, the opah, Lampris guttatus. *Science (New York, N.Y.)*, *348*(6236), 786–789.

150. Welander, P. (1971). A discussion on ocean currents and their dynamics -The thermocline problem. *Mathematical and Physical Sciences*, 270(1206), 415-421.

151. Wilmers, C. C., Nickel, B., Bryce, C. M., Smith, J. A., Wheat, R. E., & Yovovich, V. (2015). The golden age of bio-logging: How animal-borne sensors are advancing the frontiers of ecology. *Ecology*, 96(7), 1741-1753.

152. Wilson, A. D., Wikelski, M., Wilson, R. P., & Cooke, S. J. (2015). Utility of biological sensor tags in animal conservation. *Conservation Biology*, 29(4), 1065-1075.

153. Wilson, R. P., & McMahon, C. R. (2006). Measuring devices on wild animals: what constitutes acceptable practice?. *Frontiers in Ecology and the Environment*, 4(3), 147-154.

154. Wilson, R., Ducamp, J., Rees, G., Culik, B., & Neikamp, K. (1992). Estimation of location: Global coverage using light intensity. *Wildlife Telemetry: Remote Monitoring and Tracking of Animals*.

155. Woollings, T., Gregory, J. M., Pinto, J. G., Reyers, M., & Brayshaw, D. J. (2012). Response of the North Atlantic storm track to climate change shaped by ocean–atmosphere coupling. *Nature Geoscience,* 5(5), 313-317.

156. World Meteorological Organization (WMO). State of the Climate in Europe 2022 (WMO-No. 1320). *WMO*.

157. Wright, J. J., Konwar, K. M., & Hallam, S. J. (2012). Microbial ecology of expanding oxygen minimum zones. *Nature Reviews Microbiology*, *10*(6), 381-394.

158. Xu, Y., Wang, C., & Zhang, L. (2023). Record-breaking North Atlantic Sea surface temperatures in 2023. *Journal of Climate Science*, 34(9), 657-670.

8. Supplementary materials

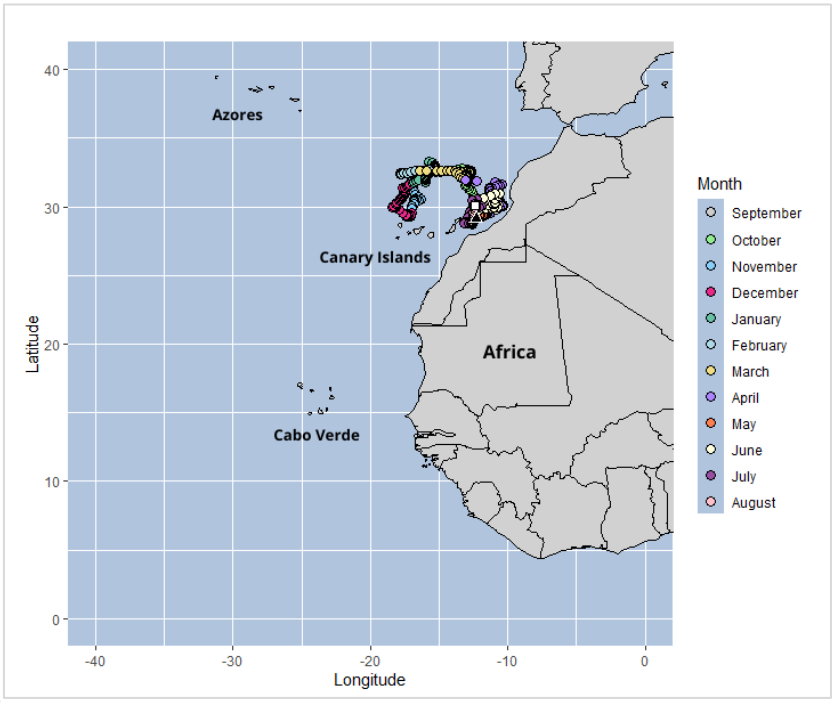

a

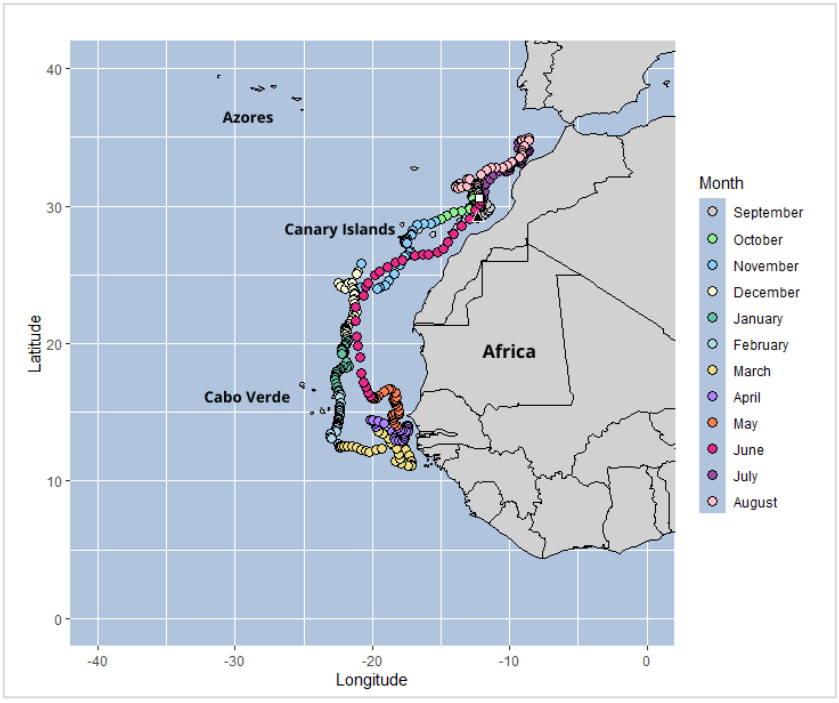

b

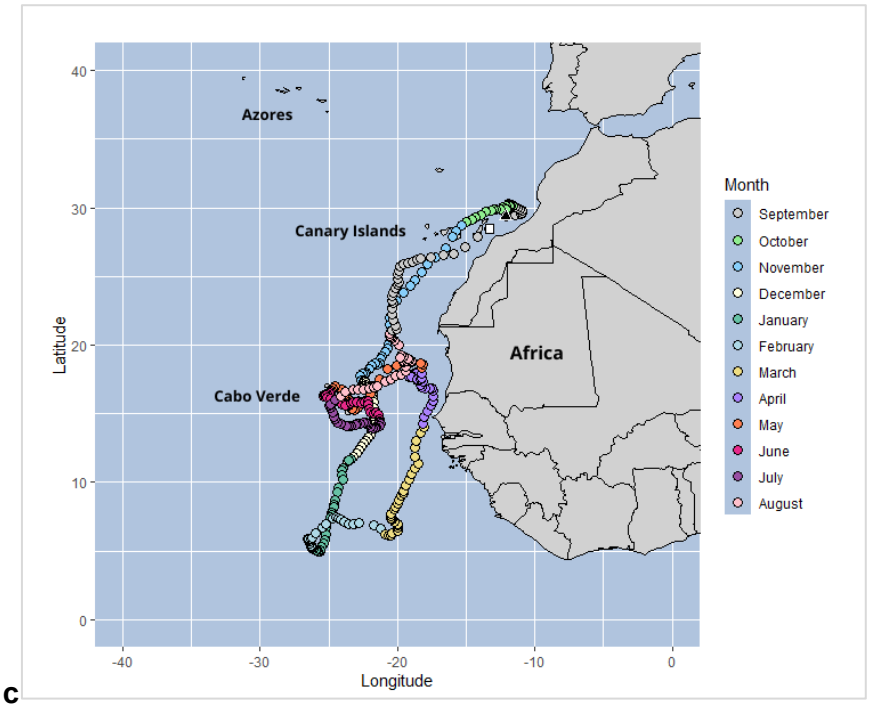
Azores
Canary Islands
Africa
Cabo Verde
Latitude
Longitude
40
30
20
10
0
-40
-30
-20
-10
0
Month
September
October
November
December
January
February
March
April
May
June
July
August

c

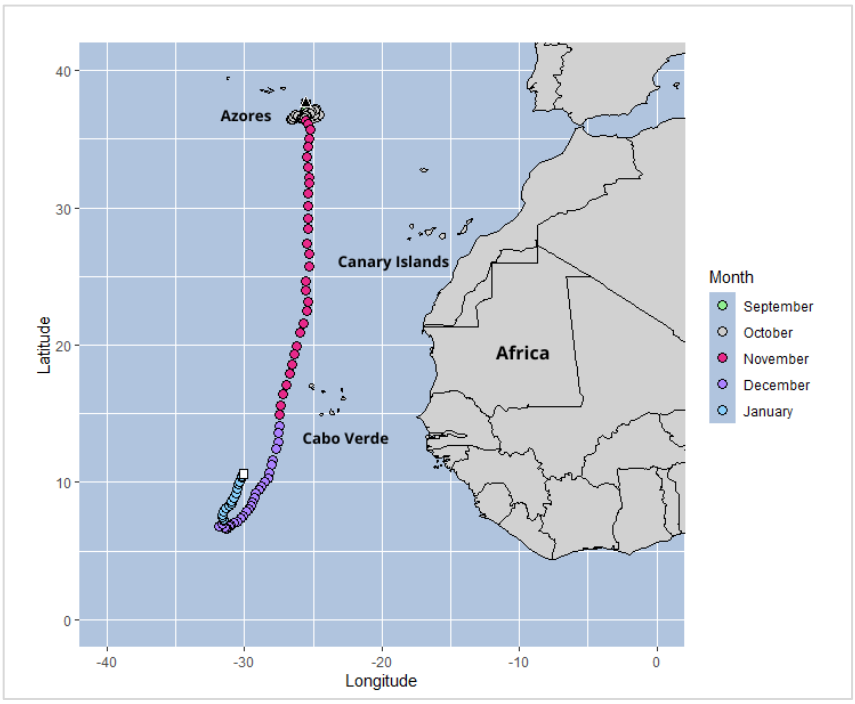
Azores
Canary Islands
Africa
Cabo Verde
Latitude
Longitude
40
30
20
10
0
-40
-30
-20
-10
0
Month
September
October
November
December
January

d

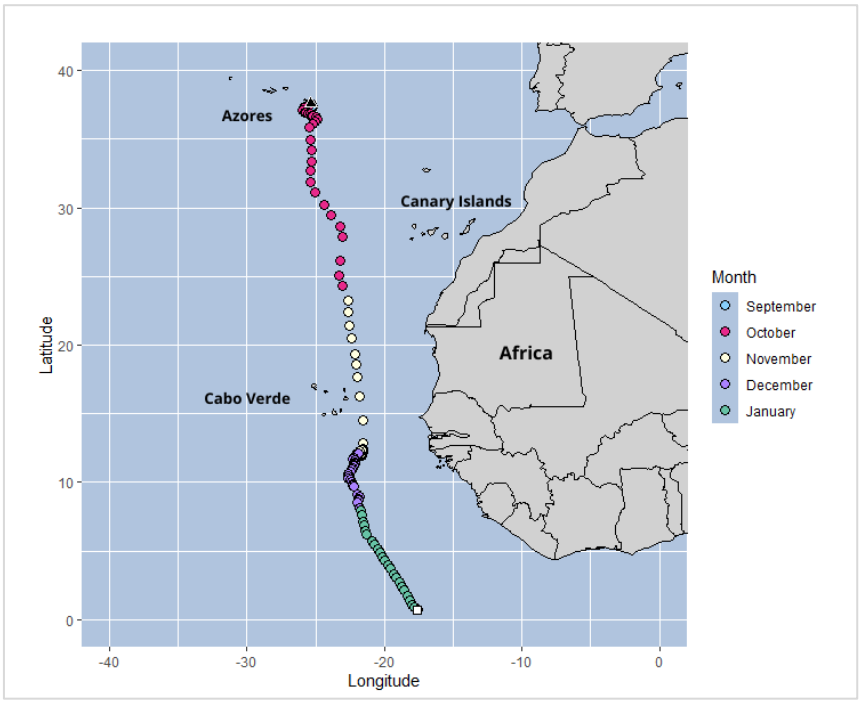
Azores
Canary Islands
Africa
Cabo Verde
Month
September
October
November
December
January
Latitude
Longitude
40
30
20
10
0
-40
-30
-20
-10
0

e

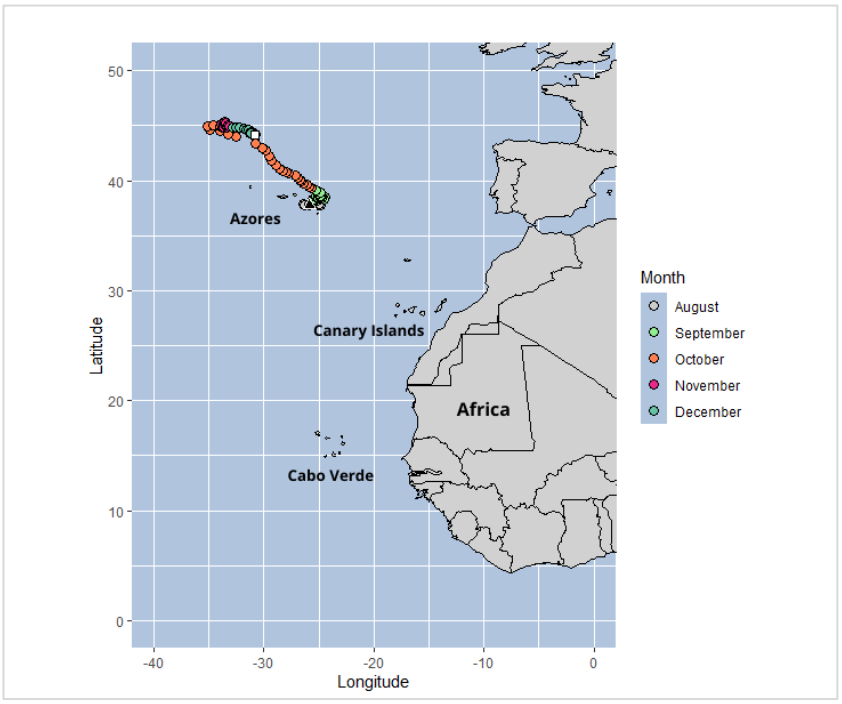
Azores
Canary Islands
Africa
Cabo Verde
Month
August
September
October
November
December
Latitude
Longitude
50
40
30
20
10
0
-40
-30
-20
-10
0

f

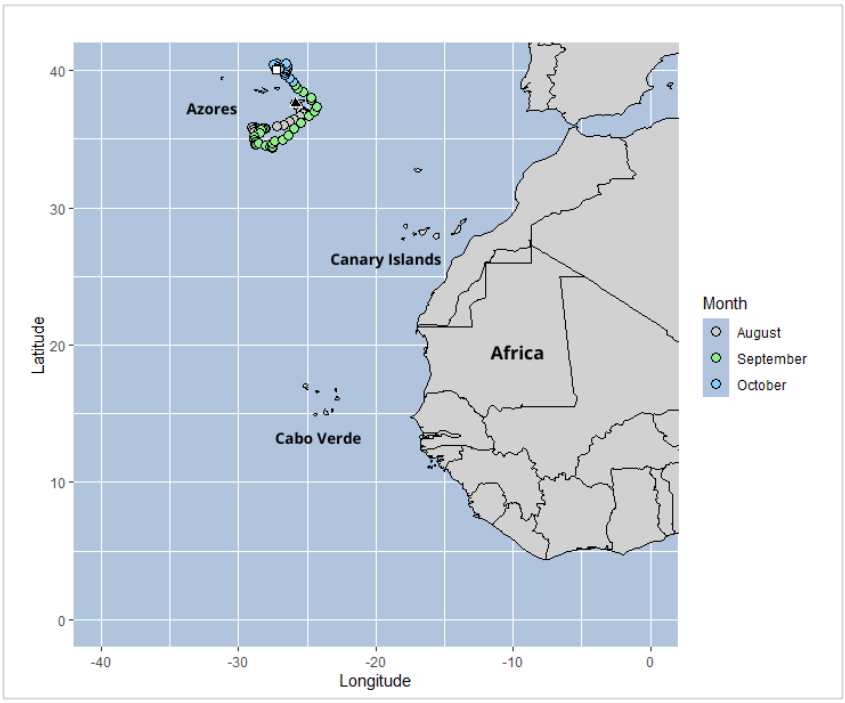
Azores
Canary Islands
Africa
Cabo Verde
Month
August
September
October
Latitude
Longitude
40
30
20
10
0
-40
-30
-20
-10
0

g

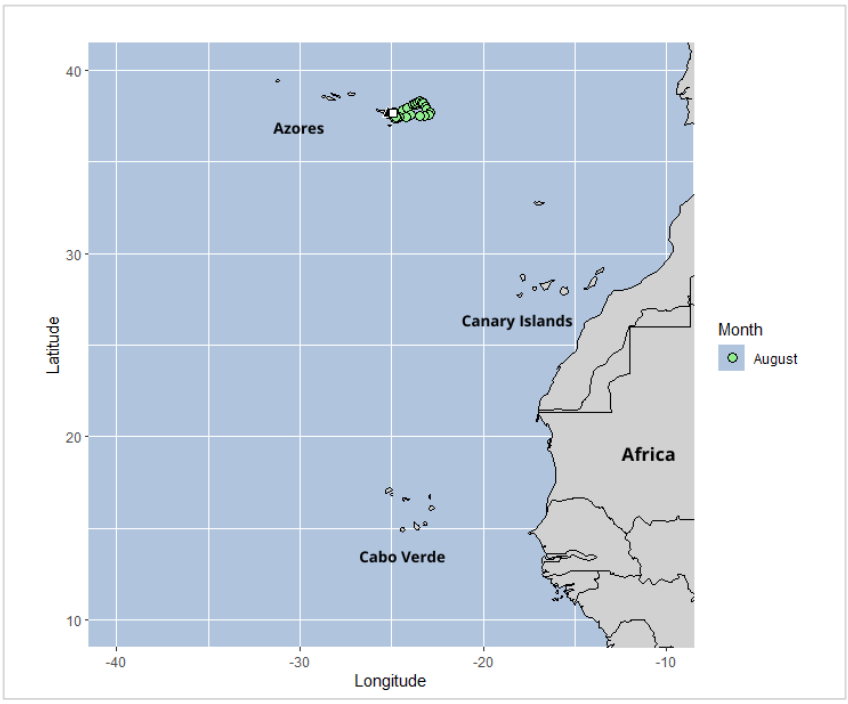
Azores
Canary Islands
Africa
Cabo Verde
Month
August
Latitude
Longitude
40
30
20
10
-40
-30
-20
-10

h

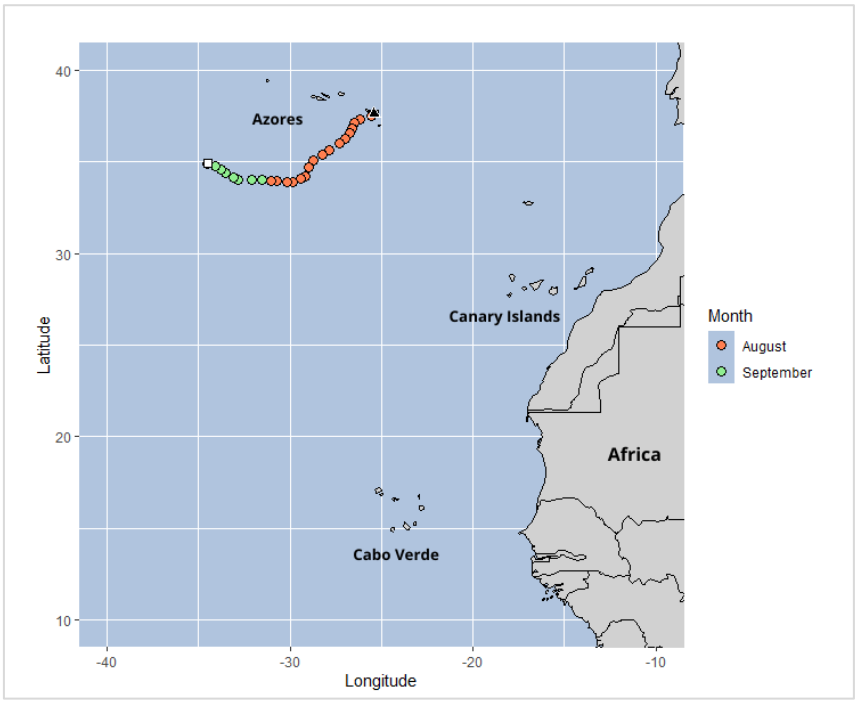

i

Figure S1. Monthly movement patterns. The black triangles represent the tagging sites, and the white quadrilaterals represent the endpoints of each track. (a) BET1 (b) BET2 (c) BET3 (d) BET4 (e) BET5 (f) BET6 (g) BET7 (h) BET8 (i) BET9.

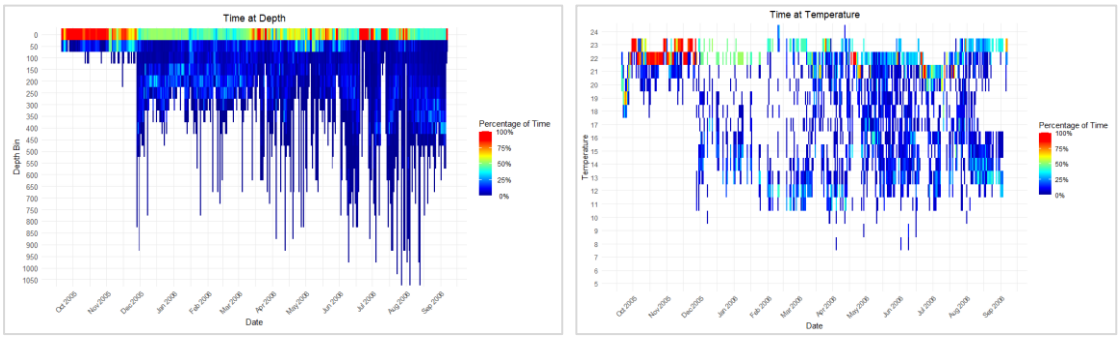

a

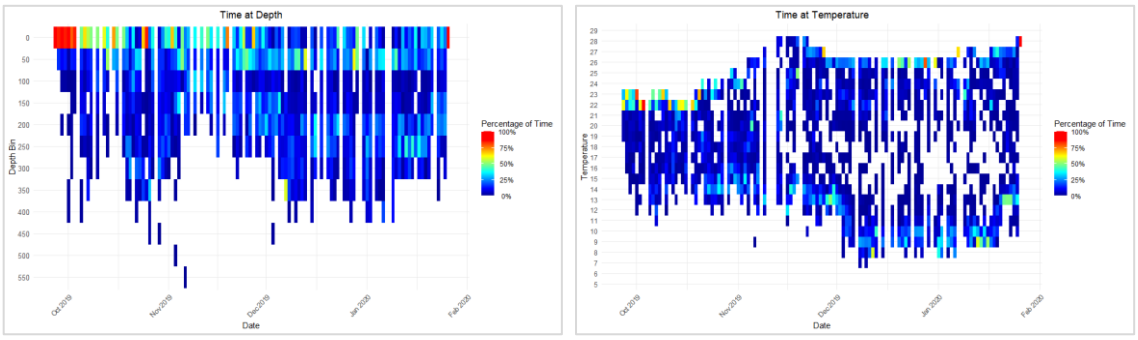

b

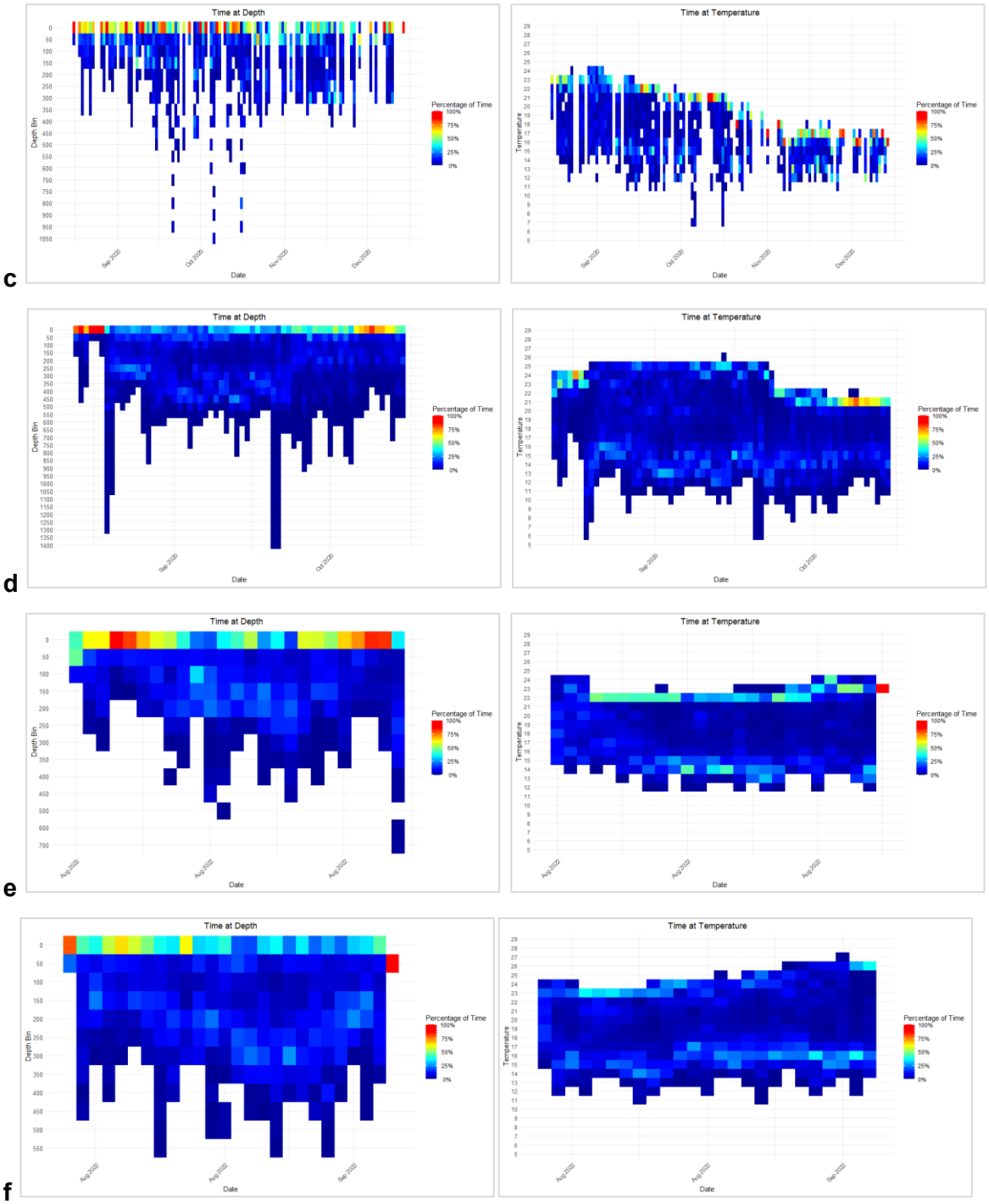

Figure S2. Time spent at different depths (left) and temperatures (right). In the depth graphs, the y-axis shows depth bins (in meters), while in the temperature graphs, the y-axis shows temperature bins (in degrees). The x-axis in both represents the date. The colour scale indicates the percentage of time tuna spent at each depth or temperature bin, with red representing 100% of the time and dark blue indicating 0%. (a) BET2 (b) BET5 (c) BET6 (d) BET7 (e) BET8 (f) BET9.

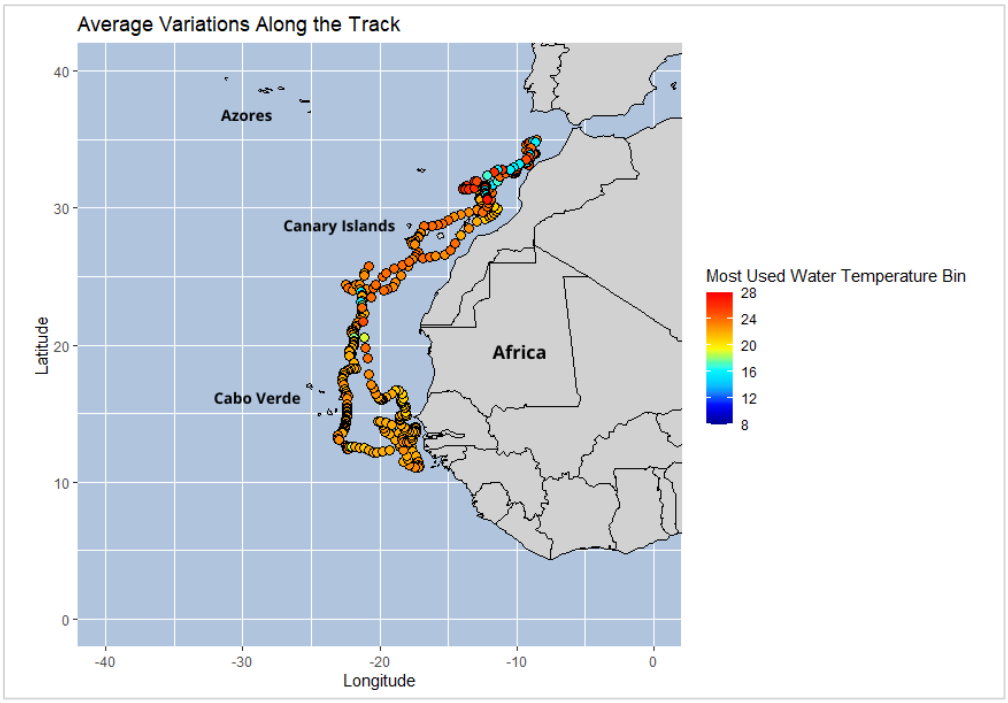
Average Variations Along the Track
Azores
Canary Islands
Africa
Cabo Verde
Latitude
Longitude
Most Used Water Temperature Bin
28
24
20
16
12
8
40
30
20
10
0
-40
-30
-20
-10
0

a

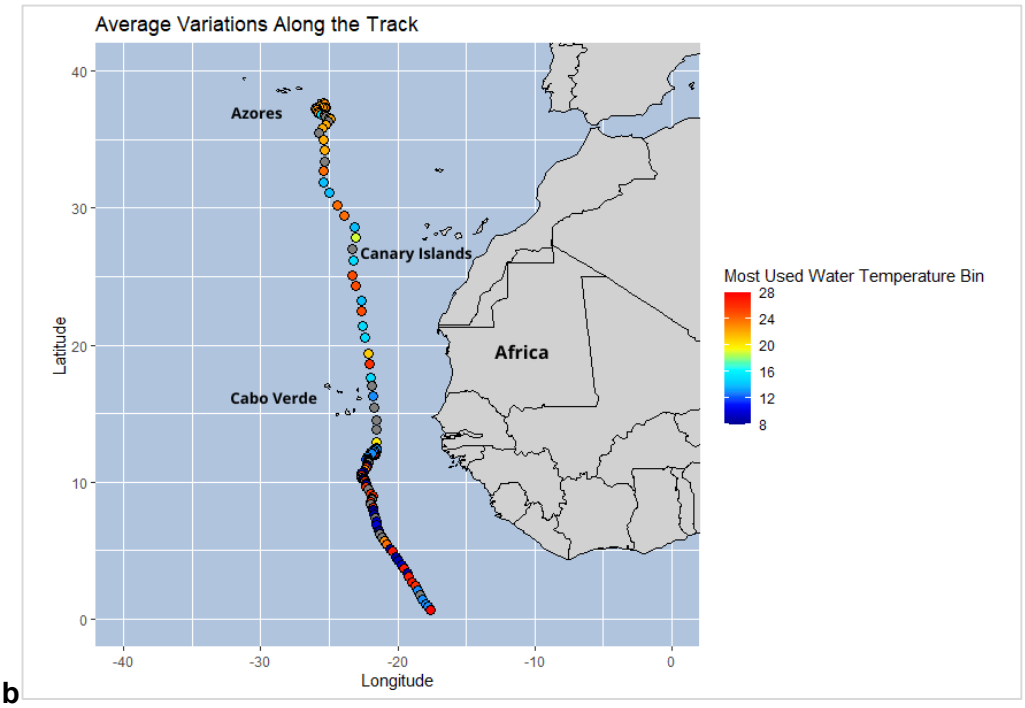
Average Variations Along the Track
Azores
Canary Islands
Africa
Cabo Verde
Latitude
Longitude
Most Used Water Temperature Bin
28
24
20
16
12
8
40
30
20
10
0
-40
-30
-20
-10
0

b

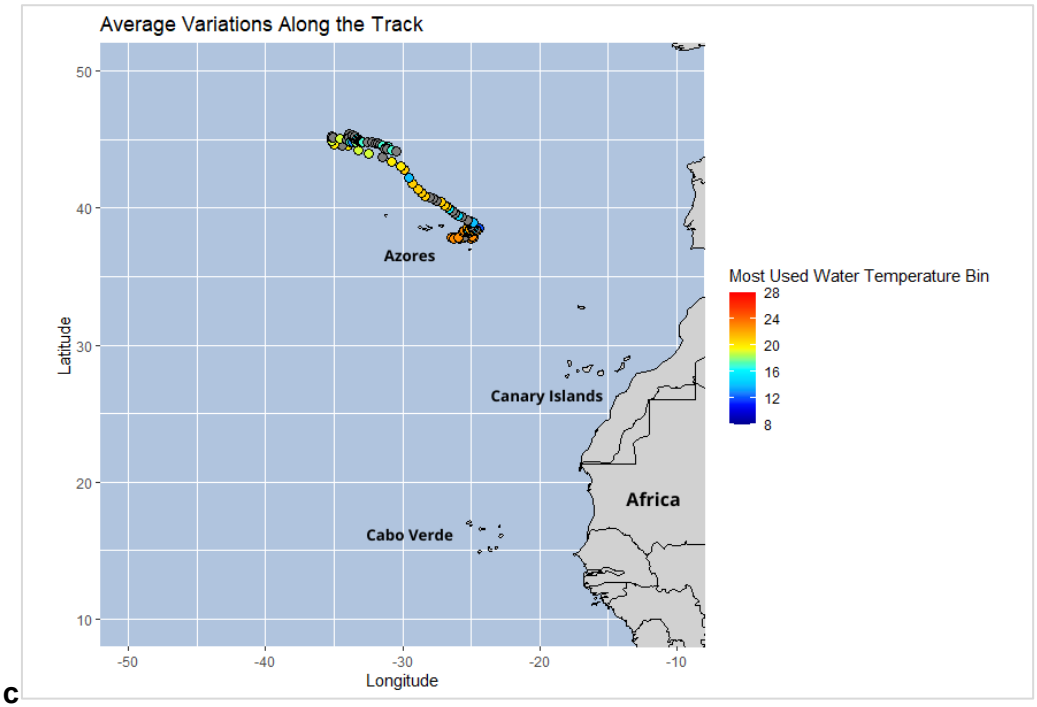
Average Variations Along the Track
Azores
Canary Islands
Africa
Cabo Verde
Latitude
Longitude
Most Used Water Temperature Bin
28
24
20
16
12
8
50
40
30
20
10
-50
-40
-30
-20
-10

c

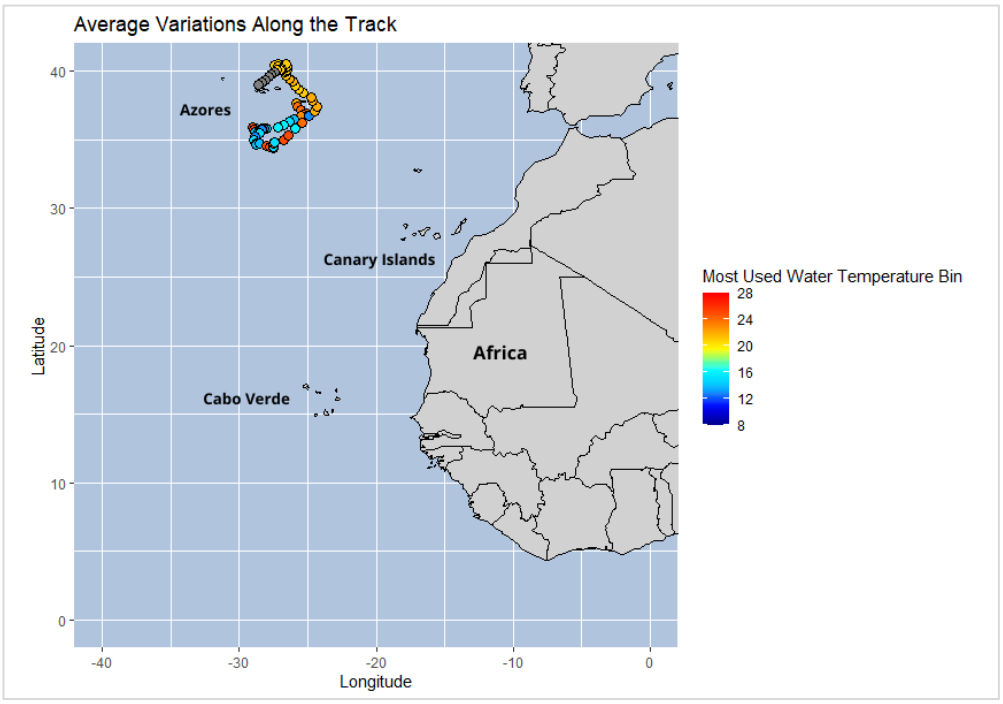
Average Variations Along the Track
Azores
Canary Islands
Africa
Cabo Verde
Latitude
Longitude
Most Used Water Temperature Bin
28
24
20
16
12
8
40
30
20
10
0
-40
-30
-20
-10
0

d

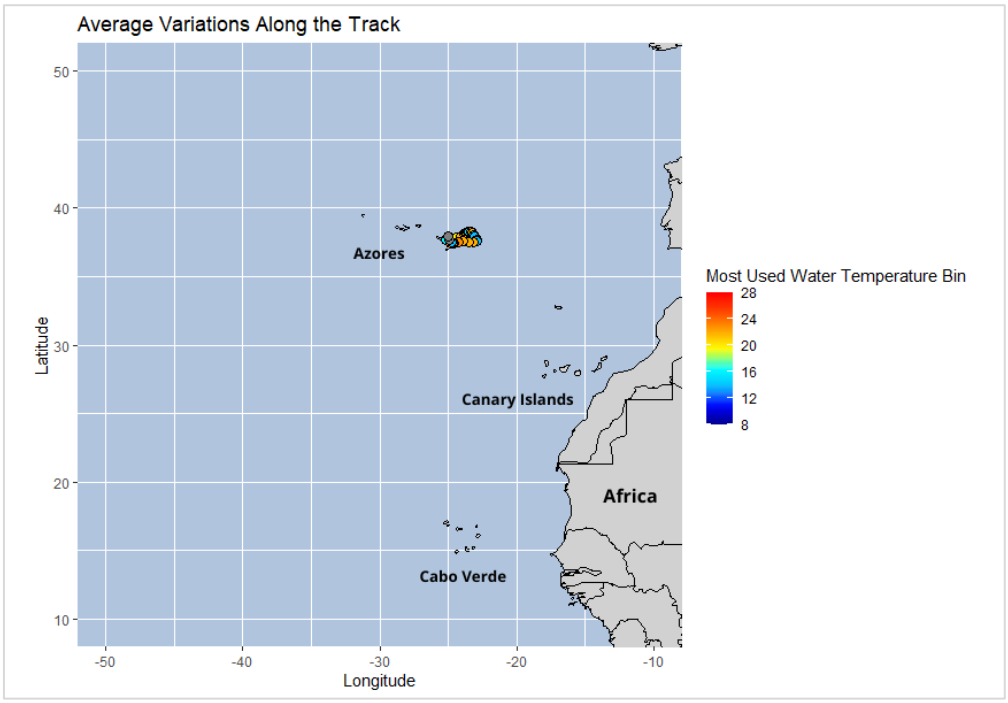

e

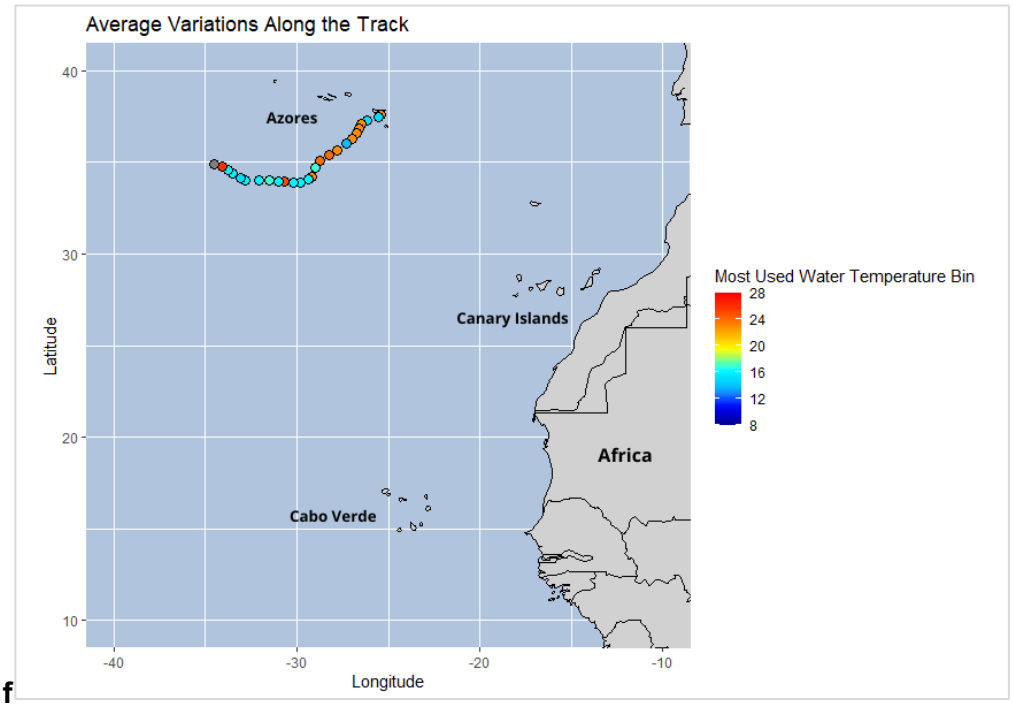

f

Figure S3. Average variations in most used ambient temperature bins along the track. The colour scale represents the water temperature (°C), with warmer temperatures in red and cooler temperatures in yellow. (a) BET2 (b) BET5 (c) BET6 (d) BET7 (e) BET8 (f) BET9.

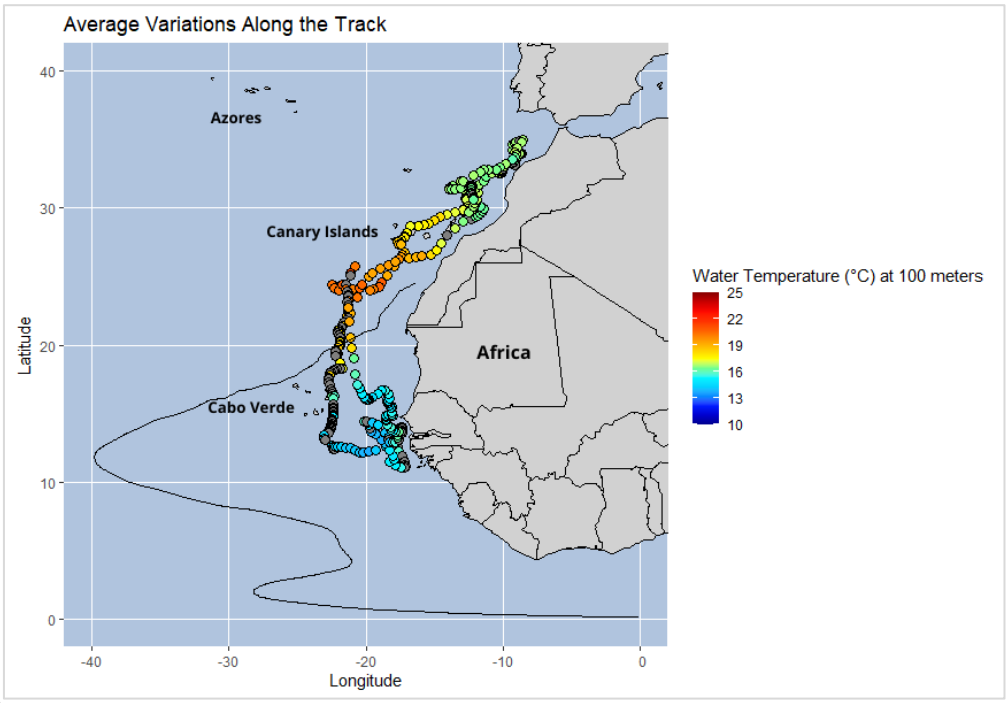
Average Variations Along the Track
Azores
Canary Islands
Africa
Cabo Verde
Latitude
Longitude
Water Temperature (°C) at 100 meters
25
22
19
16
13
10
40
30
20
10
0
-40
-30
-20
-10
0

a

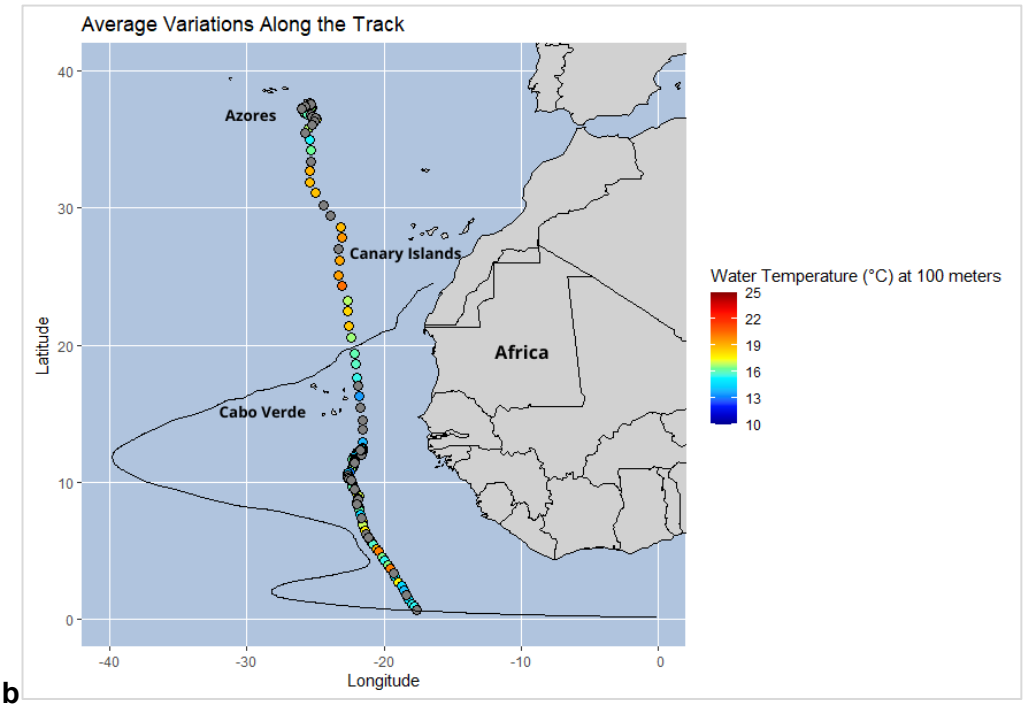
Average Variations Along the Track
Azores
Canary Islands
Africa
Cabo Verde
Latitude
Longitude
Water Temperature (°C) at 100 meters
25
22
19
16
13
10
40
30
20
10
0
-40
-30
-20
-10
0

b

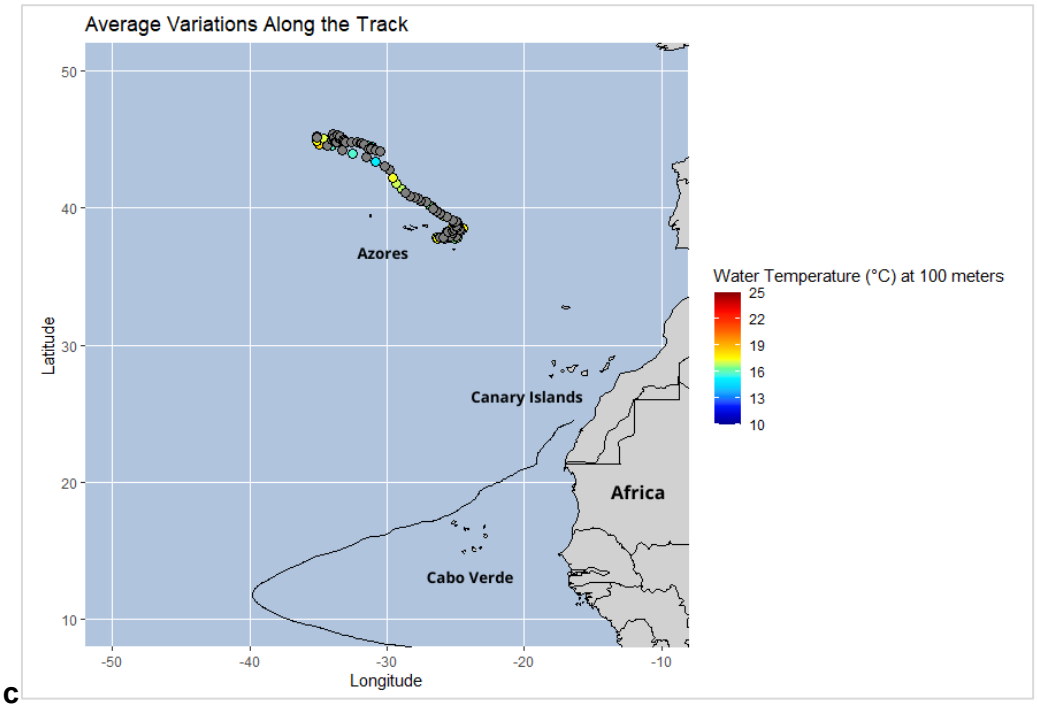
Average Variations Along the Track
Azores
Canary Islands
Africa
Cabo Verde
Water Temperature (°C) at 100 meters
25
22
19
16
13
10
Latitude
Longitude
50
40
30
20
10
-50
-40
-30
-20
-10

c

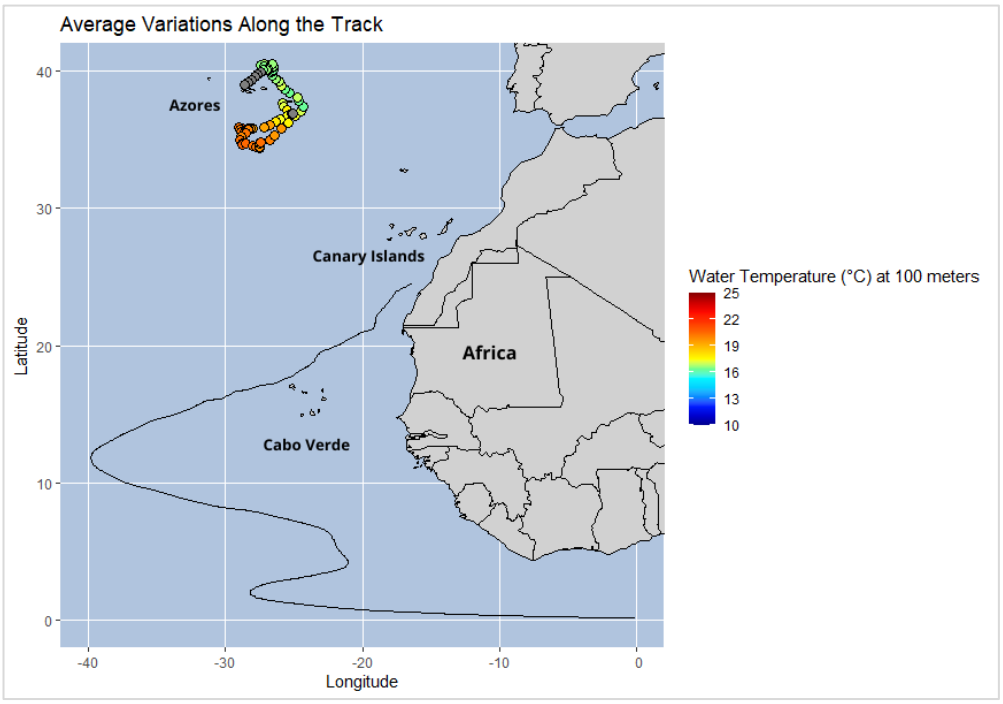
Average Variations Along the Track
Azores
Canary Islands
Africa
Cabo Verde
Water Temperature (°C) at 100 meters
25
22
19
16
13
10
Latitude
Longitude
40
30
20
10
0
-40
-30
-20
-10
0

d

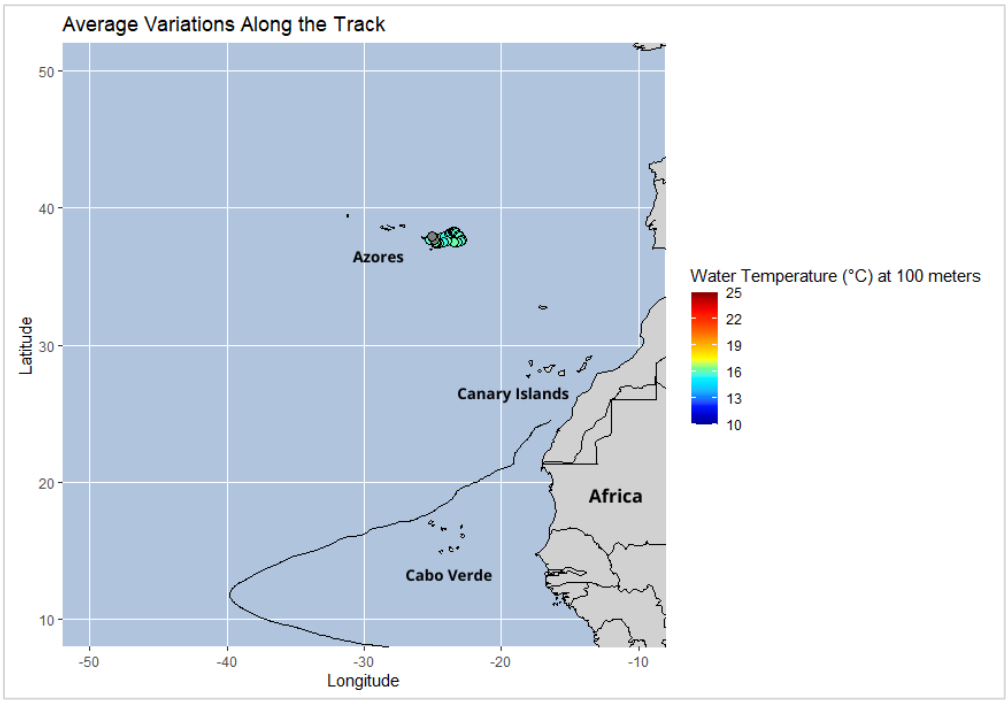

e

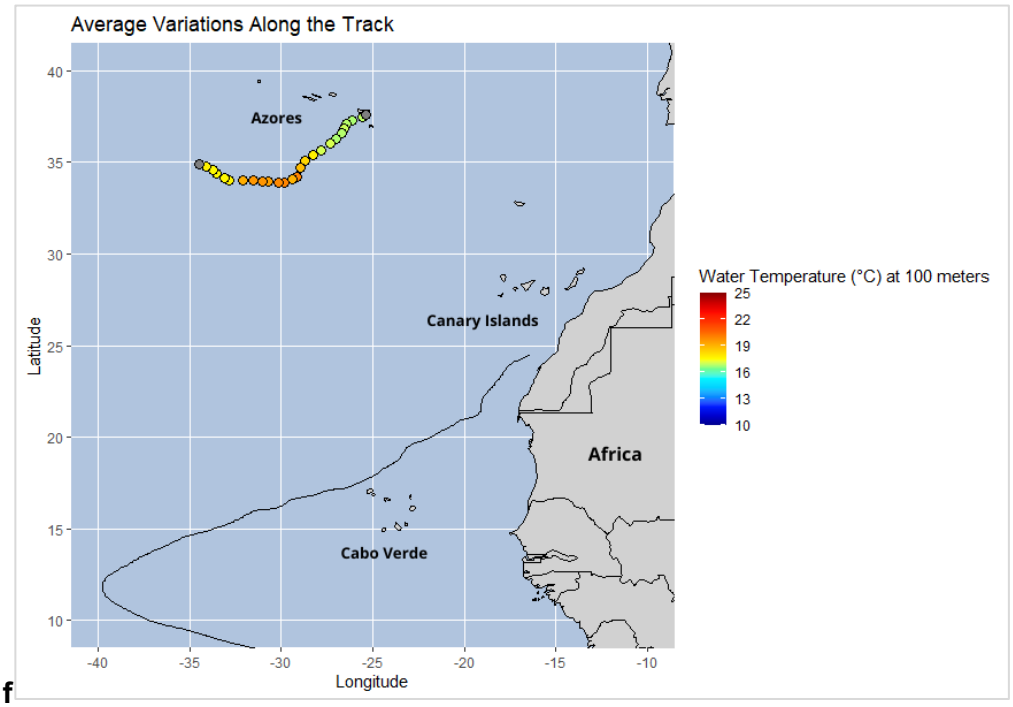

f

Figure S4. Average water temperature variations at a depth of 100 meters along the track overlaid with the OMZ boundary obtained from modelled dissolved oxygen concentrations (at 100 m). The colour scale represents water temperature (°C), with warmer temperatures shown in red and cooler temperatures in blue. (a) BET2 (b) BET5 (c) BET6 (d) BET7 (e) BET8 (f) BET9.

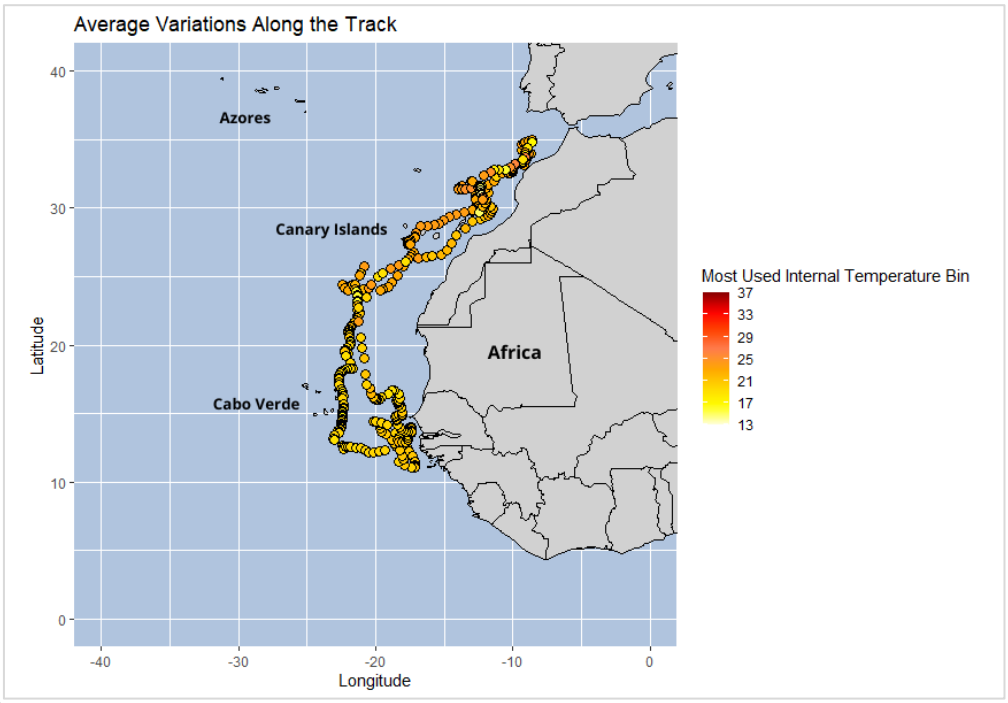
Average Variations Along the Track
Azores
Canary Islands
Africa
Cabo Verde
Latitude
Longitude
Most Used Internal Temperature Bin
37
33
29
25
21
17
13
40
30
20
10
0
-40
-30
-20
-10
0

a

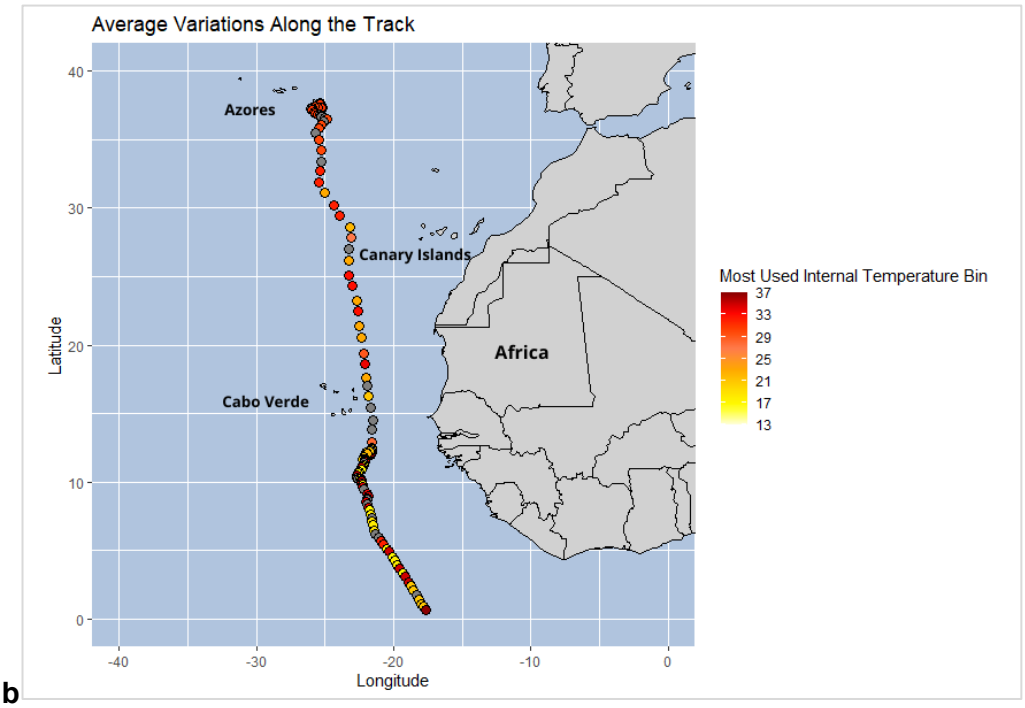
Average Variations Along the Track
Azores
Canary Islands
Africa
Cabo Verde
Latitude
Longitude
Most Used Internal Temperature Bin
37
33
29
25
21
17
13
40
30
20
10
0
-40
-30
-20
-10
0

b

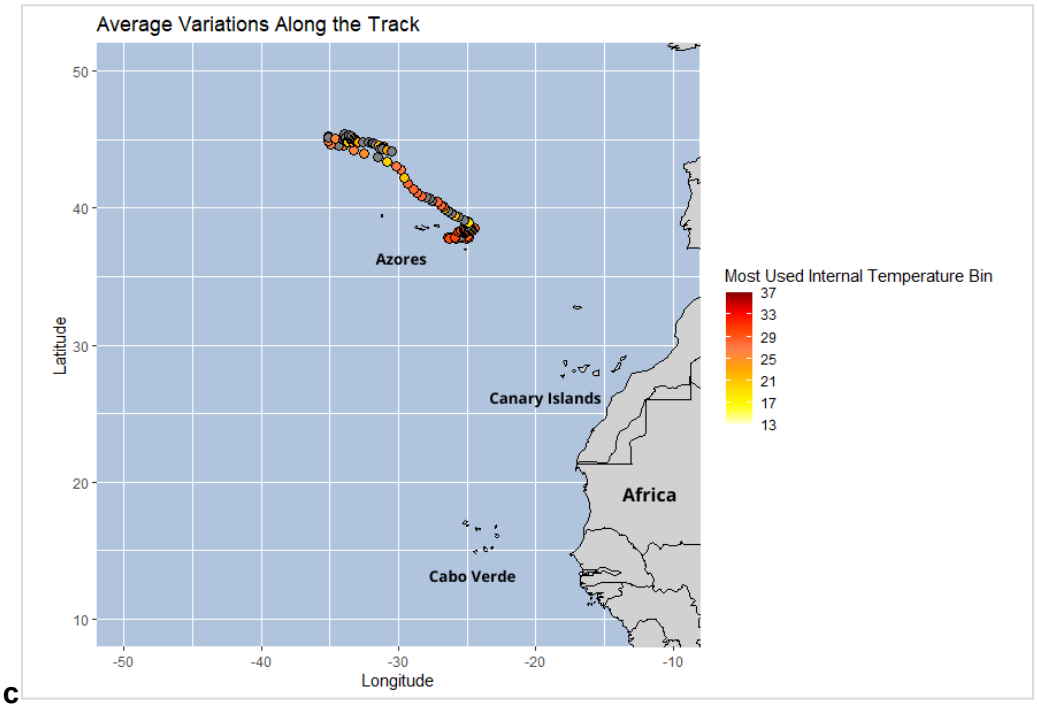
Average Variations Along the Track
Azores
Canary Islands
Africa
Cabo Verde
Latitude
Longitude
Most Used Internal Temperature Bin
37
33
29
25
21
17
13
50
40
30
20
10
-50
-40
-30
-20
-10

c

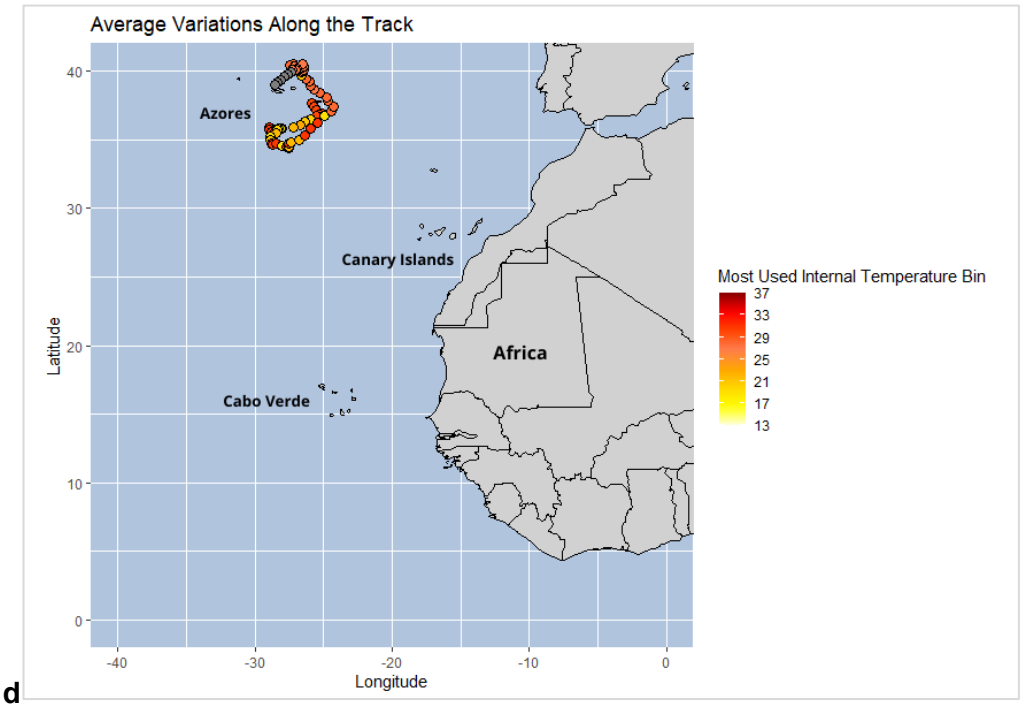
Average Variations Along the Track
Azores
Canary Islands
Africa
Cabo Verde
Latitude
Longitude
Most Used Internal Temperature Bin
37
33
29
25
21
17
13
40
30
20
10
0
-40
-30
-20
-10
0

d

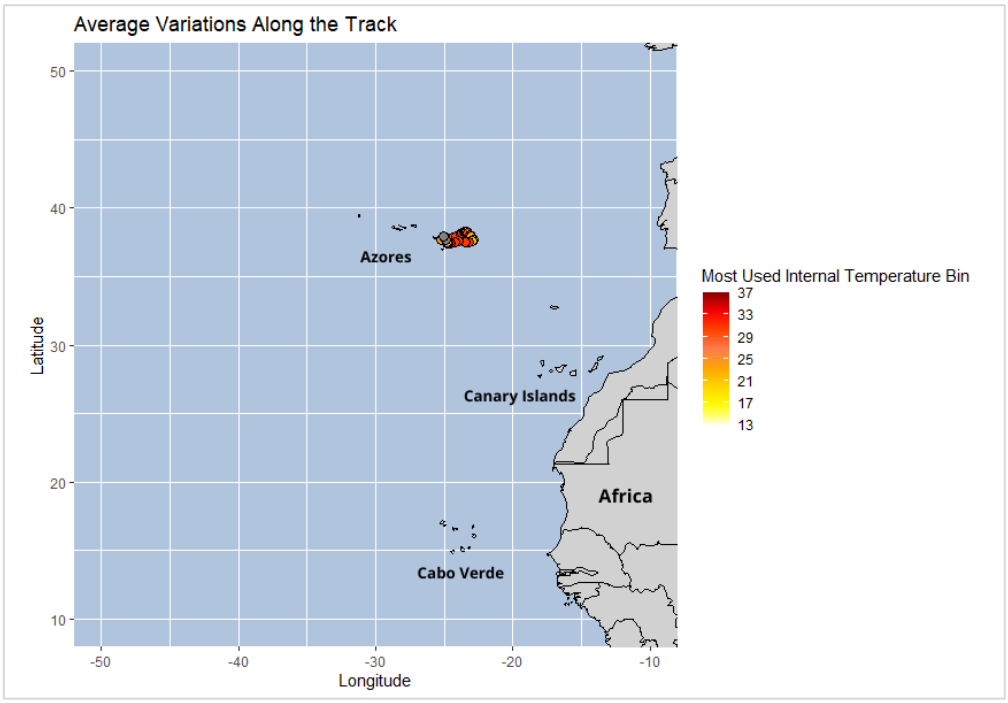

e

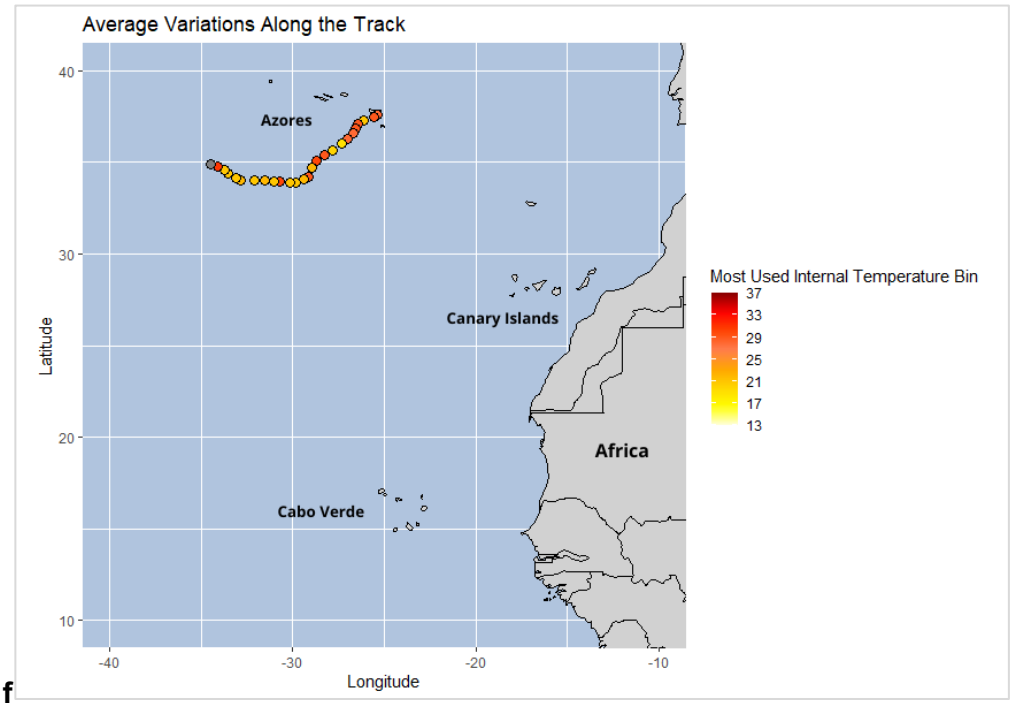

f

Figure S5. Average variations in most used internal temperature bins along the track. The colour scale represents the water temperature (°C), with warmer temperatures in red and cooler temperatures in yellow. (a) BET2 (b) BET5 (c) BET6 (d) BET7 (e) BET8 (f) BET9.

INSTITUTO DE **CIÊNCIAS BIOMÉDICAS ABEL SALAZAR**